Use of artificial intelligence to locate and treat weeds in Midwestern United States corn (*Zea mays*) and soybean (*Glycine max*) cropping systems

by

Isaac Harrison Barnhart

B.S., Sterling College (KS), 2017
M.S., Kansas State University, 2020

AN ABSTRACT OF A DISSERTATION

submitted in partial fulfillment of the requirements for the degree

DOCTOR OF PHILOSOPHY

Department of Agronomy
College of Agriculture

KANSAS STATE UNIVERSITY
Manhattan, Kansas

2024

Abstract

Site-specific weed management (SSWM) is defined as the process of managing weeds where they are growing as opposed to treating the whole field and treating areas with no weeds. Artificial intelligence (AI), the process of creating intelligent machines, has become a part of everyday life in modern society. Utilizing convolutional neural networks and object detection algorithms, weeds can be distinguished from crops, and herbicide applications can target weeds where they are growing. The objectives of this dissertation were to 1) train open-sourced object detection algorithms to detect in central Kansas soybean (*Glycine Max* [L.] Merr.) fields, focusing on Palmer amaranth (*Amaranthus palmeri* S. Watson, henceforth denoted as *A. palmeri*), 2) determine herbicide efficacy and cost savings of SSWM herbicide applications using a ONE SMART SPRAY research sprayer, an intelligent dual-boom sprayer using AI technology to locate and spray weeds growing within crops, and 3) compare traditional broadcast (BCST) applications with spot-spray (SS) herbicide applications using a commercial-sized ONE SMART SPRAY sprayer. Images were obtained from two soybean fields in 2021 containing *A. palmer*i infestations and were annotated with bounding boxes to identify both *A. palmeri* and soybean plants. In this study, the YOLOv5 object detection algorithm was identified as having the highest mean average precision scores and was therefore selected for further analysis. The precision, recall, and F1 evaluation metrics found for the test image dataset was 0.71, 0.70, and 0.71, respectively. Regression analysis revealed that our trained YOLOv5 model evaluation metrics were higher when identifying *A. palmeri* plants 2 cm in height at low plants m^{-2}. For the second objective, corn (*Zea mays* L) and soybean field trials were conducted in Manhattan, KS and Seymour, IL with the research-sized ONE SMART SPRAY. Simultaneous herbicide applications of residual BCST + foliar SS, base-rate foliar BCST + SS “Spike” rates, and SS

only were compared in corn (*Zea mays* L.) and soybean trials. Specific SS thresholds tested included an herbicide efficacy, balanced, savings, and traditional BCST applications were tested for comparison. Results showed that both residual BCST + foliar SS and "Spike" approaches provided weed-free area not different than traditional broadcast applications, in many cases. The greatest savings were achieved by SS only applications, but weed-free area was almost always significantly less than for other treatments. Simultaneous BCST + SS of soil residual and foliar herbicides, respectively, provided the most weed-free area with the greatest cost savings for both crops. Thirdly, we tested a commercial-sized ONE SMART SPRAY and compared traditional broadcast applications with SS only and simulated two-boom/two-tank applications using the foliar base rate + "Spike" approach. Treatments included SS only, low rate BCST + high rate SS, and high rate BCST + low rate SS applications. Results indicated that high rate BCST + low rate SS applications provided the highest weed-free area, but savings were not different from a broadcast application in soybeans. In corn, thresholds were not different, but both applications with BCST applications demonstrated greater weed-free area than SS only treatments. Overall, this research demonstrated that 1) open-sourced object detection algorithms can be custom trained to identify *A. palmeri* in soybean crops, with opportunities to train and identify other weed species in other crops, 2) intelligent AI sprayers show potential in providing weed-free area comparable to traditional BCST applications, especially systems that utilize two-tank/two-boom technology for simultaneous BCST and SS applications, and 3) herbicide costs were significantly reduced for SS applications compared to traditional BCST applications.

Use of artificial intelligence to locate and treat weeds in Midwestern United States corn (*Zea mays*) and soybean (*Glycine max*) cropping systems

by

Isaac Harrison Barnhart

B.S., Sterling College (KS), 2017
M.S., Kansas State University, 2020

A DISSERTATION

submitted in partial fulfillment of the requirements for the degree

DOCTOR OF PHILOSOPHY

Department of Agronomy
College of Agriculture

KANSAS STATE UNIVERSITY
Manhattan, Kansas

2024

Approved by:

Major Professor
Johanna Anita Dille

Copyright

Abstract

Site-specific weed management (SSWM) is defined as the process of managing weeds where they are growing as opposed to treating the whole field and treating areas with no weeds. Artificial intelligence (AI), the process of creating intelligent machines, has become a part of everyday life in modern society. Utilizing convolutional neural networks and object detection algorithms, weeds can be distinguished from crops, and herbicide applications can target weeds where they are growing. The objectives of this dissertation were to 1) train open-sourced object detection algorithms to detect in central Kansas soybean (*Glycine Max* [L.] Merr.) fields, focusing on Palmer amaranth (*Amaranthus palmeri* S. Watson, henceforth denoted as *A. palmeri*), 2) determine herbicide efficacy and cost savings of SSWM herbicide applications using a ONE SMART SPRAY sprayer, an intelligent dual-boom sprayer using AI technology to locate and spray weeds growing within crops, and 3) compare traditional broadcast (BCST) applications with spot-spray (SS) herbicide applications using a commercial-sized ONE SMART SPRAY sprayer. Images were obtained from two soybean fields in 2021 containing *A. palmer*i infestations and were annotated with bounding boxes to identify both *A. palmeri* and soybean plants. In this study, the YOLOv5 object detection algorithm was identified as having the highest mean average precision scores and was therefore selected for further analysis. The precision, recall, and F1 evaluation metrics found for the test image dataset was 0.71, 0.70, and 0.71, respectively. Regression analysis revealed that our trained YOLOv5 model evaluation metrics were higher when identifying *A. palmeri* plants 2 cm in height at low plants m^{-2}. For the second objective, corn (*Zea mays* L) and soybean field trials were conducted in Manhattan, KS and Seymour, IL with the research-sized ONE SMART SPRAY. Simultaneous herbicide applications of residual BCST + foliar SS, base-rate foliar BCST + SS “Spike” rates, and SS only were

compared in corn (*Zea mays* L.) and soybean trials. Specific SS thresholds tested included an herbicide efficacy, balanced, savings, and traditional BCST applications were tested for comparison. Results showed that both residual BCST + foliar SS and "Spike" approaches provided weed-free area not different than traditional broadcast applications, in many cases. The greatest savings were achieved by SS only applications, but weed-free area was almost always significantly less than for other treatments. Simultaneous BCST + SS of soil residual and foliar herbicides, respectively, provided the most weed-free area with the greatest cost savings for both crops. Thirdly, we tested a commercial-sized ONE SMART SPRAY sprayer and compared traditional broadcast applications with SS only and simulated two-boom/two-tank applications using the foliar base rate + "Spike" approach. Treatments included SS only, low rate BCST + high rate SS, and high rate BCST + low rate SS applications. Results indicated that high rate BCST + low rate SS applications provided the highest weed-free area, but savings were not different from a broadcast application in soybeans. In corn, thresholds were not different, but both applications with BCST applications demonstrated greater weed-free area than SS only treatments. Overall, this research demonstrated that 1) open-sourced object detection algorithms can be custom trained to identify *A. palmeri* in soybean crops, with opportunities to train and identify other weed species in other crops, 2) intelligent AI sprayers show potential in providing weed-free area comparable to traditional BCST applications, especially systems that utilize two-tank/two-boom technology for simultaneous BCST and SS applications, and 3) herbicide costs were significantly reduced for SS applications compared to traditional BCST applications.

Table of Contents

List of Figures

List of Tables

Acknowledgements

My time as a Ph.D. student/candidate has been incredible. I never thought that I would enjoy the experience as much as I did, but I can now say for certain that I did. It was interesting starting a Ph.D. in the middle of a pandemic, seeing the university transition from a completely remote environment to finishing my degree in a normal, face-to-face setting. This and the experiences that went with them are events that I will be able to talk about for the rest of my life!

I want to sincerely thank my advisor Dr. Anita Dille for all her support, dedication, and professionalism throughout the process. Dr Dille never takes advantage of her students, and I can say with absolute certainty that she cares for her students and wants nothing more for them to succeed. I also appreciated her management style, letting me manage my own time while never doubting that I would get the work done. Also, she made herself available for me and other students to come and ask questions, which was very nice. I could not have done any of this without her support, and for that, I sincerely thank her.

I would like to thank Dr. Greg Robert Kruger for his mentorship through the years. Dr. Kruger was the driving force behind the academic-industry ONE SMART SPRAY collaboration, so I have him to thank in large part for organizing the team that enabled me to develop my skillsets in teamwork, collaboration, and data analysis. This partnership was like nothing else I experienced in my graduate program; it gave me the opportunity to work with industry and allowed me to work with something which I have become very passionate about. Through this work, I have met and established professional relationships that will be with me throughout the rest of my career. I thank him not only for his support in this project, but also for taking the time to talk to me and to give me advice regarding a future career.

On that note, I would like to extend my thanks to those who worked on that collaboration. Thanks to Dr. Chris Proctor for allowing me to work with him to test commercial sized ONE SMART SPRAY machines in Nebraska. I learned what it takes to establish and evaluate on-farm research trials through this partnership. Chris has been very supportive, patient, knowledgeable, and has been a joy to work with. I would like to thank Dr. Rodrigo Werle for his mentorship; while we didn't physically work together, we have corresponded and shared ideas multiple times, and he has given me multiple references. I am very thankful for that. Special thanks to Kalvin Miller, whom I worked directly with in establishing the small plot trials in Kansas and Illinois. Kalvin and I spent many hours together making sure that the correct treatments were applied on the correct plots. Without Kalvin's knowledge, expertise, and connections, this project would have fallen flat. Special thanks to Dr. Andrew Hunt, BASF data analyst responsible for the North American ONE SMART SPRAY trials. Andrew gave me access to raw data and provided me feedback that helped me develop my data analysis skills to where they are today. I learned a lot from him, and he was more than willing to help both myself and others on multiple occasions. Finally, I would like to thank Thiago Vitti and Zaim Ugljic, both of whom are currently graduate students from the University of Lincoln-Nebraska and the University of Wisconsin-Madison, respectively. Thiago and I spent many hours working together in the Nebraska experiment sites, and I have come to appreciate him as a colleague and friend. He is very knowledgeable, works very hard, and has been a tremendous help to me and everyone around me. I would like to sincerely thank him for that. I have also greatly enjoyed getting to know Zaim, and while the distance between our trials was a bit too far to travel to, I greatly enjoyed working with him and conversing with him about various agronomic subjects. To both

of you, I am very thankful that our paths crossed, and I greatly anticipate working with you in the future!

I am very thankful for Russell Dille and Dustan Ridder, both of whom work for the Kansas State research farms at Ashland Bottoms and the North Farm here in town. I sincerely appreciate Dustan's help in getting these experiment sites established. I wish to thank Russell for working with me on this and almost everything else, from helping with experiment establishment, harvest, and for being so supportive throughout the entire process. I greatly appreciated working with both of you. Also, an additional thanks to Jane Lingenfelser for allowing me to use her truck to transport farm equipment. Additionally, she let me use her tractor and planter in 2023, which was a huge help. A special thanks to Dr. Peter Tomlinson for allowing me to use his RGN tractor trailer to transport equipment on. Lastly, I wish to thank Chris Weber for his hard work and dedication to helping the weed science graduate students during his time as an assistant scientist for the KSU Weed Extension program. He is truly selfless and has contributed so much to so many.

I would like to extend a special thanks to the landowners who allowed us to do research on their land. This includes Eric Lund (Salina, KS) and Alan Hildebrand (Junction City, KS).

Additionally, I would like to thank my supervisory committee: Dr. Kraig Roozeboom, Dr. Douglas Goodin, and Dr. Sarah Lancaster. I wish to thank Drs. Roozeboom and Lancaster for the use of their farm equipment, and Dr. Goodin for the use of his computer to help train my AI models.

Lastly, I am thankful for every current and former graduate student I have had the pleasure of working with. Your friendship, assistance, and support throughout this process has meant/means the world to me. This includes Dr. Ednaldo Borgato, Tyler Meyeres, Monica

Marrs, Chad Lammers, Ethan Denson, Alec Adam, Alex Hewitt, Lily Ziehmer, Joanna Schroeder de Souza, and Sachin Dhanda. Additional thanks to Luke Chism, who has continued to support and befriend me even after starting work outside of Kansas State, and for the many hundreds of hours spent teaching me how to hunt, fish, trap, and garden. I have enjoyed getting to know all of you, and hope that our paths can cross again!

I have had so many wonderful interactions in this short time during my Ph.D., and I would like to say again that I am extremely thankful for each one of you. My graduate school experience would not have been the same without you!

Dedication

"Trust in the Lord with all your heart and lean not on your own understanding; in all your ways acknowledge Him, and He will make your paths straight." ~ Proverbs 3:5-6

"Delight yourself in the Lord, and He will give you the desires of your heart." ~ Psalm 37:4

This dissertation is dedicated to my Lord and Savior Jesus Christ, who has blessed me with so many wonderful opportunities during my Ph.D. I wish to glorify, honor, and praise Him with all that I think, say, and do.

I would like to dedicate this dissertation also to my wife, Claire. I am very grateful for her love and support throughout all this process. For over 3 years now, she has worked to put me through school, and I will be forever grateful for this. I love you very much and look forward to holding our son or daughter very soon!!

Lastly, I wish to dedicate this dissertation to my immediate family: My father (Kurt), mother (Anita), and my sister (Evelyn). Thank you for your love, support, and prayers. I love you all very much.

Preface

Before coming to Kansas State University to earn my graduate degrees, I had the opportunity to work as a custom pesticide/fertilizer applicator and tractor trailer driver in central Kansas. Even though I had previous experience working as a farm hand and doing farm-related work, this was the position that inspired my interest in agronomy, specifically weed control. Having operated a variety of row-crop sprayers and liquid/dry application systems over thousands of acres, I had the opportunity to learn the business first-hand. I became familiar with herbicides, insecticides, fungicides, spray adjuvants, both dry and liquid fertilizer products, and lime applications.

It was during this time that I noticed the large quantities of pesticides that were applied to our cropping systems. I especially took an interest in herbicides, as herbicides constituted most of my pesticide applications. This was not only my experience, but is the experience of many agricultural professionals, as herbicides make up the largest category of pesticide applications around the world. Although these applications are necessary to prevent costly yield losses, I became aware just how expensive these applications were for farmers. During the time I spent in the cab of the application tractors, I began to wonder if there were ways that could reduce the quantity of herbicides applied. 'Surely,' I thought, 'there has to be a way to help reduce herbicide waste, environmental contamination, and input expenses for farmers.'

Fast-forwarding to 2020, when I had the opportunity to begin my Ph.D. studies, I became especially interested in artificial intelligence (AI) and how it could be used for precision weed management. Many researchers were (and remain) excited about it because of the opportunities to identify weeds using a concept that has potential to be superior to previous electronic means of weed identification. However, the concept was still very new, and was very limited in terms of

practical uses for farmers. To illustrate the infancy, it wasn't until a research team led by Alex Krizhevsky, Ilya Sutskever, and Geoffrey Hinton released AlexNet in 2012 that people realized that AI for image classification (and later, object detection) was, in fact, practical. Since AlexNet, the AI options for visual object identification have exploded, including for precision weed detection.

When we began this research, we wanted to determine if it was feasible to train AI object detection algorithms on pictures of weeds collected in central Kansas, and how accurate they would be when making detections. To keep this process as simple as possible, we focused only on one weed species and one crop. Although the idea behind this was practical, it was still difficult to practically use this algorithm because we had no knowledge of how to build an intelligent sprayer and how to deploy the model for weed detection. Fortunately, we were able to form a partnership with BASF®, giving us the opportunity to test their novel Smart Sprayer. This sprayer has since become known as the ONE SMART SPRAY, stemming from the joint venture of Bosch® and BASF® that came together to build these sprayers. Although we did not use our specific algorithm that we trained, the process of training our algorithm contributed greatly to our understanding of how the ONE SMART SPRAY system makes detections. If we had not embarked upon this first project, we would have been at a great disadvantage in terms of fully understanding and appreciating the ONE SMART SPRAY research project.

The dissertation that follows highlights the results of my Ph.D. work that I have become very passionate about. I am very grateful to my adviser, Dr. Anita Dille, for supporting my endeavors in these projects, as well as all those who participated in the academic-industry collaboration that allowed us to conduct this research. I am also very grateful to be a part of a collaboration that never lost sight of the end goal, which was to help farmers control weeds while

helping farmers reduce herbicide costs and thus, help to increase cropping system profitability. The results obtained in this research were very encouraging and illustrate that the future is bright for AI and precision weed management. My dream is that this technology will one day become available to farmers across the world, as it would greatly help to increase sustainability and ensure cropping system productivity for generations to come. For those reading this preface, I challenge you to pick up the research baton that I am handing off and continue to make great strides to help this dream become a reality!

Chapter 1 - Literature review

1.1 Artificial intelligence, machine learning, and neural networks: an overview

Artificial Intelligence (AI) is defined as the science behind producing and creating intelligent machines (McCarthy 2007). These AI machines are modeled after the human brain and are programmed to make decisions as the mind does (Boden 1996). AI was first proposed in the 1950s by Alan Turing when he published an article entitled "Computing Machinery and Intelligence" (Turing 1950), in which he described a test (known as the 'Turing Test') to determine whether computers could imitate human intelligence (Haenlein and Kaplan 2019; Kaul et al. 2020). Between 1964 and 1966, Joseph Weizenbaum created ELIZA, a language processing tool that could simulate human conversation and was one of the first programs able to pass the Turing Test (Haenlein and Kaplan 2019). Another example of early AI innovation is the "General Problem Solver" program created by Herbert Simon, Cliff Shaw, and Allen Newell (Haenlein and Kaplan 2019). Today, AI is characterized mostly by complicated neural networks and deep learning programs. What began as a series of "if-then" statements has developed into complex algorithms that have found their way into almost every aspect of modern society (Kaul et al. 2020).

Modern-day AI comes in many forms, ranging from (but not limited to) self-driving cars, personal assistants on smart phones (i.e. "Siri"), online chatbots, conversationalist AI such as ChatGPT (OpenAI 2023), and self-checkout technology at the grocery store. These systems can "learn" by discovering patterns and automatically generating insights by using machine learning (ML) (Kelly 2023). Machine learning is defined as algorithms that emulate human intelligence by making inferences from the surrounding environment (El Naqa and Murphy 2015). Global

data is expected to reach 175 zettabytes (1.75×10^{14} gigabytes) by 2025 (Reinsel et al. 2018); this accumulation of "Big Data" must be processed with ML methods because older, traditional methods will quickly be overwhelmed by these data (Oracle 2022).

Deep learning (DL) is a subcategory of ML that provides AI systems with the ability to learn by using networks that resemble a human brain's neural networks (Kelly 2023). These networks can make sense of patterns, trends, noise, and sources of confusion in data (Kelly 2023). These networks are often referred to as artificial neural networks (ANNs) due to their similarities to the human brain (Tavanaei et al. 2019). Just as in the human brain, these neural networks are made up of connected neurons. Input neurons are activated through environmental stimuli, and other neurons are activated as a result (Schmidhuber 2015). Artificial neural networks can therefore learn complicated and often non-linear relationships and solve problems that traditional computing cannot (Basu et al. 2010). Different ANNs are often used for speech recognition, image classification, facial recognition software, medical diagnostics, and even fraud detection (Akash 2023; Kalita 2022).

One of the most well-known ANN applications is image recognition via computer vision (Akash 2023). A breakthrough for image classification came in 2012, when AlexNet (Krizhevsky et al. 2012) was used in the ImageNet Large Scale Visual Recognition Challenge, or ILSVRC (Standford University 2020; Tavanaei et al. 2019). AlexNet won the competition and was the first successful application of DL, thereby demonstrating that DL was in fact practical (Briggs and Carnevali 2023). AlexNet is a deep convolutional neural network (DCNN, also known as convolutional neural networks, or CNNs), consisting of eight layers of neurons and a total of 60 million parameters (Tavanaei et al. 2019). DCNNs are a specialized type of ANN for computer vision (Meel 2023) and analyze imagery by passing input imagery into arrays and assigning a

likelihood of the image belonging to a certain class (Chatterjee 2019). DCNNs are used for image problems instead of ANNs because ANNs are unable to extract complicated image features (Mwiti 2022). The input arrays are passed through several convolutional, activation, pooling, and fully connected layers prior to making a classification decision (Chatterjee 2019). Interestingly, DCNNs were developed based on working neurons of animal visual cortexes, allowing computers to "see" and classify imagery as humans do (Chatterjee 2019). In addition to image classification, DCNNs have been used for speech recognition (Nassif et al. 2019), text recognition (Wang et al. 2012), and object detection (Dhillon and Verma 2020).

1.2 Site-specific weed management

In most situations, weed infestations left uncontrolled cause more crop losses than insects, fungi, or other pests (Gharde et al. 2018). For instance, weed interference in corn production has been estimated to cause 50% yield loss annually, valued at $26.7 billion (Soltani et al. 2016), and soybean annual yield losses due to weeds has been valued at $16.2 billion (Soltani et al. 2017). Weeds are ideally managed using a "zero tolerance" strategy because even one weed escape can produce many seeds and contribute to many more years of weed infestations (Barber et al. 2015). Herbicides are the most frequently used tool in the United States for weed control, costing growers between $4 and 5 billion each year (Atwood and Paisley-Jones 2017). However, the number of herbicide-resistant weeds is continually increasing, with 518 unique cases confirmed as of April 2023 (Heap 2023). Because herbicides are usually applied via whole-field broadcast applications, overapplications of herbicides have been linked with rises in occurrence of herbicide resistance, human and animal health risks, environmental pollution, and increased input costs for farmers (Ferreira et al. 2019).

To reduce herbicide overapplications and the problems that come with it, herbicide applications should focus on targeting weeds where they are growing in the field rather than broadcast applications throughout the whole field. This practice is a component of site-specific weed management (SSWM), which is defined as the process of "varying weed management within a crop field to match the variation in location, density, and composition of the weed population" (Fernández-Quintanilla et al. 2018; Wiles 2009). SSWM for precision herbicide spraying has been the focus of many weed scientists and engineers for more than 30 years (Swinton 2005). In the early days of SSWM, fields were mapped manually by superimposing a grid on a field and measuring weed densities at pre-determined points (Weis and Sökefeld 2010). Weed densities at each location were sampled via quadrats, and spray maps could be generated to either activate or deactivate nozzles or vary the rate of herbicides applied. Although this has been shown to effectively control weeds in some studies, it is a very labor-intensive and time-consuming process that is not economically advantageous as compared to whole field broadcast applications (Rider et al. 2006).

SSWM has also been accomplished using aerial imagery and remote sensing. Satellite imagery has been used to identify weed infestations, but often insufficient spatial resolution makes this challenging at field-level (Casady et al. 2005; Weis and Sökefeld 2010). A new opportunity for high-resolution weed detection arose when commercial-grade unmanned aerial vehicles (UAVs) started to gain popularity in the mid-2010s (Alkobi 2019). Lower-cost sensors could be mounted to these autonomous UAVs, allowing for very high spatial and temporal resolution data to be collected. UAVs have been found to be more accurate when compared to traditional weed scouting (Rasmussen et al. 2018; Rozenberg et al. 2021), as UAV imagery can capture discrete weed density data over a large area without being subject to human

interpretation errors. Rosenberg et al. (2018) found that images collected using low-cost UAV systems could distinguish weeds from onion crops using maximum likelihood and support vector machine classification. Jurado-Expósito et al. (2021) used UAV imagery and ground-sampled weed density data to create management maps using cokriging. Sapkota et al. (2020) used UAV data to identify cotton (*Gossypium hirsutum* L.) crop rows using the Hough transformation and classify weeds using object-based classifications. In Castaldi et al. (2017), UAV imagery was used to identify weeds and to create a patch-spraying map, which was uploaded to a precision sprayer for targeted applications. Using this method, the authors observed significant herbicide savings. Through using high-resolution imagery captured with UAVs, weeds have been successfully detected and mapped for both fallow and in-crop situations.

1.3 Deep convolutional neural networks in site-specific weed management

A major component of SSWM includes using AI through DCNNs for weed detection. DCNNs can be trained on custom image datasets using the processes of transfer learning (Roman 2020). Transfer learning involves taking information used in one problem to solve another, similar problem (Ghazi et al. 2017). Typically, this involves using pre-trained models such as the ResNet (Keras 2023a) or VGG (Keras 2023b) models, which are trained on very large datasets such as the Microsoft Common Objects in Context database (Lin et al. 2014). During transfer learning, the model weights are updated using a different image database, thus allowing different image problems to be solved. Transfer learning is usually preferred rather than training DCNNs from scratch, with the latter being very complicated and time-consuming (Ruder 2021).

There are two main uses of DCNNs for weed detection: Image classification and object detection. Image classification consists of assigning a single class to an input image (Vadapalli

2020). A simple example that is often referred to is the 2013 “Dogs vs. Cats” Kaggle competition that required contestants to use a DCNN to correctly classify images of dogs and cats (Kaggle 2013). Many studies have shown that weeds can be detected using image classification. Yu et al. (2020) used AlexNet, GoogLeNet (Szegedy et al. 2014), and VGGNet (Simonyan and Zisserman 2015) and concluded that VGGNet detected crabgrass species (*Digitaria* spp.), doveweed (*Murdannia nudiflora* L. Brenan), dallisgrass (*Paspalum dilatatum* Poir.), and tropical sungrass (*Urochloa distachya* L. T.Q. Nguyen) with an overall accuracy of 1, or 100%. In a similar study, Yu et al. (2019) found that VGGNet accurately classified spotted spurge (*Euphorbia macualta* L.), ground ivy (*Glechoma hederacea* L.), and dandelion (*Taraxacum officinale* Web.) in perennial ryegrass (*Lolium perenne* L.) turfgrass imagery with high accuracy. Subeesh et al. (2022) found that when comparing AlexNet, GoogLeNet, InceptionV3 (Szegedy et al. 2015), and Xception (Chollet 2017) networks for weed detection in bell peppers (*Capiscum annum* L.), the InceptionV3 model performed superiorly. Additionally, Peteinatos et al. (2020) used 93,000 images to train VGG16 (Simonyan and Zisserman 2015), ResNet-50 (He et al. 2015), and Xception models for weed detection in corn (*Zea mays* L.), sunflower (*Helianthus annuus* L.), and potato (*Solanum tuberosum* L.) crops. They observed varying levels of success among the models, with accuracy rates between 77 and 98%.

A major shortfall of weed classification is that classification does not locate individual weeds in an image. Because detecting and localizing pests is more applicable than classifying images of pests (Chen et al. 2021), DCNN object detection is often preferred over image classification. Object detection refers to computer vision tasks that localize and identify objects in digital images (Brownlee 2021). Multiple free and open-sourced object detection models are available for use, including the You Only Look Once (YOLO)-series models, which were first

introduced by Redmon et al. (2016). The YOLO models are single-stage object detectors, localizing and classifying objects in a single pass of the neural network (Barnhart et al. 2022; Forson 2017). At the present time, more recent releases of the YOLO-series models are YOLO version 8 (YOLOv8), (Ultralytics 2023) and YOLO-World (Liu et al. 2024). Other single-stage models include the Single Shot Detection (SSD) models (Liu et al. 2016), SqueezeDet (Wu et al. 2019), and the DetectNet (Tao et al. 2016) models (Hollemans 2018). In contrast, two-stage object detectors localize objects and classify the localized objects in two separate stages (Boesch 2023). Widely used two-stage object detection models include the regional convolutional neural network (R-CNN) models such as Fast R-CNN (Girshick 2015), Faster R-CNN (Ren et al. 2016), and Mask R-CNN (He 2018). In general, single-stage object detectors can detect objects faster than two-stage detectors, but two-stage detectors are generally more accurate (Boesch 2023). However, this is not always the case, as YOLO models have been shown to outperform two-stage object detectors in some situations (Barnhart et al. 2022; Chen et al. 2021). Several models such as YOLOv8 provide different sizes of models with different detection accuracies and inference speeds. For instance, YOLOv8n has a mean average precision (mAP) of 37.3 and an inference speed of 80.4 ms, whereas YOLOv8x has a mAP and an inference speed of 53.9 and 479.1 ms, respectively (Ultralytics 2023). Smaller models can be useful for smaller platforms with less computing power (Hussain et al. 2020; Xiao et al. 2019), whereas larger, more powerful computational systems are better suited for larger models with slower inference speeds.

Object detection evaluation metrics include precision, recall, mean average precision (mAP), and F1 scores. Prior to computing these metrics, an Intersection over Union (IoU) threshold must be chosen. IoU is a number from 0 to 1 which indicates the percentage of overlap between detected objects and ground truth bounding boxes (Hofesmann 2020). IoU thresholds

between 0.5 and 0.75 are the most common (Vijayabhaskar 2020), with many weed detection studies selecting a threshold of 0.5 (Fatima et al. 2023; Jiang et al. 2019; Thanh Le et al. 2021). IoU thresholds are used to compute true positive (TP), false positive (FP), and false negative (FN) detections. Detections with overlap percentages below the chosen threshold are FP detections, whereas detections above the thresholds are TP detections (Henderson and Ferrari 2017). FN detections are objects with ground truth bounding boxes but do not have any detection bounding box overlap. Precision is the quotient of the number of TP predictions divided by the total number of TP + FP predictions (Barnhart et al. 2022; Hussain et al. 2021). When a model makes a low number of TP predictions or a high number of FP predictions, precision scores are reduced (Gad 2021). Recall is computed by dividing the TP by the sum of the TP and FN detections. Recall measures how well a model identifies TP predictions; higher recall scores indicate more TP detections (Barnhart et al. 2022; Huilgol 2020; Hussain et al. 2021). A model's F1 score is the harmonic mean between precision and recall (Barnhart et al. 2022; Zhong et al. 2019). F1 scores demonstrate the model's ability to capture both TP values (recall) and to also be accurate (precision) (Allwright 2022). Precision, recall, and F1 values range from 0 to 1, with 0 and 1 being the worst and best scores, respectively. The average precision (AP) is determined by graphing the precision-recall curve for each object detection class, and the average of the AP scores is the main average precision (mAP) for the model (Barnhart et al. 2022). mAP scores range from 0 to 1, with higher scores indicating better model performance.

Object detection has been used to identify weeds in many studies. In Barnhart et al. (2022), the authors achieved a mAP of 0.77 when using YOLOv5 (Ultralytics 2022) to identify Palmer amaranth (*Amaranthus palmeri* S. Watson) in soybeans (*Glycine max* L. Merr.). Ahmad et al. (2021) found that YOLOv3 (Redmon and Farhadi 2018) was fast and accurate for

localizing and detecting weeds, but achieved relatively low AP scores of 43.28%, 26.30%, 89.89%, and 57.8% for common cocklebur (*Xanthium strumarium* L.), foxtail species (*Setaria* spp.), redroot pigweed (*Amaranthus retroflexus* L.), and giant ragweed (*Ambrosia trifida* L.), respectively. Additionally, the overall mAP score was 54.3% and relatively low. Sharpe et al. (2020) used YOLOv3 to identify grasses, sedges, and broadleaves with F1 scores of 0.96, 0.96, and 0.93, respectively. When trying to detect hedge bindweed (*Convolvulus sepium* L. var. *americanus* Sims) in sugar beets (*Beta vulgaris* L.), Gao et al. (2020) found that YOLOv3 detected sugar beets well (AP = 0.938) but struggled to detect hedge bindweed (AP = 0.726). Finally, Sivakumar et al. (2020) found that late-season weed escapes in soybean crops could be detected with Faster R-CNN and SSD models; Faster R-CNN was determined to be the best-performing model in this study. The authors also noted that by reducing Faster R-CNN (a two-stage detector) to 200 proposals, the inference speed could be as fast as SSD, thus combining speed and accurate weed detections. Recently, and after the publication in Chapter 2, YOLOv8 has been used to identify Caosu (*Phlomoides umbrosa* (Turcz.) Kamelin & Makhm) (Guo et al. 2023) and undefined crops and weeds (Kumar et al. 2024). Guo et al. (2023) achieved success identifying Caosu with precision, recall, mAP50, and F1-scores of 91.1%, 86.7%, 92.6%, and 88.85%, respectively, and Guo et al. (2023) claimed to achieve an accuracy of 86% in crop and weed identification in a "real-time agricultural environment." These examples show that weed detection with object detection DCNNs is both possible and feasible with modern technologies.

After object detection models have been trained and evaluated, they can be deployed on a variety of weed control platforms. These platforms range from precision sprayers, robots, and UAV systems. Hussain et al. (2020) trained both YOLOv3 and tiny-YOLOv3 (Adarsh et al. 2020) to identify common lambsquarters (*Chenopodium album* L.) and potato and uploaded the

trained tiny-YOLOv3 model to a prototype precision sprayer developed by their team. The authors reported an herbicide savings of 42% during trials. Ruigrok et al. (2020) trained a YOLOv3 model to detect volunteer potatoes growing in sugar beet fields, uploaded the trained model to a precision spraying robot, and reported 96% of the volunteer potatoes sprayed while only incorrectly spraying 3% of the sugar beet crop. This methodology is not only limited to weed control; for example, Mustafid et al. (2022) trained an SSD Mobilenet V3-small (pkulzc 2019) model to detect cabbage (*Brassica oleracea* L.) plants. The model was uploaded to a robotic sprayer so that crop protection products such as insecticides and fungicides were applied only to the cabbages. The robotic sprayer used a Raspberry Pi 4 (Raspberry Pi 2023), a relatively inexpensive processor that can allow such sprayers to be constructed at a lower cost. The authors reported an average cabbage detection accuracy of 88%, with an average accuracy of spraying position reported as 80%.

1.4 Commercial AI application equipment

Commercial field sprayers that enable SSWM have been on the market for several years; however, these systems utilize multispectral sensing rather than artificial intelligence. For example, companies such as Weed-It® (Weed-It, 7221 CJ Steenderen, The Netherlands) manufacture external sensors that can be retrofitted to existing commercial sprayers and can activate and deactivate nozzles/boom sections when weeds are detected. These sensors typically use vegetative indices such as the Normalized Difference Vegetation Index (Kriegler et al. 1969), which detects plant vegetation by subtracting the near infrared (NIR) band from the red radiation band, divided by the NIR band plus the red band of the electromagnetic spectrum (Huang et al.

2020). However, these systems are limited in that they detect only green vegetation, thereby limiting spraying options to fallow applications (Weed-It 2023).

In addition to multispectral-powered field sprayers, sprayers powered by AI for in-crop applications are becoming available on the market. These sprayers include the ONE SMART SPRAY (ONE SMART SPRAY 2023), the John Deere® See & Spray™ Ultimate (John Deere 2023), and Greeneye Technology™ sprayers (Greeneye Technology 2023a). These companies differ from one another slightly in that the ONE SMART SPRAY and See and Spray™ Ultimate are factory-fitted with AI application equipment, whereas sprayers are retrofitted with Greeneye™ equipment and thereby upgrade existing sprayers with spot-spraying capabilities (Greeneye Technology 2023b). These sprayers are different than the Weed-it® system in that they are capable of both fallow (green on brown) and in-crop (green-on-green) site-specific herbicide applications. By using an approach such as crop row removal or object detection, weeds can be located by the sprayers' AI systems and targeted for herbicide application within the field, thus reducing the need for whole-field applications (Rai et al. 2023).

1.5 Dissertation objectives

AI has been shown to be effective in identifying and locating weeds in many agronomic and horticultural cropping systems, including but not limited to corn and soybeans (Ahmad et al. 2021), sugar beet (Gao et al. 2020), lettuce (*Lactuca* L.) (Osorio et al. 2020), and bermudagrass (*Cynodon dactylon* (L.) Pers.) turf crops (Yu et al. 2020). AI is a rapidly changing field (Pan 2016), with advances, upgrades, and new algorithms seemingly released every day. Because of this, AI-empowered weed control is also changing, thus making it critical to evaluate these new technologies to better understand how they can influence weed control. Two very important

pieces to this are (1) the backbone AI algorithm(s), and (2) commercial AI herbicide application systems. Commercial sprayers utilize AI algorithms to recognize and treat weeds, so understanding how both fit into agronomic cropping systems is very important. The overall objective of this dissertation is to evaluate how well AI weed control tools can detect and control weeds using open-sourced object detection algorithms and a commercial AI sprayer. For chapter 2, we focused on detecting Palmer amaranth (*Amaranthus palmeri* S. Watson) in soybean, as *A. palmeri* is frequently designated as the most problematic weed in the United States (WSSA 2016). In chapters 3 and 4, we switch from an algorithm focus to an evaluation of a commercial AI field sprayer, using a ONE SMART SPRAY sprayer. Thus, specific objectives of chapters 2, 3, and 4 were to:

Chapter 2:

1. Develop an annotated image database of *A. palmeri* and soybean with multiple weed densities and soybean row spacings that can be used to fine-tune object detection algorithms.
2. Compare multiple open-source algorithms' effectiveness in detecting *A. palmeri*.
3. Evaluate the relationship between *A. palmeri* growth features (diameter, height, density, and ground cover) and *A. palmeri* detection ability.

Chapter 3:

1. Evaluate the weed control efficacy of different commercial AI sprayer herbicide treatment programs, including one-pass versus two-pass programs, spot-sprayed treatments only, and simultaneous broadcasted residual and spot-sprayed foliar herbicides.
2. Determine if sensor weed detection threshold settings influences weed control.

3. Determine the seasonal cost for each herbicide program, comparing each with a traditional broadcast treatment.

Chapter 4

1. Evaluate the weed control efficacy of a commercial AI field sprayer using a two-tank simulated approach versus a traditional broadcast and a spot spray only approach (using a commercial-sized field sprayer).
2. Determine herbicide cost savings using treatments with spot spray applications applied with commercial field sprayers.

1.6 References

Adarsh P, Rathi P, Kumar M (2020) YOLOv3-Tiny: Object detection and recognition using one stage improved model." Pages 687-694 *in* Proceedings from the 6th International Conference on Advanced Computing and Communication Systems. Coimbatore, India: Institute of Electrical and Electronics Engineers

Ahmad A, Saraswat D, Aggarwal V, Etienne A, Hancock B (2021) Performance of deep learning models for classifying and detecting common weeds in corn and soybean production systems. Comput Electron Agric 184:106081

Akash S (2023) Top 10 applications of artificial neural networks in 2023. Available online: https://www.analyticsinsight.net/top-10-applications-of-artificial-neural-networks-in-2023/. Accessed: March 29, 2023

Alkobi J (2019) The evolution of drones: From military to hobby & commercial. Available online: https://percepto.co/the-evolution-of-drones-from-military-to-hobby-commercial/. Accessed: March 30, 2023

Allwright S (2022) How to interpret F1 score (simply explained). Available online: https://stephenallwright.com/interpret-f1-score/. Accessed: April 4, 2023

Atwood D, Paisley-Jones C (2017) Pesticide industry sales and usage, 2008-2012 market estimates. Washington DC: Environmental Protection Agency. 13 p

Barber TL, Smith KL, Scott RC, Norsworthy JK, Vangilder AM (2015) Zero tolerance: A community-based program for glyphosate-resistant Palmer amaranth management. Little Rock, AR: University of Arkansas Division of Agriculture Research and Extension. 2 p

Barnhart IH, Lancaster S, Goodin D, Spotanski J, Dille JA (2022) Use of open-source object detection algorithms to detect Palmar amaranth (*Amaranthus palmeri*) in soybean. Weed Sci 70:648-662

Basu JK, Bhattacharyya D, Kim T (2010) Use of artificial neural network in pattern recognition. Int J Softw Eng Ap 4:23-34

Boden MA, ed (1996) Artificial Intelligence: Handbook of Perception and Cognition. 2nd edition. San Diego, CA: Academic Press, Inc. XV p

Boesch G (2023) Object detection in 2023: The definitive guide. Available online: https://viso.ai/deep-learning/object-detection/. Accessed: April 3, 2023

Briggs J, Carnevali L (2023) AlexNet and ImageNet: The birth of deep learning. Available online: https://www.pinecone.io/learn/imagenet/. Accessed: March 29, 2023

Brownlee J (2021) A gentle introduction to object recognition with deep learning. Available online: https://machinelearningmastery.com/object-recognition-with-deep-learning/. Accessed: April 3, 2023

Casady GM, Hanley RS, Seelan SK (2005) Detection of leafy spurge (*Euphorbia esula*) using multidate high-resolution satellite imagery. Weed Sci 19:462-467

Castaldi F, Pelosi F, Pascucci S, Casa R (2017) Assessing the potential of images from unmanned aerial vehicles (UAV) to support herbicide patch spraying in maize. Precis Agric 18:76-94

Chatterjee CC (2019) Basics of the classical CNN. Available online: https://towardsdatascience.com/basics-of-the-classic-cnn-a3dce1225add. Accessed: March 30, 2023

Chen JW, Lin WJ, Cheng HJ, Hung CL, Lin CY, Chen SP (2021) A smartphone-based application for scale pest detection using multi-object detection methods. Electronics 10:372

Chollet F (2017) Xception: Deep learning with depthwise separable convolutions. Pages 1251-11258 *in* Proceedings of the 2017 IEEE Conference on Computer Vision and Pattern Recognition. Honolulu, HI: Institute of Electrical and Electronics Engineers

Dhillon A, Verma GK (2020) Convolutional neural network: a review of models, methodologies and applications to object detection. Lect Notes Artif Int 9:85-112

El Naqa I, Murphy MJ (2015) What is Machine Learning? Pages 3-11 *in* El Naqa I, Li R, Murphy MJ, eds. Machine Learning in Radiation Oncology. Switzerland: Springer

Fatima HS, ul Hassan I, Hasan S, Khurram M, Stricker D, Afzal MZ (2023) Formation of a lightweight, deep learning-based weed detection system for a commercial autonomous laser weeding robot. Appl Sci 13:3997

Fernández-Quintanilla C, Peña JM, Andújar D, Dorado J, Riberio A, López-Granados F (2018) Is the current state of the art of weed monitoring suitable for site-specific weed management in arable crops? Weed Res 58:259-272

Ferreira ADS, Freitas DM, da Silva GC, Pistori H, Folhes MT (2019) Unsupervised deep learning and semi-automatic data labeling in weed discrimination. Comput Electron Agr 165:104963

Forson E (2017) Understanding SSD MultiBox—Real-Time Object Detection in Deep Learning. Available online: https://towardsdatascience.com/understanding-ssdmultibox-real-time-object-detection-in-deep-learning-495ef744fab. Accessed: April 3, 2023

Gad AF (2021) Evaluating Deep Learning Models: The Confusion Matrix, Accuracy, Precision, and Recall. Available online: https://www.kdnuggets.com/2021/02/evaluating-deep-learning-models-confusion-matrix-accuracy-precision-recall.html. Accessed: April 4, 2023

Gao J, French AP, Pound MP, He Y, Pridmore TP, Pieters JG (2020) Deep convolutional neural networks for image-based *Convolvulus sepium* detection in sugar beet fields. Plant methods 16:29

Gharde Y, Singh PK, Dubey RP, Gupta PK (2018) Assessment of yield and economic losses in agriculture due to weeds in India. Crop Protec 107:12-18

Ghazi et al. (2017) Plant identification using deep neural networks via optimization of transfer learning parameters. Neurocomputing 235:228-235

Girshick R (2015) Fast R-CNN. arXiv database 1504.08083v2

Greeneye Technology (2023a) Greeneye: Spray less, grow more. Available online: https://greeneye.ag/. Accessed: September 21, 2023

Greeneye Technology (2023b) Introducing Greeneye's selective spraying system, designed for seamless integration and maximum profitability. Available online: https://greeneye.ag/technology/. Accessed: September 21, 2023

Guo B, Ling S, Tan H, Wang S, Wu C, Yang D (2023) Detection of the grassland weed Phlomoides umbrosa using multi-source imagery and an improved YOLOv8 network. Agronomy 13:3001

Haenlein M, Kaplan A (2019) A Brief History of Artificial Intelligence: On the Past, Present, and Future of Artificial Intelligence. Calif Manage Rev 61:5-14

He K, Gkioxari G, Dollár P, Girshick R (2018) Mask R-CNN. arXiv database 1703.06870

He K, Zhang X, Ren S, Sun J (2015) Deep residual learning for image recognition. arXiv database 1512.03385

Heap I (2023) The international herbicide-resistant weed database. Available online: https://www.weedscience.org/Home.aspx. Accessed: March 30, 2023

Henderson P, Ferrari V (2017) End-to-end training of object class detectors for mean average precision. Pages 198–213 *in* Lai SH, Lepetit V, Nishino K, Sato Y, eds. Computer Vision—ACCV 2016. ACCV 2016 (Lecture Notes in Computer Science, Vol. 10115). Cham, Switzerland: Springer

Hofesmann E (2020) IoU a better detection evaluation metric. Available online: https://towardsdatascience.com/iou-a-better-detection-evaluation-metric-45a511185be1. Accessed: April 4, 2023

Hollemans M (2018) One-stage object detection. Available online: https://machinethink.net/blog/object-detection/. Accessed: April 3, 2023

Huang S, Tang L, Hupy JP, Wang Y, Shao G (2020) A commentary review on the use of normalized difference vegetation index (NDVI) in the era of popular remote sensing. J Forestry Res 32:1-6

Huilgol P (2020) Precision vs. Recall—An Intuitive Guide for Every Machine Learning Person. Available online: https://www.analyticsvidhya.com/blog/2020/09/precision-recall-machine-learning/. Accessed: April 4, 2023

Hussain N, Farooque AA, Schumann AW, Abbas F, Acharya B, McKenzie-Gopsill A, Barrett R, Afzaal H, Zaman QU, Cheema MJM (2021) Application of deep learning to detect lamb's quarters (*Chenopodium album* L.) in potato fields of Atlantic Canada. Comput Electron Agric 182:106040

Hussain N, Farooque AA, Schumann AW, McKenzie-Gopsill A, Esau T, Abbas F, Acharya B, Zaman Q (2020) Design and development of a smart variable rate sprayer using deep learning. Remote Sens 12:4091

Jiang Y, Li C, Paterson AH, Robertson JS (2019) DeepSeedling: deep convolutional network and Kalman filter for plant seedling detection and counting in the field. Plant Methods 15:141

John Deere (2023) See & Spray TM Ultimate: Targeted, in-crop spraying. Available online: https://www.deere.com/en/sprayers/see-spray-ultimate/. Accessed: September 21, 2023

John Deere (2023) See & Spray™ Ultimate: Targeted, in-crop spraying. Available online: https://www.deere.com/en/sprayers/see-spray-ultimate/. Accessed: March 30, 2023

Jurado-Expósito M, López-Granados F, Jiménez-Brenes FM, Torres-Sánchez J (2021) Monitoring the spatial variability of knapweed (*Centaurea diluta* Aiton) in wheat crops using geostatistics and UAV imagery: probability maps for risk assessment in site-specific control. Agronomy 11:880

Kaggle (2013) Dogs vs cats. Available online: https://www.kaggle.com/c/dogs-vs-cats. Accessed: March 31, 2023

Kalita D (2022) An overview and application of neural networks. Available online: https://www.analyticsvidhya.com/blog/2022/03/an-overview-and-applications-of-artificial-neural-networks-ann/. Accessed: March 29, 2023

Kaul V, Enslin S, Gross SA (2020) History of artificial intelligence in medicine. Gastrointest Endosc 92:807-812

Kelly K (2023) What is artificial intelligence: Types, history, and future. Available online: https://www.simplilearn.com/tutorials/artificial-intelligence-tutorial/what-is-artificial-intelligence. Accessed: March 29, 2023

Keras (2023a) ResNet and ResNetV2. Available online: https://keras.io/api/applications/resnet/#resnet50-function. Accessed: March 31, 2023

Keras (2023b) VGG16 and VGG19. Available online: https://keras.io/api/applications/vgg/#vgg19-function. Accessed: March 31, 2023

Kriegler FJ, Malila WA, Nalepka RF, Richardson W (1969) Preprocessing transformations and their effect on multispectral recognition. Remote Sens Environ VI:97-132

Krizhevsky A, Sutskever I, Hinton GE (2012) Imagenet classification with deep convolutional neural networks. Adv Neur In 25:1097-1105

Kumar P, Misra U (2024) Deep learning for weed detection: YOLO V8 algorithm's performance in agricultural environments. Pages 255-258 *in* Proceedings of the 2024 2nd International Conference on Disruptive Tecchnologies (ICDT). Greater Noida, India: Institute of Electrical and Electronics Engineers

Lin TY, Marie M, Belongie S, Hays J, Perona P, Ramanan D, Dollár P, Zitnick CL (2014) Microsoft COCO: Common objects in context. Pages 740-755 *in* Fleet D, Pajdla T, Schiele B, Tuytelaars T, eds. Computer Vision – ECCV 2014. Springer, Cham

Liu W, Anguelov D, Erhan D, Szegedy C, Reed S, Fu CY, Berg AC (2016) SSD: Single shot multibox detector. Pages 21-37 *in* Proceedings of the 14th European Conference on Computer Vision, Part 1. Amsterdam: European Conference on Computer Vision.

Cheng T, Song L, Ge Y, Liu W, Wang X, Shan Y (2024) YOLO-World: Real-time open-vocabulary object detection. arXiv 2401.17270

McCarthy J (2007) What is artificial intelligence? Stanford, CA: Computer Science Department, Stanford University. 2 p

Meel V (2023) ANN and CNN: Analyzing differences and similarities. Available online: https://viso.ai/deep-learning/ann-and-cnn-analyzing-differences-and-similarities/. Accessed: March 29, 2023

Mustafid MA, Subrata IDM, Pramuhadi G, Harahap IS (2022) Design and performance test of autonomous precision spraying robot for cabbage cultivation. IOP Conf. Ser: Earth Environ Sci 1038:012044

Mwiti D (2022) Image classification with convolutional neural networks (CNNs). Available online: https://www.kdnuggets.com/2022/05/image-classification-convolutional-neural-networks-cnns.html. Accessed: March 31, 2023

Nassif AB, Shahin I, Attili I, Azzeh M, Shaalan K (2019) Speech recognition using deep neural networks: A systematic review. IEEE Access 7:19143-19165

ONE SMART SPRAY (2023) Smart spraying solution. Available online: https://www.onesmartspray.com/. Accessed: September 18, 2023

OpenAI (2023) ChatGPT. Available online: https://openai.com/blog/chatgpt. Accessed: March 20, 2023

Oracle (2022) The evolution of big data and the future of the data lakehouse. Available online: https://www.oracle.com/a/ocom/docs/big-data/big-data-evolution.pdf. Accessed: March 29, 2023

Osorio K, Puerto A, Pedraza C, Jamaica D, Rodríguez L (2020) A deep learning approach for weed detection in lettuce crops using multispectral images. AgriEngineering 2:471-488

Pan Y (2016) Heading toward artificial intelligence 2.0. Engineering 2:409-413

Peteinatos GG, Reichel P, Karouta J, Andújar D, Gerhards R (2020) Weed identification in maize, sunflower, and potatoes with the aid of convolutional neural networks. Remote Sens 12:4185

Pkulzc (2019) Release MobileNet V3 models and SSDLite models with MobileNet V3 backbone. Github repository available online: https://github.com/tensorflow/models/blob/master/research/object_detection/samples/configs/ssdlite_mobilenet_v3_small_320x320_coco.config (Accessed: 18 September 2023)

Rai N, Zhang Y, Ram BG, Schumacher L, Yellavajjala RK, Bajwa S, Sun X (2023) Applications of deep learning in precision weed management: A review. Comput Electron Agr 206:107698

Rasmussen J, Nielsen J, Streibig JC, Jensen JE, Pedersen KS, Olsen SI (2018) Pre-harvest weed mapping of *Cirsium arvense* in wheat and barley with off-the-shelf UAVs. Precis Agric 20:983-999

Raspberry Pi (2023) Raspberry Pi 4. Available online: https://www.raspberrypi.com/products/raspberry-pi-4-model-b/ (Accessed: 18 September 2023)

Redmon J, Divvala S, Girshick R, Farhadi A (2016) You only look once: Unified, real-time object detection. Pages 779-788 *in* Proceedings from the IEEE Conference on Computer Vision and Pattern Recognition (CVPR). Las Vegas, NV: Institute of Electrical and Electronics Engineers

Redmon J, Farhadi A (2018) YOLOv3: An incremental improvement. arXiv database 1804.02767

Reinsel D, Gantz J, Rydning J (2018) The digitization of the world from edge to core. Framingham, MA: IDC White Paper #US44413318. 3 p

Ren S, He K, Girshick R, Sun J (2016) Faste R-CNN: Towards real-time object detection with region proposed networks. arXiv database 1506.01497

Rider TW, Vogel JW, Dille JA, Dhuyvetter KC, Kastens TL (2006) An economic evaluation of site-specific herbicide application. Precis Agric 7:379-392

Roman V (2020) CNN transfer learning & fine tuning. Available online: https://towardsdatascience.com/cnn-transfer-learning-fine-tuning-9f3e7c5806b2. Accessed: March 31, 2023

Rozenberg G, Kent R, Blank L (2021) Consumer-grade UAV utilized for detecting and analyzing late-season weed spatial distribution patterns in commercial onion fields. Precis Agric 22:1317-1332

Ruder S (2021) Recent advances in language model fine-tuning. Available online: https://www.ruder.io/recent-advances-lm-fine-tuning/. Accessed: March 31, 2023

Ruigrok T, van Henten E, Booij J, van Boheemen K, Kootstra G (2020) Application-Specific Evaluation of a Weed-Detection Algorithm for Plant-Specific Spraying. Sensors 20:7262

Schmidhuber J (2015) Deep learning in neural networks: An overview. Neural Networks 61:85-117

Sharpe SM, Schumann AW, Yu J, Boyd NS (2020) Vegetation detection and discrimination within vegetable plasticulture row-middles using a convolutional neural network. Precis Agric 21:264-277

Simonyan K, Zisserman A (2015) Very deep convolutional networks for large-scale image recognition. arXiv database 1409.1556

Sivakumar ANV, Li J, Scott S, Psota E, Jhala AJ, Luck JD, Shi Y (2020) Comparison of object detection and patch-based classification deep learning models on mid- to late-season weed detection in UAV imagery. Remote Sens 12:2136

Soltani N, Dille JA, Burke IC, Everman WJ, VanGessel MJ, Davis VM, Sikkema PH (2016) Potential corn yield losses from weeds in North America. Weed Technol 30:979-984

Soltani N, Dille JA, Burke IC, Everman WJ, VanGessel MJ, Davis VM, Sikkema PH (2017) Perspectives on potential soybean yield losses from weeds in North America. Weed Technol 31:148-154

Stanford University (2020) ImageNet Large Scale Visual Recognition Challenge (ILSVRC). Available online: https://www.image-net.org/challenges/LSVRC/. Accessed: March 29, 2023

Subeesh A, Bhole S, Singh K, Chandel NS, Rajwade YA, Rao KVR, Kumar SP, Jat D (2022) Deep convolutional neural network models for weed detection in polyhouse grown bell peppers. Artif Intell Agr 6:47-54

Swinton SM (2005) Economics of site-specific weed management. Weed Sci 53:259-263

Szegedy C, Liu W, Jia Y, Sermanet P, Reed S, Anguelov D, Erhan D, Vanhoucke V, Rabinovich A (2014) Going deeper with convolutions. arXiv database 1409.4842

Szegedy C, Vanhoucke V, Ioffe S, Shlens J, Wonja Z (2015) Rethinking the Inception architecture for computer vision. arXiv database 1512.00567

Tao A, Barker J, Sarathy S (2016) DetectNet: Deep neural network for object detection in DIGITS. NVIDIA Developer Technical Blog. Available online: https://developer.nvidia.com/blog/detectnet-deep-neural-network-object-detection-digits/. Accessed: April 3, 2023

Tavanaei A, Ghodrati M, Kheradpisheh SR, Masquelier T, Maida A (2019) Deep learning in spiking neural networks. Neural Networks 111:47-63

Thanh Le VN, Truong G, Alameh K (2021) Detecting weeds from crops under complex field environments based on Faster RCNN. Pages 350-355 *in* Proceedings of the IEEE Eighth International Conference on Communications and Electronics. Phu Quoc Island, Vietnam: Institute of Electrical and Electronics Engineers

Turing A (1950) Computing Machinery and Intelligence. Mind LIX:433-460

Ultralytics (2022) yolov5. Github repository, available online: https://github.com/ultralytics/yolov5. Accessed: April 4, 2023

Ultralytics (2023) YOLOv8 docs. Available online: https://docs.ultralytics.com/. Accessed: April 3, 2023

Vadapalli P (2020) Using convolutional neural networks for image classification. Available online: https://www.upgrad.com/blog/using-convolutional-neural-network-for-image-classification/. Accessed: March 31, 2023

Vijayabhaskar J (2020) A coder's guide to IoU, non-max suppression, and mean average precision. Available online: https://vijayabhaskar96.medium.com/practitioners-guide-to-iou-non-max-suppression-and-mean-average-precision-e09de73a2bd8. Accessed: April 4, 2023

Wang T, Wu J, Coates A, Ng AY (2012) End-to-end text recognition with convolutional neural networks. Pages 3304-3308 *in* Proceedings of the 21st International Conference on Pattern Recognition. Tsukuba, Japan: ICPR2012

Weed-It (2023) Our applications. Available online: https://www.weed-it.com/our-applications. Accessed: September 21, 2023

Weis M, Sökefeld M (2010) Detection and identification of weeds. Pages 119-134 *in* Oerke EC, Gerhards R, Menz G, Sikora R, eds. Precision Crop Protection - the Challenge and Use of Heterogeneity. Springer, Dordrecht

Wiles LJ (2009) Beyond patch spraying: site-specific weed management with several herbicides. Precis Agric 10:277-290

Wu B, Wan A, Iandola F, Jin PH, Keutzer K (2019) SqueezeDet: Unified, small, low power fully convolutional neural networks for real-time object detection for autonomous driving. arXiv database 1612.01051

Xiao D, Shan F, Li Z, Le BT, Liu X, Li X (2019) A target detection model based on improved tiny-yolov3 under the environment of mining truck. IEEE Access 7:123757-123764

Yu J, Schumann AW, Cao Z, Sharpe SM, Boyd NS (2019) Weed detection in perennial ryegrass with deep learning convolutional neural network. Front Plan Sci 10:1422

Yu J, Schumann AW, Sharpe SM, Li X, Boyd NS (2020) Detection of grassy weeds in bermudagrass with deep convolutional neural networks. Weed Sci 68:545-552

Yu J, Schumann AW, Sharpe SM, Li X, Boyd NS (2020) Detection of grassy weeds in bermudagrass with deep convolutional neural networks. Weed Sci 68:545-552

Zhong L, Hu L, Zhou H (2019) Deep learning based multi-temporal crop classification. Remove Sens Environ 221:430-443

[WSSA] Weed Science Society of America (2016) WSSA Survey Ranks Palmer Amaranth as the Most Troublesome Weed in the U.S., Galium as the Most Troublesome in Canada. https://wssa.net/2016/04/wssa-survey-ranks-palmer-amaranth-as-the-most-troublesome-weed-in-the-u-s-galium-as-the-most-troublesome-in-canada. Accessed: September 21, 2023

Chapter 2 - Use of open-source object detection algorithms to detect Palmer amaranth (*Amaranthus palmeri*) in soybean

Note: This manuscript has been published in Weed Science and can be found with the following citation: Barnhart IH, Lancaster S, Goodin D, Spotanski J, Dille JA (2022) Use of open-source object detection algorithms to detect Palmer amaranth (*Amaranthus palmeri*) in soybean. Weed Sci 70:648-662

2.1 Abstract

Site-specific weed management using open-source object detection algorithms could accurately detect weeds in cropping systems. We investigated object detection algorithms to detect Palmer amaranth (*Amaranthus palmeri* S. Watson, henceforth referred to as *A. palmeri*) in soybean [*Glycine max* (L.) Merr.]. The objectives were to (1) develop an annotated image database of *A. palmeri* and soybean to fine-tune object detection algorithms, (2) compare effectiveness of multiple open-source algorithms in detecting *A. palmeri*, and (3) evaluate the relationship between *A. palmeri* growth features and *A. palmeri* detection ability. Soybean field sites were established in Manhattan, KS, and Gypsum, KS, with natural populations of *A. palmeri*. Totals of 1,108 and 392 images were taken aerially and at ground level, respectively, between May 27 and July 27, 2021. After image annotation, 4,492 images were selected. Annotated images were used to fine-tune open-source faster regional convolutional (Faster R-CNN) and single-shot detector (SSD) algorithms using a Resnet backbone, as well as the "You Only Look Once" (YOLO) series algorithms. Results demonstrated that YOLO v. 5 achieved the highest mean average precision score of 0.77. For both *A. palmeri* and soybean detections within this algorithm, the highest F1 score was 0.72 when using a confidence threshold of 0.298. A lower confidence threshold of 0.15 increased the likelihood of species detection, but also increased the likelihood of false-positive detections. The trained YOLOv5 data set was used to

identify *A. palmeri* in a data set paired with measured growth features. Linear regression models predicted that as *A. palmeri* densities increased and as *A. palmeri* height increased, precision, recall, and F1 scores of algorithms would decrease. We conclude that open-source algorithms such as YOLOv5 show great potential in detecting *A. palmeri* in soybean-cropping systems.

Key words: Artificial intelligence, TensorFlow, YOLOv5, Faster R-CNN, Single Shot Detector, site-specific weed management.

2.2 Introduction

Site-specific weed management (SSWM) involves adapting weed management strategies to match weed variation within a given field (Fernández-Quintanilla et al. 2018). In agriculture, weeds often grow in distinct patches rather than uniformly across a field (Maxwell and Luschei 2005); as a result, broadcast herbicide applications often treat areas of the field where no weeds are present. In theory, using SSWM could result in increased herbicide savings, decreased herbicide expenses, and decreased environmental contamination (Arsenijevic et al. 2021; Barroso et al. 2004; dos Santos Ferreira et al. 2019). An additional benefit is that SSWM could allow for the economical application of multiple herbicide mechanisms of action (MOAs) so that more expensive chemistries could be applied only where needed. Not only would this be less expensive for the farmer, but applications with diversified MOAs help to slow the development of herbicide-resistant weeds (Evans et al. 2015). In modern agriculture, successful weed control can be very difficult due to increases in herbicide-resistant weed cases, rising costs of herbicides, and shortages of crop protection products brought on by economic consequences of the COVID-19 pandemic (Dayan 2021; Mordor Intelligence 2022). As such, strategies such as SSWM that aim to reduce input quantities and costs could potentially benefit farmers and contribute to the sustainability of cropping systems around the world (Bongiovanni and Lowenberg-Deboer 2004).

The key component to SSWM involves the accurate detection of weed positions within a given field, but the development of a robust and accurate detection system for field conditions remains a challenge (Gao et al. 2020). One of the ways this challenge is being addressed is by applying artificial intelligence using convolutional neural networks (CNNs). Convolutional neural networks are a type of deep neural network that excel at pattern recognition and can be

utilized in a variety of tasks ranging from image analysis to audio file analysis (Albawi et al. 2017). The most common use of CNNs in the agricultural sector involves image analysis; CNNs analyze the textural, spectral, and spatial features of images and can extract features unseen by the human eye (Albawi et al. 2017; Sapkota et al. 2020). Fruit counting, weed detection, disease detection, and grain yield estimation are ways that CNNs have been used in agriculture (Biffi et al. 2021; Hussain et al. 2020, 2021; Sivakumar et al. 2020; Yang et al. 2019).

Two approaches to documenting and treating weeds in the field are real-time in situ weed detection and herbicide application and scouting and developing weed maps to guide SSWM (Cardina et al. 1997; Somerville et al. 2020). In situ weed detection involves recognizing weeds in real time and can lead to plants being treated in a timelier manner. Platforms that have been developed to detect weeds in situ include "smart" sprayers, autonomous weeding robots, and unmanned aerial spraying vehicles (Sivakumar et al. 2020), most of which use some type of CNN technology. CNNs have been shown to be accurate in tasks such as segmentation (dividing images into regions based on pixel similarities), image classification (assigning a label to an image based on the objects present), and object detection (identifying objects within an image) (Biffi et al. 2021; Sivakumar et al. 2020; Stanford 2022; ThinkAutomation 2022). Object detection CNNs are typically at the forefront of in situ weed detection, as there is often greater value in detecting and localizing agricultural pests as opposed to assigning labels to images with pests located in them (Chen et al. 2021).

In recent years, open-source object detection algorithms have become available, such as those from the TensorFlow Object Detection API (Huang et al. 2017), the "You Only Look Once" (YOLO) algorithm series (first introduced by Redmon et al. 2016), and the Detectron algorithm series (Lin et al. 2018). These object detectors have been used to implement a variety

of computer vision tasks, including cancer cell detection (Al Zorgani et al. 2022), facial recognition (Mattman and Zhang 2019), underwater fish detection (Xu and Matzner 2018), and projects related to the development of self-driving vehicles (Kulkarni et al. 2018). Open-source algorithms are typically pretrained on very large data sets, such as the Microsoft COCO (Common Objects in Context) data set (Lin et al. 2014). Through utilizing a process called transfer learning, pretrained algorithm parameters can be fine-tuned to detect custom objects. Transfer learning involves using information learned from one object detection algorithm and applying this information to identify different, yet related, objects (Ghazi et al. 2017). This eliminates the need to train algorithms from scratch, which is a very computationally expensive and time-consuming process (Ruder 2021). Open-source algorithms fine-tuned to identify agricultural crops and weeds have been used in a variety of studies, including late-season species detection in soybean [*Glycine max* (L.) Merr.] of Palmer amaranth (*Amaranthus palmeri* S. Watson), waterhemp (*Amaranthus tuberculatus* (Moq.) Sauer], common lambsquarters (*Chenopodium album* L.), velvetleaf (*Abutilon theophrasti* Medik.), and *Setaria* spp. (Sivakumar et al. 2020); detection of wild radish (*Raphanus raphanistrum* L.) and capeweed [*Arctotheca calendula* (L.) Levyns] in barley (*Hordeum vulgare* L.) (Thanh Le et al. 2021); and weed detection in a variety of crops, including lettuce (*Lactuca sativa* L.) (Osorio et al. 2020), carrots (*Daucus carota* L. var. *sativus* Hoffm.) (Ying et al. 2021), corn (*Zea mays* L.) (Ahmad et al. 2021), and onions (*Allium cepa* L.) (Parico and Ahamed 2020).

For this study, we focused on detecting *A. palmeri* in soybean-cropping systems using open-source object detection algorithms. *Amaranthus palmeri* has been designated the most problematic weed in the United States (WSSA 2016), and it can reduce soybean yields by as much as 68% (Klingaman and Oliver 1994; Kumar et al. 2021). Therefore, controlling this weed

is very important for United States soybean producers. Large numbers of training images are necessary to train object detection algorithms to identify custom objects (Pokhrel 2020); however, nonproprietary image databases of *A. palmeri* are often unavailable. In addition, even though algorithms have been previously trained on *A. palmeri* in the midwestern United States (Sivakumar et al. 2020), we did not find many studies that investigated the relationship of model evaluation metrics as influenced by *A. palmeri* growth features, including canopy diameter, plant height, percent ground cover, and weed density. Understanding the relationship between algorithm evaluation metrics and *A. palmeri* growth features could benefit precision weed applications. For example, future databases could focus on collecting images of *A. palmeri* plants with growth features best detected by the algorithm. In addition, farmers and agricultural professionals could gain a better understanding of which field conditions would benefit the most from deploying these algorithms. For instance, *A. palmeri* infestations with large plants and high populations may not be the best environments to use this technology for site-specific applications.

We hypothesized that as weed diameter and height increase, object detection algorithms will be better able to identify *A. palmeri* plants; however, as *A. palmeri* density and ground cover increases, ability to identify will decrease. Object detection algorithms can have difficulty detecting both small objects (Li et al. 2017) and detecting all object occurrences if objects are present in high densities in an image (Sun et al. 2022). The specific objectives of this study were (1) to develop an annotated image database of *A. palmeri* and soybean with multiple weed densities and soybean row spacings that can be used to fine-tune object detection algorithms, (2) compare multiple open-source algorithms' effectiveness in detecting *A. palmeri*, and (3) evaluate

the relationship between *A. palmeri* growth features (diameter, height, density, and ground cover) and *A. palmeri* detection ability.

2.3 Materials and methods

2.3.1 Image acquisition

To establish conditions representative of multiple *A. palmeri* densities and soybean-cropping systems, field locations were identified at the Kansas State University, Department of Agronomy Ashland Bottoms Research Farm near Manhattan, KS (39.122°N, 96.635°W) and at the Lund Research Farm near Gypsum, KS (38.797°N, 97.448°W) in 2021. At each location, 24 plots of soybeans were planted at a seeding rate of 331,000 seed ha^{-1}: 12 plots were planted at 38-cm-wide row spacing, and 12 plots were planted at 76-cm-wide row spacing; plot dimensions were 3.1-m wide and 9.1-m long. Both field sites had a naturally occurring population of *A. palmeri* that was allowed to germinate and grow with the soybeans. These field locations allowed multiple densities of *A. palmeri* to be photographed while growing among soybean in different row spacings, providing a greater diversity of field situations to be "seen" by each algorithm.

The training database was built with 1,500 images taken of *A. palmeri* only, soybean only, or both species between May 27 and July 27 (Table 1). Imagery was taken both with a TG-610 handheld camera (OM Digital Solutions, Hachioji-City, Tokyo, Japan), and with a DJI Inspire 1 unmanned aerial vehicle (UAV) equipped with a Zenmuse X5R RAW camera (DJI, Shenzhen, China). The TG-610 has a sensor size of 28 mm^2, whereas the Zenmuse X5R has a larger sensor size of 225 mm^2. To increase the variability of the photographed vegetation, aboveground altitudes at which the images were taken varied from 1.5 m to 8 m, often with the minimum height chosen on any given day determined by vegetation height. For example, as the

plants increased in height, it became necessary to increase the UAV flight altitude to prevent propeller downdraft from collapsing the plants. To add an additional source of variability, images were also collected under a variety of lighting conditions.

2.3.2 Field-collected data

To model algorithm evaluation metrics related to *A. palmeri* growth features, plant height, canopy diameter, and density were taken weekly between the middle rows of each plot from 1 to 4 wk after planting (WAP) and 1 to 5 WAP for the Manhattan and Gypsum plots, respectively. *Amaranthus palmeri* density was measured each week in a 0.25-m^2 quadrat placed at random within these rows. A total of four height and diameter measurements were recorded from random plants within the quadrats. Within this study, *A. palmeri* height was defined as the tallest measurable structure, and diameter was defined as the widest portion of the plant within the top 20 cm. In plots with a total of fewer than four *A. palmeri* plants observed, height and diameter measurements corresponded to the total number of observable plants. Data were taken on *A. palmeri* plants after the formation of the first true leaf and any growth stage afterward, as cotyledons proved to be too difficult to annotate on the image data set. On these same dates, five photos were taken within the middle of each plot with the handheld camera, approximately 1.5 m above the canopy. Five photos were taken to provide a representative sample of the plot, as plots were 9.1 m in length. These images were kept separate from the training data set and were used to evaluate algorithm performance within each plot.

2.3.3 Image processing and data annotation

Raw image outputs from the handheld and the Zenmuse cameras produced images with dimensions that were too large and would exceed processor memory capacity. To begin, every input image was cropped to dimensions of 2,880 × 2,880 pixels to remove the "fish-eye" effect that often accompanies aerial imagery (Gurtner et al. 2007). Next, these images were tiled into smaller dimensions of 1,024 × 1,024 pixels using Python 3.9.7 (Python Software Foundation 2022) and the Pillow module (Clark et al. 2022). This allowed images large enough to retain features necessary for labeling, but small enough so as to not exhaust processor memory during training. Each input image was tiled into 20 new images of 1,024 × 1,024 pixels for a total of 30,000 images, which allowed for more images to be added to the training database. Images in which no plant features were visible or those of poor quality were simply discarded and not labeled; in all, 4,492 images were selected for labeling.

Images were labeled using the annotation tool LabelImg (Tzutalin 2015), which allows users to draw rectangular bounding boxes around objects within imagery and assign classes to each box. In many cases, the presence of multiple classes of objects can lead to better detection results due to the presence of multiple feature gradients (Oza and Patel 2019). Therefore, we chose to annotate two classes for this study: *A. palmeri* and soybean. Using the same methods described by Sivakumar et al. (2020), bounding boxes were drawn over both individual and patches of *A. palmeri* and soybean. In the event of irregularly shaped plants or patches of plants, multiple bounding boxes were drawn to encompass the entirety of the plant features. Labeling partial sections of irregularly shaped plants has been shown to be beneficial to object detectors (Sharpe et al. 2018, 2020a; Zhuang et al. 2022), so these irregular features were not ignored. In any given image, both plant species could be present, so they were labeled accordingly.

Amaranthus palmeri plants were labeled at all growth stages ranging from the formation of the first true leaf through inflorescence, and soybeans were labeled from the VE-VC stage through the R2 stage (Fehr et al. 1971) (Figure 1). *Amaranthus palmeri* plants visible within each labeled image ranged from no plants (only soybean labeled) to roughly 115 labeled specimens. Throughout the image data set, soybean growth stage was homogeneous on each plant date, but *A. palmeri* could have multiple growth stages visible due to its ability to emerge throughout the growing season (Jha and Norsworthy 2009; Shyam et al. 2021). Figure 2 illustrates the image labeling process.

The images that were selected for labeling contained a total of 10,494 and 10,312 *A. palmeri* and soybean annotations across all growth stages, respectively. The data set was then divided into 90% training and 10% test images, used to train and evaluate the algorithms, respectively. The training and test data sets consisted of 4,042 and 450 images, respectively. The aforementioned images taken over the plots for analysis of *A. palmeri* growth features and algorithm evaluation metrics were not included in the training or testing data sets but were kept separate for further analysis.

2.3.4 Algorithm selection

Three open-source algorithm architectures were used in this study: faster regional convolutional neural network (Faster R-CNN), single-shot detector (SSD), and two YOLO algorithms. Faster R-CNN algorithms are a modern development of what are called regional-based CNNs, first proposed by Girshick et al. (2014). This approach was revolutionary, in that it was one of the first large-scale successful approaches to addressing the task of object localization and detection (Balasubramanian 2021). As input images are fed into the algorithm, areas of

interest based on groups of pixels are extracted from the image and fed into the neural network (Oinar 2021). The architecture has been updated with the development of Fast R-CNN in 2015 (Girshick 2015) and finally with Faster R-CNN in 2016 (Ren et al. 2017), with each version being faster in detection speed than the previous. Faster R-CNN is known as a two-stage object detector, in that it first extracts regions of interest where it is likely that the objects will be and then classifies these regions of interest (Du et al. 2020). Consequently, Faster R-CNN is known to perform better in terms of detection accuracy but has slower detection speeds (Sivakumar et al. 2020).

SSD and YOLO algorithms were proposed by Liu et al. (2016) and Redmon et al. (2016), respectively. Considered single-stage object detectors, they are generally faster and less computationally expensive than Faster R-CNN algorithms (Liu et al. 2016), allowing for faster detection and suitable for real-time detection applications. Instead of extracting regions of interest as R-CNN algorithms do, they accomplish object localization and classification in one forward pass of the neural network (Forson 2017). As in Sivakumar et al. (2020), Faster R-CNN was chosen for this project due to its detection performance, whereas SSD and YOLO algorithms were chosen due to their inference speeds.

The backbone models refer to the specific neural networks behind the architectures and allow for feature extraction from the input image (Shimao 2019). These networks are interchangeable, with multiple networks able to be used as backbone models (Li et al. 2020). For this study, the Faster R-CNN architecture backed with the ResNet (He et al. 2016) network was chosen with multiple layers, including ResNet-50, ResNet-101, ResNet-152, and Inception ResNet-V2 (Szegedy et al. 2017). Additionally, ResNet-50 and ResNet-152 were also chosen as backbone models for the SSD architecture.

For the YOLO algorithms, YOLOv4 (Bochkovskiy et al. 2020) and YOLOv5 (Jocher et al. 2020) were used, both running on the Cross Stage Partial (CSP) Darknet53 (Bochkovskiy et al. 2020) network. YOLOv5 also implements a Path Aggregation Network, allowing for both increased propagation of lower-level features and improvements in using localization signals (Carlos and Ulson 2021). This allows for an increase in accuracy when localizing an object (Carlos and Ulson 2021). Additionally, the YOLOv5 algorithm consists of four releases: YOLOv5s, YOLOv5m, YOLOv5l, and YOLOv5x (ultralytics 2022b). YOLOv5x was chosen for this experiment, as it is considered the most accurate object detector of the four (Carlos and Ulson 2021). Both YOLO algorithms were obtained from their respective GitHub repositories (Alexey 2022; Jocher 2022a). YOLO algorithms down-sample input images by a factor of 32 when training (Hui 2018), so input images with width and height dimensions divisible by 32 are necessary. Our input image dimensions of 1,024 × 1,024 pixels fit this criterion. All Faster R-CNN and SSD algorithms were obtained from the TensorFlow 2 Detection Model Zoo (TensorFlow 2021); the respective algorithms with input dimension requirements of 1,024 × 1,024 pixels were chosen. All YOLO and TensorFlow models selected were pretrained, thus eliminating the need to train from scratch (Ruder 2021).

2.3.5 Training

All algorithms were trained on a virtual Ubuntu 18.04 computer available on Paperspace, a virtual machine learning platform (Paperspace Cloud Computing, https://www.paperspace.com). The computer was equipped with an Intel® Xeon® E5-2623 v4 processor (Intel Technologies, Santa Clara, California, United States) equipped with 16 CPU

cores and 60 GB of RAM. To increase training speed, training was done utilizing a NVIDIA P6000 Graphics Processing Unit (GPU) with 24 GB of RAM (NVIDIA, Santa Clara, CA, USA).

For all algorithms, the default training hyperparameters were accepted, except for the learning rates for both the TensorFlow algorithms and batch sizes for all algorithms. As algorithm loss was monitored during training, learning rate had to be lowered below default settings for most Faster R-CNN and SSD algorithms due to an issue with exploding gradients. When doing so, we also lowered the warm-up learning rate to a value below the learning rate to avoid errors during training. As input images were large, batch sizes were reduced to prevent exhausting the GPU's memory capacity. Larger batch sizes were possible with smaller algorithms (i.e., Faster R-CNN ResNet-52 and Faster R-CNN ResNet-101), but batch sizes had to be reduced for larger algorithms (i.e., Faster R-CNN Inception ResNet-V2) to avoid the "Resource Exhausted Error:" (TensorFlow 2017) indicating that the GPU was out of memory. Because batch size has been said to not be a significant factor in affecting algorithm performance (Ghazi et al. 2017), we did not expect this to affect the outcome of our algorithms. Algorithm training information is presented in Table 2.

During the image annotation process, all annotations were saved in Pascal VOC format. Pascal VOC format is compatible with TensorFlow algorithms, but not with YOLO algorithms. Therefore, before training the YOLO algorithms, copies of the annotations were saved in a separate folder and converted to YOLO format using Python 3.9.7. The script that was used can be obtained on the Convert PascalVOC Annotations to YOLO GitHub website (vdalv 2017).

All algorithms were trained for the default 100,000 steps, except for the Faster R-CNN Inception Resnet-V2, YOLOv4, and YOLOv5 algorithms. The default number of training steps for the Faster R-CNN Inception ResNet-V2 algorithm is 200,000, but upon monitoring the loss,

it was determined that no further increases in algorithm training were being made, and training was terminated early. YOLOv4 training involves iterations, thereby defining a batch size before training and an iteration completing when the algorithm has processed the number of images specified in the batch size. Finally, YOLOv5 output metrics were reported after each completed epoch, which is defined as one iteration through the entire training data set (Brownlee 2018). Upon viewing an output of the evaluation metrics for each epoch, we terminated algorithm training after 41 epochs, and the best weights were automatically saved for analysis.

Image augmentation is an important aspect of model training, as it allows for a more comprehensive set of images to be passed through the algorithm and reduce overfitting (Shorten and Khoshgoftaar 2019). Each of the algorithms contained code to automatically augment images during algorithm training, according to each algorithm's default settings. The Faster R-CNN architecture augmentations included random horizontal flips, hue adjustments, contrast adjustments, saturation adjustments, and random image cropping. The SSD architectures used random horizontal flips and random image cropping augmentations. For the YOLO algorithms, the YOLOv4 augmentations included random image saturation, exposure, and hue adjustments (Alexey 2020). Finally, the YOLOv5 model used random mosaicking. This process involves combining an input image with three random images from the training data set. The new mosaic is then passed through the algorithm for training (Jocher 2022b).

2.3.6 Algorithm evaluation and statistical analysis

To measure overall performance of the algorithms, the metrics of precision, recall, and F1 score were computed for the test data set (Shung 2018). Using an intersect over union (IoU) threshold of 0.5 (50%) between the annotated objects and the predicted bounding boxes (Henderson and

Ferrari 2017), true-positive (TP) and false-positive (FP) detections are determined. IoU is defined as the overlap between the ground truth bounding boxes drawn during annotation and the predicted bounding box determined by the computer (Jin et al. 2022), divided by the total area of each bounding box (Figure 3). IoU values greater than or equal to 0.5 were considered TP, and values less than 0.5 were considered FP predictions (Henderson and Ferrari 2017).

Precision is the ratio between the number of TP predictions and the total number of positive predictions, with the lowest value being 0 and the highest value being 1 (Hussain et al. 2021). Precision is reduced when an algorithm makes many incorrectly positive, or FP, predictions or a low number of TP predictions but is increased by larger numbers of correct predictions and low FP detections (Gad 2021). Precision was computed with the following equation:

$$\text{Precision} = \frac{\text{TP}}{\text{TP} + \text{FP}} \quad [1]$$

Recall, also referred to as the TP rate (Hussain et al. 2021), is a measure of how well a given algorithm identifies TP predictions (Huilgol 2020). Also ranging from 0 to 1, a higher recall indicates better TP predictions. Recall was computed as follows:

$$\text{Recall} = \frac{\text{TP}}{\text{TP} + \text{FN}} \quad [2]$$

where FN denotes false-negative detections.

The F1 score is the harmonic mean between precision and recall (Zhong et al. 2019), with the best score being 1 and the worst being 0 (Hussain et al. 2021). It was calculated as:

$$\text{F1} = 2 \times \frac{\text{Precision} \times \text{recall}}{\text{Precision} + \text{recall}} \quad [3]$$

The average precision (AP) for each class is determined by graphing a precision–recall curve for each test image for both classes and computing the area beneath each curve (Henderson and Ferrari 2017). The AP is then used to find the mean AP (mAP) of the algorithm, which was

calculated from an IoU threshold of 0.5 in this study using the following equation (Jin et al. 2022):

$$\text{mAP} = \frac{\sum_{i=1}^{N} \text{AP}i}{N} \quad [4]$$

where *N* corresponds to the total number of object classes. Values for mAP range from 0 to 1, with higher values corresponding to larger areas beneath the curve. For this study, the algorithm with the largest mAP was selected to analyze the model evaluation metrics for the photos taken above the individual plots.

For each measurement date, an average for each plot was determined for all field-collected data (*A. palmeri* height, diameter, and density). *Amaranthus palmeri* coverage was computed by multiplying the average canopy area by the average density per plot, assuming a circular shape:

$$\text{T} = \pi r^2 n \quad [5]$$

where T is the average total *A. palmeri* coverage (m^2), *r* is the average *A. palmeri* radius (m), and *n* is the average weed density (plants m^{-2}).

Each test image taken over the plots was passed through the best-performing algorithm, and precision, recall, and F1 scores were generated. Each evaluation metric was averaged within its respective plot. Statistical analysis was done using R v. 4.1.2 (R Core Team 2021). Regression models (see "Results and Discussion" section) were used to test whether field-measured data (*A. palmeri* density, height, and coverage) significantly predicted algorithm evaluation metrics. Data were combined over all collection dates and locations for this analysis, as regression assumptions were checked visually for each location and were determined to meet all assumptions (data not shown) (Osborne and Waters 2002). Best regression models were selected based on the Akaike information criterion (AIC) values, such that the model with the

lowest AIC value was selected for each evaluation metric. AIC values and weights (indicating the total predicative power among all tested models) were found using the AICCMODAVG package in R (Mazerolle 2020). Density and coverage were found to be highly collinear (data not shown), so these variables were never included in the same model together.

2.4 Results and Discussion

2.4.1 Algorithm comparison

The results of algorithm training are presented in Figure 4. After training, it was shown that YOLOv5 achieved the highest overall mAP value of 0.77. YOLOv4 and Faster R-CNN ResNet50 both achieved acceptable results with mAP values of 0.70, followed by SSD ResNet152 and Faster R-CNN Inception ResNet(v2) with values of 0.68. In most cases, the mAP values for the single-stage detectors (YOLO and SSD) on this data set were equal or superior to those of the two-stage detectors. Faster R-CNN models are generally considered accurate object detectors (Sivakumar et al. 2020), but they can be sensitive to background noise and often have difficulty detecting small objects (Amin and Galasso 2017; Roh and Lee 2017). Our test data set contained images of multiple *A. palmeri* and soybean growth stages, including very small plants of both species. This could explain why the single-stage object detectors often outperformed the Faster R-CNN models in this study. Additionally, we were not surprised to see the higher performances of YOLOv4 and YOLOv5 algorithms, as previous versions of YOLO have been reported to detect weeds faster than Faster R-CNN algorithms and with greater accuracy than SSD algorithms (Ahmad et al. 2021). Given these results, YOLOv5 was selected for further analysis.

The YOLOv5 algorithm in this study was trained for 41 epochs (Figure 5), taking approximately 15 h to complete. Training was monitored based on the changes in mAP per epoch. Algorithm training was terminated after mAP values were seen to "plateau," thus indicating no further meaningful gains in algorithm performance were expected. During training, YOLOv5 saved the best-performing weights, which were used to compute all further algorithm evaluations. In the precision–recall curve for YOLOv5 (Figure 6), the AP of *A. palmeri* (0.788) is greater than that of soybean (0.756), indicating that detection was slightly better for *A. palmeri* than for soybean. This could be related to differences in the way that the species were annotated. As soybean increased in size, larger bounding boxes were drawn over multiple plants, as there was a high level of overlap between individual plants (Figure 7). Separating out the individual plants would have been both difficult and time-consuming. On the other hand, although there were some overlaps observed with *A. palmeri*, these were much less pronounced and allowed for more individual weed plants to be annotated. Therefore, individual *A. palmeri* plants were presumably easier for the YOLOv5 algorithm to identify.

When using YOLOv5 for detection, users can specify a confidence threshold as an input parameter to the detection script (ultralytics 2022a). This confidence threshold acts to limit the number of FP scores displayed in the final prediction (Wenkel et al. 2021). In our algorithm, lower confidence thresholds increased the likelihood of detecting either an *A. palmeri* or soybean plant, but the FP detection rates increased as a result. Figure 8 illustrates the F1 scores calculated on the test image data set. Interpretation of Figure 8 indicates that at a confidence threshold of 0.298, the highest F1 score (0.72) was achieved for both classes. This indicates that at this threshold, both precision and recall will be optimized for best detection results. As this

confidence threshold is a recommended value, users still have the option to set the threshold to a value of their choosing.

There were differences between detections using lower (0.15) and higher (0.70) confidence thresholds (Figure 9). With multiple objects present in this image, YOLOv5 confidence in object detections ranged from low (0.36) to high (0.86); values are displayed immediately following the class prediction on each box. If this algorithm were to be used by a precision ground sprayer or a similar platform, we propose that using a lower confidence threshold would result in more *A. palmeri* plants being identified and treated. Consequently, the likelihood of soybean being incorrectly detected as *A. palmeri* would increase, but in soybean-cropping systems with herbicide-tolerant traits, this would not result in crop damage, assuming all current labels for such applications were followed. An increase in *A. palmeri* FP detections would likely lead to more herbicide being applied to the field. Interestingly, *A. palmeri* FP detections were not just limited to soybean; other broadleaf weeds such as carpetweed (*Mollugo verticillata* L.) and *A. theophrasti* were sometimes detected as *A. palmeri* with lower confidence intervals (Figure 10). This suggests that some weeds with features similar to *A. palmeri* plants would be sprayed if confidence intervals were lowered upon deployment. Regardless, further research is needed to determine which threshold would be optimal to reduce the volume of herbicides applied, while still achieving acceptable weed control.

2.4.2 Modeling YOLOv5 evaluation metrics

Only data for the *A. palmeri* class were used to model *A. palmeri* physical characteristics in relation to YOLOv5 evaluation metrics. For all regression models analyzed, the model P-values

were significant, indicating that all ground-measured variables affected the evaluation metrics (Table 3). However, it was determined that model 5, which included the main effects and interaction effect of *A. palmeri* density and height, was the model that best fit the data. For precision, recall, and the F1 score, the model carried 72%, 86%, and 91% of the weights from the models that were compared, respectively. Therefore, this model was selected to describe the relationship between model evaluation metrics for density and height.

For all evaluation metrics analyzed with model 5, the interaction coefficient for density and height was significant (P = 0.049, 0.016, and 0.010 for precision, recall, and F1 score, respectively) (Table 4). As smaller weeds are generally more susceptible to control (Kieloch and Domaradzki 2011), we chose to model our results with four heights representing *A. palmeri* plants at early growth stages. The results of these predictions by the YOLOv5 algorithm indicated that smaller, younger *A. palmeri* plants growing at lower densities were detected better than taller plants (Figure 11). The results were as anticipated for density, but the prediction suggesting that YOLOv5 detection ability was greater for smaller plants was surprising, as species identification is often easier on larger plants with distinctive features. This may have been because there were a greater number of *A. palmeri* annotations of younger, smaller plants as opposed to larger, more mature plants. Additionally, larger plants have canopies that overlap with each other, making it difficult to distinguish and label large individual plants. Regardless, these predictions were encouraging, as algorithms that can detect smaller weeds are of more practical use, because weeds can be controlled much more easily when they are younger and smaller in size (Naghashzadeh and Beyranvand 2015).

In relation to weed density affecting algorithm performance, our study conflicts with Yu et al. (2020), in that they found that images with higher weed densities generally led to better

algorithm detection results than those with lower weed densities. However, the study by Yu et al. (2020) utilizes image classification rather than object detection. Rather than localizing the weeds within the image, the entire input image was classified with the weed species that were visible. Image classification for weed detection comes with some disadvantages, however, as the location of individual weeds was not provided, and multiple weed species within an image were not able to be detected (Ahmad et al. 2021). With object detection algorithms, object localization within the image allows for weeds to be located and controlled where they occur. However, we hypothesize that this application is best suited for postemergence applications (in the case of using precision herbicide application technology) where weed density is relatively low. Fields with very high weed densities would likely not benefit from a site-specific herbicide application, as the volume of herbicide needed for control would likely not be statistically different from a whole-field broadcast application. Further research is needed to determine the optimum weed density beyond which precision weed control has no economic or environmental benefits.

The overall precision, recall, and F1 scores computed for the 450 images in the test data set were 0.71, 0.70, and 0.71, respectively (data not shown). A precision of 0.71 indicates that the YOLOv5 algorithm was 71% accurate in successfully predicting *A. palmeri* and soybeans. Likewise, a recall of 0.70 indicates that the algorithm correctly predicted 70% of the plants belonging to either class (Jin et al. 2022). These results were lower than previously reported by other YOLO weed detectors (Jin et al. 2022; Zhuang et al. 2022). However, our "test" data set consisted of images randomly selected from the large-input database and had a variety of *A. palmeri* growth stages and population densities. When evaluating YOLOv5 evaluation metrics on images taken within the plots with lower *A. palmeri* densities and shorter plant heights, the algorithm precision, recall, and F1 scores greatly improved. Based on the regression model fit to

the data, *A. palmeri* plants 2-cm tall and growing at a density of 1 plant m^{-2} would be detected with precision, recall, and F1 scores of 0.87, 0.93, and 0.89, respectively.

YOLO algorithms have been used previously for weed detection. Ahmad et al. (2021) achieved an overall mAP score of 0.543 when using YOLOv3 (Redmon and Farhadi 2018) to detect redroot pigweed (*Amaranthus retroflexus* L.), giant ragweed (*Ambrosia trifida* L.), common cocklebur (*Xanthium strumarium* L.), and green foxtail [*Setaria viridis* (L.) P. Beauv.]. Hussain et al. (2020) developed an in situ sprayer using both YOLOv3 and YOLOv3-tiny (Adarsh et al. 2020) as backbone algorithms to detect *C. album*, achieving mAP scores of 0.932 and 0.782, respectively. Sharpe et al. (2020b) achieved good detection results when training the YOLOv3 algorithm to identify general classes of grasses, broadleaves, and sedge species; further, they found that including multiple classes (as opposed to a single class) in their algorithm increased precision, recall, and F1 metrics. Hu et al. (2021) used YOLOv3 and YOLOv4 to detect 12 different weed species common to rice (*Oryza sativa* L.) and found that YOLOv4 achieved a mAP score that was 0.116 higher than YOLOv3. Our best mAP score was slightly lower than some of these YOLO weed detectors; however, it must be mentioned that this data set was collected with multiple cameras covering a variety of *A. palmeri* densities and growth stages. Data sets such as those collected by Jin et al. (2022) and Zhuang et al. (2022) consisted of a handheld camera taking multiple images at a consistent height. In this study, we collected imagery ranging from 1.5 m to 8 m above ground level. While many data sets collected consist of "ideal" specimens including plants grown in greenhouses or photos of individual plants, our data set was based on what a field sprayer or application UAV would observe in the field. As a result, during the labeling process, several overlapping bounding boxes had to be drawn, and it was impossible for each image to contain labels for individual plants.

In conclusion, this research demonstrated that YOLOv5, a free and open-source object detection algorithm, can detect *A. palmeri* in soybean-cropping systems. As site-specific herbicide applications become more widespread due to the potential for herbicide savings and environmental benefits, open-source algorithms such as YOLOv5 could enable increased development and adoption of precision weed detectors. Furthermore, this research suggests that our algorithm may be better at detecting smaller as opposed to larger *A. palmeri* plants. Upon further refinement and training of the algorithm, it may be of great use to growers, as smaller weeds are much more susceptible to control than larger ones.

Future research and improvements to our model will include adding more images to the data set. We included different imagery heights in this study to create a data set that could be utilized by multiple precision agriculture platforms such as precision ground sprayers and pesticide application UAVs. In the future, construction of specialized data sets that consist of imagery for each type of platform would be collected. For instance, imagery collected to train an algorithm for a precision ground sprayer should be at a height consistent with the sensors on the sprayer itself, that is, 60 cm above the target canopy. In this experiment, we trained the object detectors to identify two species (*A. palmeri* and soybean), and a future goal is to expand the number of weed species that can be detected by the YOLOv5 model. An increase in both the number of images and number of annotated weed species in these specialized data sets would increase the mAP of the YOLOv5 algorithm and reduce errors in object detection (Linn et al. 2019). Equal distribution of annotations among species is important when collecting these images. With further improvements to the algorithm, field tests will need to be carried out to both optimize weed detection and to treat weeds in real time using a precision ground sprayer with high-resolution cameras oriented close to plant canopies.

2.5 Acknowledgements

This research received no specific grant from any funding agency or the commercial or not-for-profit sectors. No conflicts of interest have been declared. This is contribution no. 23-042-J from the Kansas Agricultural Experiment Station.

2.6 References

Adarsh P, Rathi P, Kumar M (2020) YOLO v3-Tiny: object detection and recognition using one stage improved model. Pages 687–694 *in* Proceedings from the 6th International Conference on Advanced Computing and Communication Systems (ICACCS). Coimbatore, India: Institute of Electrical and Electronics Engineers

Ahmad A, Saraswat D, Aggarwal V, Etienne A, Hancock B (2021) Performance of deep learning models for classifying and detecting common weeds in corn and soybean production systems. Comput Electron Agric 184:106081

Albawi S, Mohammed TA, Al-Zawi S (2017) Understanding of a convolutional neural network. Pages 1–6 in Proceedings of the 2017 International Conference on Engineering & Technology. Antalya, Turkey: Institute of Electrical and Electronics Engineers

Alexey AB (2020) CFG Parameters in the [Net] Section. https://github.com/AlexeyAB/darknet/wiki/CFG-Parameters-in-the-%5Bnet%5D-section. Accessed: July 19, 2022

Alexey AB (2022) darknet. https://github.com/AlexeyAB/darknet. Accessed: February 3, 2022

Al Zorgani MM, Mehmood I, Ugail H (2022) Deep YOLO-based detection of breast cancer mitotic-cells in histopathological images. Pages 335–352 in Su R, Zhang YD, Liu H, eds. Proceedings of 2021 International Conference on Medical Imaging and Computer-Aided Diagnosis (MICAD 2021). MICAD 2021 (Lecture Notes in Electrical Engineering, Vol. 784). Singapore: Springer

Amin S, Galasso F (2017) Geometric proposals for faster R-CNN. Pages 1–6 in Proceedings of the 14th IEEE International Conference on Advanced Video and Signal Based Surveillance (AVSS). Lecce, Italy: Institute of Electrical and Electronics Engineers

Arsenijevic N, de Avellar M, Butts L, Arneson NJ, Werle R (2021) Influence of sulfentrazone and metribuzin applied preemergence on soybean development and yield. Weed Technol 35:210–215

Balasubramanian R (2021) Region–based convolutional neural network (RCNN). https://medium.com/analytics-vidhya/region-based-convolutional-neural-network-rcnn-b68ada0db871. Accessed: February 2, 2022

Barroso J, Fernandez-Quintanilla C, Maxwell BD, Rew LJ (2004) Simulating the effects of weed spatial pattern and resolution of mapping and spraying on economics of site-specific management. Weed Res 44:460–468

Biffi LJ, Mitishita E, Liesenberg V, dos Santos AA, Gonçalves DN, Estrabis NV, Silva JdA, Osco LP, Ramos APM, Centeno JAS, Schimalski MB, Rufato L, Neto SLR, Junior JM, Gonçalves WN (2021) ATSS deep learning-based approach to detect apple fruits. Remote Sens 13:54

Bochkovskiy A, Wang CY, Liao HYM (2020) YOLOv4: Optimal Speed and Accuracy of Object Detection. arXiv database 2004.10934. https://arxiv.org/abs/2004.10934. Accessed: February 2, 2022

Bongiovanni R, Lowenberg-Deboer J (2004) Precision agriculture and sustainability. Precis Agric 5:359–387

Brownlee J (2018) Difference between a Batch and an Epoch in a Neural Network. https://machinelearningmastery.com/difference-between-a-batch-and-an-epoch. Accessed: February 3, 2022

Cardina J, Johnson GA, Sparrow DH (1997) The nature and consequence of weed spatial distribution. Weed Sci 45:364–373

Carlos LMJ, Ulson JAC (2021) Real time weed detection using computer vision and deep learning. Pages 1131–1137 in Proceedings from the 14th IEEE International Conference on Industry Applications (INDUSCON). São Paulo, Brazil: Institute of Electrical and Electronics Engineers

Chen JW, Lin WJ, Cheng HJ, Hung CL, Lin CY, Chen SP (2021) A smartphone-based application for scale pest detection using multiple-object detection methods. Electronics 10:372

Clark A (2022) Pillow 9.2.0. Code. https://pypi.org/project/Pillow. Accessed: July 20, 2022

Dayan FE (2021) Market trends of the herbicide crop protection industry and impact of COVID-19. Outlook Pest Manag 32:2–4

dos Santos Ferreira A, Freitas DM, da Silva GC, Pistori H, Folhes MT (2019) Unsupervised deep learning and semi-automatic data labeling in weed discrimination. Comput Electron Agric 165:104963

Du L, Zhang R, Wang X (2020) Overview of two-stage object detection algorithms. J Phys Conf Ser 1544:012033

Evans JA, Tranel PJ, Hager AG, Schutte B, Wu C, Chatham LA, Davis AS (2015) Managing the evolution of herbicide resistance. Pest Manag Sci 72:74–80

Fehr WR, Caviness CE, Burmood DT, Pennington JS (1971) Stage of development descriptions for soybeans, Glycine max (L.) Merrill. Crop Sci 11:929–931

Fernández-Quintanilla C, Peña JM, Andújar D, Dorado J, Ribeiro A, López-Granados F (2018) Is the current state of the art of weed monitoring suitable for site-specific weed management in arable crops? Weed Res 58:259–272

Forson E (2017) Understanding SSD MultiBox—Real-Time Object Detection in Deep Learning. https://towardsdatascience.com/understanding-ssd-multibox-real-time-object-detection-in-deep-learning-495ef744fab. Accessed: February 2, 2022

Gad AF (2021) Evaluating Deep Learning Models: The Confusion Matrix, Accuracy, Precision, and Recall. https://blog.paperspace.com/deep-learning-metrics-precision-recall-accuracy. Accessed: February 3, 2022

Gao J, French AP, Pound MP, He Y, Pridmore TP, Pieters JG (2020) Deep convolutional neural networks for image-based Convolvulus sepium detection in sugar beet fields. Plant Methods 16:29

Ghazi MM, Yanikoglu B, Aptoula E (2017) Plant identification using deep neural networks via optimization of transfer learning parameters. Neurocomputing 235:228–235

Girshick R (2015) Fast R-CNN. Pages 1440–1448 in Proceedings of the IEEE International Conference on Computer Vision (ICCV). Santiago, Chile: Institute of Electrical and Electronics Engineers

Girshick R, Donahue J, Darrell T, Malik J (2014) Rich feature hierarchies for accurate object detection and semantic segmentation. Pages 580–587 in Proceedings of the IEEE Conference on Computer Vision and Pattern Recognition (CVPR). Columbus, OH: Institute of Electrical and Electronics Engineers

Gurtner A, Walker R, Boles W (2007) Vibration compensation for fisheye lenses in UAV Applications. Pages 218–225 in Proceedings from the 9th Biennial Conference of the Australian Pattern Recognition Society on Digital Image Computing Techniques and Applications (DICTA 2007). Glenelg, SA, Australia: Institute of Electrical and Electronics Engineers

He K, Zhang X, Ren S, Sun J (2016) Deep residual learning for image recognition. Pages 770–778 in Proceedings of the IEEE Conference on Computer Vision and Pattern Recognition (CVPR). Las Vegas, NV: Institute of Electrical and Electronics Engineers

Henderson P, Ferrari V (2017) End-to-end training of object class detectors for mean average precision. Pages 198–213 in Lai SH, Lepetit V, Nishino K, Sato Y, eds. Computer Vision—ACCV 2016. ACCV 2016 (Lecture Notes in Computer Science, Vol. 10115). Cham, Switzerland: Springer

Hu D, Tian Z, Li L, Ma C (2021) Rice weed detection method on YOLOv4 convolutional neural network. Pages 41–45 in Proceedings from the 2021 International Conference on Artificial Intelligence, Big Data and Algorithms (CAIBDA). Xi'an, China: Institute of Electrical and Electronics Engineers

Huang J, Rathod V, Sun C, Zhu M, Korattikara A, Fathi A, Fischer I, Wojna Z, Song Y, Guadarrama S, Murphy K (2017) Speed/accuracy trade-offs for modern convolutional object detectors. Pages 7310–7311 in Proceedings of the IEEE Conference on Computer Vision and Pattern Recognition (CVPR). Honolulu, HI: Institute of Electrical and Electronics Engineers

Hui J (2018) Real-Time Object Detection with YOLO, YOLOv2 and Now YOLOv3. https://jonathan-hui.medium.com/real-time-object-detection-with-yolo-yolov2-28b1b93e2088. Accessed: July 20, 2022

Huilgol P (2020) Precision vs. Recall—An Intuitive Guide for Every Machine Learning Person. https://www.analyticsvidhya.com/blog/2020/09/precision-recall-machine-learning. Accessed: February 3, 2022

Hussain N, Farooque AA, Schumann AW, Abbas F, Acharya B, McKenzie-Gopsill A, Barrett R, Afzaal H, Zaman QU, Cheema MJM (2021) Application of deep learning to detect lamb's quarters (Chenopodium album L.) in potato fields of Atlantic Canada. Comput Electron Agric 182:106040

Hussain N, Farooque AA, Schumann AW, McKenzie-Gopsill A, Esau T, Abbas F, Acharya B, Zaman Q (2020) Design and development of a smart variable rate sprayer using deep learning. Remote Sens 12:4091

Jha P, Norsworthy JK (2009) Soybean canopy and tillage effects on emergence of Palmeramaranth (Amaranthus palmeri) from a natural seedbank. Weed Sci 57:644–651

Jin Z, Sun Y, Che J, Bagavathiannan M, Yu J, Chen Y (2022) A novel deep learning-based method for detection of weeds in vegetables. Pest Manag Sci 78:1861–1869

Jocher G (2022a) yolov5. https://github.com/ultralytics/yolov5. Accessed: February 3, 2022

Jocher G (2022b) yolov5: data augmentation #8021. https://github.com/ultralytics/yolov5/issues/8021#issuecomment-1140326033. Accessed: July 19, 2022

Jocher G, Stoken A, Borovec J, NanoCode012, ChristopherSTAN, Changyu L, Laughing, tkianai, Hogan A, lorenzomammana, yxNONG, AlexWang1900, Diaconu L, Marc, wanghaoyang0206, et al. (2020) ultralytics/yolov5: v3.1—Bug Fixes and Performance Improvements. https://doi.org/10.5281/zenodo.4154370. Accessed: February 2, 2022

Kieloch R, Domaradzki K (2011) The role of the growth stage of weeds in their response to reduced herbicide doses. ACTA Agrobotanica 64:259–266

Klingaman TE, Oliver LR (1994) Palmer amaranth (Amaranthus palmeri) interference in soybeans (Glycine max). Weed Sci 42:523–527

Kulkarni R, Dhavalikar S, Bangar S (2018) Traffic light detection and recognition for self driving cars using deep learning. Pages 1–4 in Proceedings of the 2018 Fourth International Conference on Computing Communication Control and Automation (ICCUBEA). Pune, India: Institute of Electrical and Electronics Engineers

Kumar V, Liu R, Peterson DE, Stahlman PW (2021) Effective two-pass herbicide programs to control glyphosate-resistant Palmer amaranth (Amaranthus palmeri) in glyphosate/dicamba-resistant soybean. Weed Technol 35:128–135

Li D, Wang R, Xie C, Liu L, Zhang J, Li R, Wang F, Zhou M, Liu W (2020) A recognition method for rice plant diseases and pests video detection based on deep convolutional neural network. Sensors 20:578

Li J, Liang X, Wei Y, Xu T, Feng J, Yan S (2017) Perceptual Generative Adversarial Networks for Small Object Detection. Pages 1222–1230 in Proceedings of the IEEE Conference on Computer Vision and Pattern Recognition. Honolulu, HI: Institute of Electrical and Electronics Engineers

Lin T, Maire M, Belongie S, Bourdev L, Girshick R, Hays J, Perona P, Ramanan D, Zitnick CL, Dollár P (2014) Microsoft COCO: common objects in context. Pages 740–755 in Proceedings of the 13th European Conference on Computer Vision, Part V. Zurich, Switzerland: European Conference on Computer Vision

Lin TY, Goyal P, Girshick R, He K, Dollár P (2018) Focal Loss for Object Detection. arXiv database 1708.02002v2. https://arxiv.org/pdf/1708.02002v2.pdf. Accessed: July 20, 2022

Linn AI, Mink R, Peteinatos GG, Gerhards R (2019) In-field classification of herbicide-resistant Papaver rhoeas and Stellaria media using an imaging sensor of the maximum quantum efficiency of photosystem II. Weed Res 59:357–366

Liu W, Anguelov D, Erhan D, Szegedy C, Reed S, Fu CY, Berg AC (2016) SSD: single shot multibox detector. Pages 21–37 in Proceedings of the 14th European Conference on Computer Vision, Part 1. Amsterdam: European Conference on Computer Vision.

Mattman C, Zhang Z (2019) Deep facial recognition using Tensorflow. Pages 45–51 in Proceedings from the 2019 IEEE/ACM Third Workshop on Deep Learning on Supercomputers (DLS). Denver, CO: Institute of Electrical and Electronics Engineers

Maxwell BD, Luschei EC (2005) Justification for site-specific weed management based on ecology and economics. Weed Sci 53:221–227

Mazerolle MJ (2020) AICcmodavg: Model Selection and Multimodel Inference Based on (Q)AIC(c). https://cran.r-project.org/package=AICcmodavg. Accessed: February 17, 2022

Mordor Intelligence (2022) Crop Protection Chemicals Market—Growth, Trends, COVID-19 Impact, and Forecast (2022–2027). https://www.mordorintelligence.com/industry-reports/global-crop-protection-chemicals-pesticides-market-industry. Accessed: January 28, 2022

Naghashzadeh M, Beyranvand AF (2015) Broad-leaved weeds in chickpea (Cicer arietinum L.) as affected by plant density and Lentagran herbicide application. Electron J Biol 11:90–92

Oinar C (2021) Object Detection Explained: R-CNN. https://towardsdatascience.com/object-detection-explained-r-cnn-a6c813937a76. Accessed: February 2, 2022

Osborne JW, Waters E (2002) Four assumptions of multiple regression that researchers should always test. Pract Assess Res Eval 8:1–5

Osorio K, Puerto A, Pedraza C, Jamaica D, Rodriguez L (2020) A deep learning approach for weed detection in lettuce crops using multispectral images. AgriEngineering 2:471–488

Oza P, Patel VM (2019) One-class convolutional neural network. IEEE Signal Proc Let 26:2

Parico AIB, Ahamed T (2020) An aerial weed detection system for green onion crops using the you only look once (YOLOv3) deep learning algorithm. Eng Agric Environ Food 13:42–48

Pokhrel S (2020) Collecting Data for Custom Object Detection. https://towardsdatascience.com/collecting-data-for-custom-object-detection-e7d888c1469b. Accessed: January 31, 2022

Python Software Foundation (2022) Python Language Reference. Version 3.9.7. http://www.python.org Accessed: March 3, 2022

R Core Team (2021) R: A Language and Environment for Statistical Computing. Vienna, Austria: R Foundation for Statistical Computing. https://www.R-project.org. Accessed: February 3, 2022

Redmon J, Divvala S, Girshick R, Farhadi A (2016) You only look once: unified, real-time object detection. Pages 779–788 in Proceedings from the IEEE Conference on Computer Vision and Pattern Recognition (CVPR). Las Vegas, NV: Institute of Electrical and Electronics Engineers

Redmon J, Farhadi A (2018) YOLOv3: An Incremental Improvement. arXiv database 1804.02767. https://arxiv.org/abs/1804.02767. Accessed: February 16, 2022

Ren S, He K, Girshick R, Sun J (2017) Faster R-CNN: towards real-time object detection with region proposal networks. IEEE T Pattern Anal 39:1137–1149

Roh MC, Lee JY (2017) Refining Faster-RCNN for accurate object detection. Pages 514–517 in Proceedings of the Fifteenth IAPR International Conference on Machine Vision Applications (MVA). Nagoya, Japan: Institute of Electrical and Electronics Engineers

Ruder S (2021) Recent Advances in Language Model Fine-Tuning. https://ruder.io/recent-advances-lm-fine-tuning. Accessed: January 31, 2022

Sapkota B, Singh V, Cope D, Valasek J, Bagavathiannan M (2020) Mapping and estimating weeds in cotton using unmanned aerial systems-borne imagery. AgriEngineering 2:350–366

Sharpe SM, Schumann AW, Boyd NS (2018) Detection of Carolina geranium (Geranium carolinianum) growing in competition with strawberry using convolutional neural networks. Weed Sci 67:239–245

Sharpe SM, Schumann AW, Boyd NS (2020a) Goosegrass detection in strawberry and tomato using a convolutional neural network. Sci Rep 10:9548

Sharpe SM, Schumann AW, Yu J, Boyd NS (2020b) Vegetation detection and discrimination within vegetable plasticulture row-middles using a convolutional neural network. Precis Agric 21:264–277

Shimao (2019) How Do Backbone and Head Architecture Work in Mask R-CNN? https://stats.stackexchange.com/questions/397767/how-do-backbone-and-head-architecture-work-in-mask-r-cnn/401107. Accessed: February 3, 2022

Shorten C, Khoshgoftaar TM (2019) A survey on image data augmentation for deep learning. J Big Data 6:60

Shung KP (2018) Accuracy, Precision, Recall or F1? https://towardsdatascience.com/accuracy-precision-recall-or-f1-331fb37c5cb9. Accessed: April 28, 2022

Shyam C, Chahal PS, Jhala AJ, Jugulam M (2021) Management of glyphosate-resistant Palmer amaranth (Amaranthus palmeri) in 2,4-D-, glufosinate-, and glyphosate-resistant soybean. Weed Technol 35:136–143

Sivakumar ANV, Li J, Scott S, Psota E, Jhala AJ, Luck JD, Shi Y (2020) Comparison of object detection and patch-based classification deep learning models on mid- to late-season weed detection in UAV imagery. Remote Sens 12:2136

Somerville GJ, Sønderskov M, Mathiassen SK, Metcalfe H (2020) Spatial modelling of within-field weed populations: a review. Agronomy 10:1044

Stanford (2022) Tutorial 3: Image Segmentation. https://ai.stanford.edu/~syyeung/cvweb/tutorial3.html. Accessed: July 19, 2022

Sun W, Dai L, Zhang X, Chang P, He X (2022) RSOD: Real-time small object detection algorithm in UAV-based traffic monitoring. Appl Intell 52:8448–8463

Szegedy C, Ioffe S, Vanhoucke V, Alemi AA (2017) Inception-v4, Inception-ResNet and the impact of residual connections on learning. Pages 4278–4284 in Proceedings of the Thirty-First AAAI Conference on Artificial Intelligence. San Francisco, CA: Association for the Advancement of Artificial Intelligence Press

TensorFlow (2017) Resource Exhausted: OOM when Allocating Tensor with Shape [2304,384] Traceback (most recent call last): #1993. https://github.com/tensorflow/models/issues/1993#issue-244306864. Accessed: July 20, 2022

TensorFlow (2021) TensorFlow 2 Detection Model Zoo. https://github.com/tensorflow/models/blob/master/research/object_detection/g3doc/tf2_detection_zoo.md. Accessed: February 2, 2022

Thanh Le VN, Truong G, Alameh K (2021) Detecting weeds from crops under complex field environments based on Faster RCNN. Pages 350–355 in Proceedings from the 2020 IEEE Eighth International Conference on Communications and Electronics (ICCE). Phu Quoc Island, Vietnam: Institute of Electrical and Electronics Engineers

ThinkAutomation (2022) ELI5: What Is Image Classification in Deep Learning? https://www.thinkautomation.com/eli5/eli5-what-is-image-classification-in-deep-learning. Accessed: April 28, 2022

Tzutalin (2015) LabelImg. Code https://github.com/tzutalin/labelImg. Accessed February 2, 2022

ultralytics (2022a) yolov5 / detect.py. https://github.com/ultralytics/yolov5/blob/master/detect.py. Accessed: February 15, 2022

ultralytics (2022b) v6.1—TensorRT, TensorFlow Edge TPU and OpenVINO Export and Inference. https://github.com/ultralytics/yolov5/releases. Accessed: July 19, 2022

vdalv (2017) Convert PascalVOC Annotations to YOLO. Code. https://gist.github.com/vdalv/321876a7076caaa771d47216f382cba5. Accessed: July 18, 2022

[WSSA] Weed Science Society of America (2016) WSSA Survey Ranks Palmer Amaranth as the Most Troublesome Weed in the U.S., Galium as the Most Troublesome in Canada. https://wssa.net/2016/04/wssa-survey-ranks-palmer-amaranth-as-the-most-troublesome-weed-in-the-u-s-galium-as-the-most-troublesome-in-canada. Accessed: January 28, 2022

Wenkel S, Alhazmi K, Liiv T, Alrshoud S, Simon M (2021) Confidence score: the forgotten dimension of object detection performance evaluation. Sensors 21:4350

Xu W, Matzner S (2018) Underwater fish detection using deep learning for water power applications. Pages 313–318 in Proceedings of the 2018 International Conference on Computer Science and Computational Intelligence (CSCI). Las Vegas, NV: Institute of Electrical and Electronics Engineers

Yang Q, Shi L, Han J, Zha Y, Zhu P (2019) Deep convolutional neural networks for rice grain yield estimation at the ripening stage using UAV-based remotely sensed images. Field Crop Res 235:142–153

Ying B, Xu Y, Zhang S, Shi Y, Liu L (2021) Weed detection in images of carrot fields based on improved YOLO v4. Trait Signal 38:341–348

Yu J, Schumann AW, Sharpe SM, Li X, Boyd NS (2020) Detection of grassy weeds in bermudagrass with deep convolutional neural networks. Weed Sci 68:545–552

Zhong L, Hu L, Zhou H (2019) Deep learning based multi-temporal crop classification. Remote Sens Environ 221:430–443

Zhuang J, Li X, Bagavathiannan M, Jin X, Yang J, Meng W, Li T, Li L, Wang Y, Chen Y, Yu J (2022) Evaluation of different deep convolutional neural networks for detection of broadleaf weed seedlings in wheat. Pest Manag Sci 2022:521–529

2.7 Figures

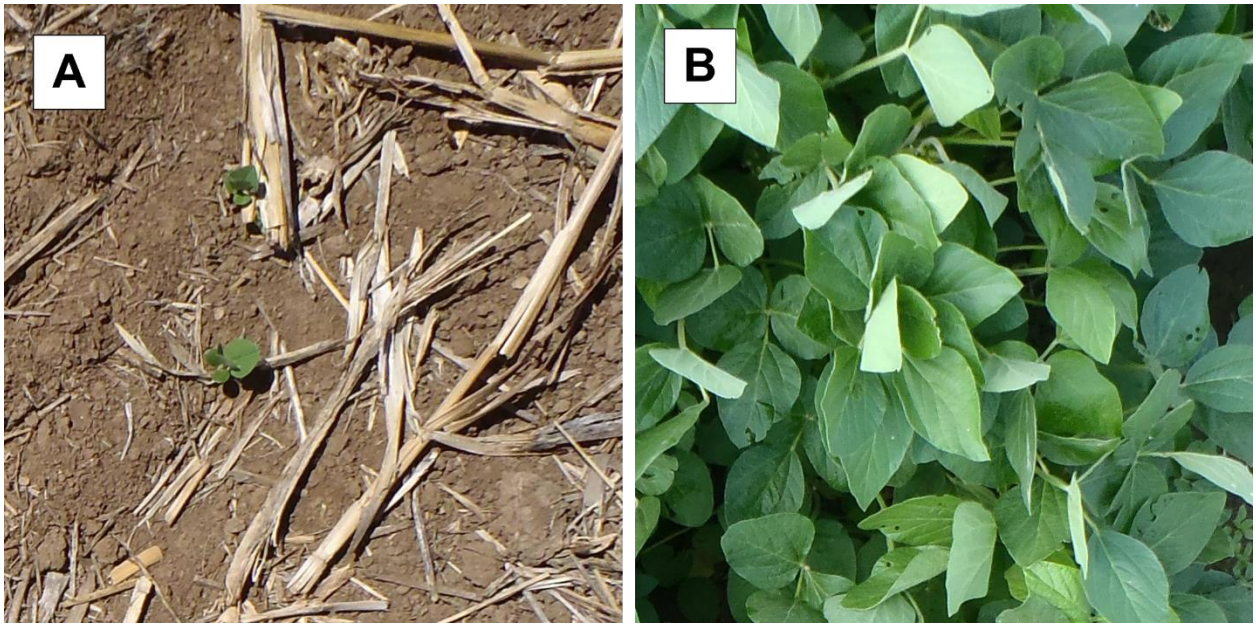

Figure 2.1 Examples of images collected for soybean in the VE - VC (A) and R2 (B) growth stages.

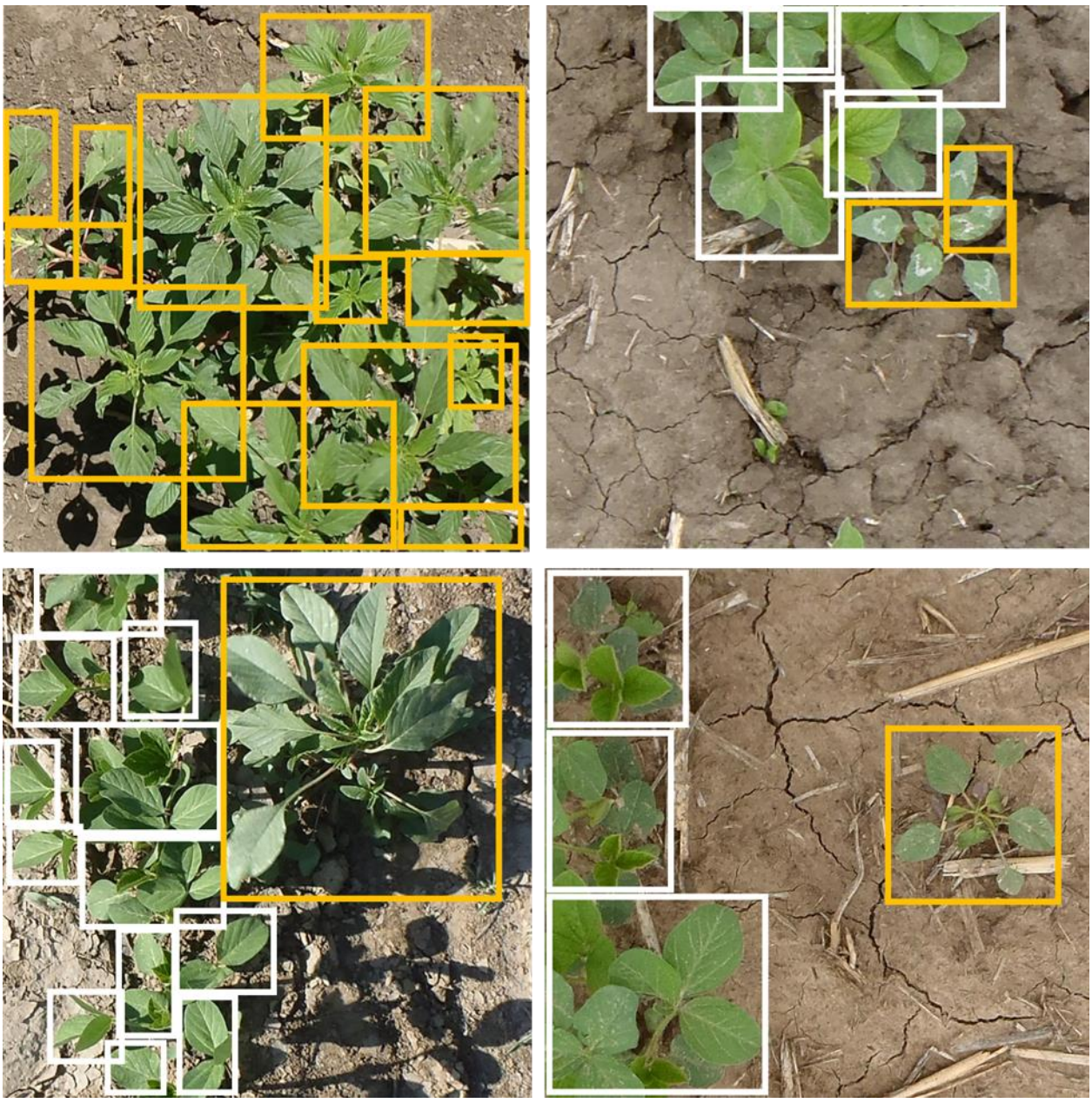

Figure 2.2 Illustration of the annotation process. *Amaranthus palmeri* and soybean plants are labeled in this figure with orange and white boxes, respectively. Bounding boxes overlap with neighboring bounding boxes when plant features are irregular. In cases where a single bounding box could not encompass a plant without including a plant of another species, multiple irregular bounding boxes were drawn on a single specimen.

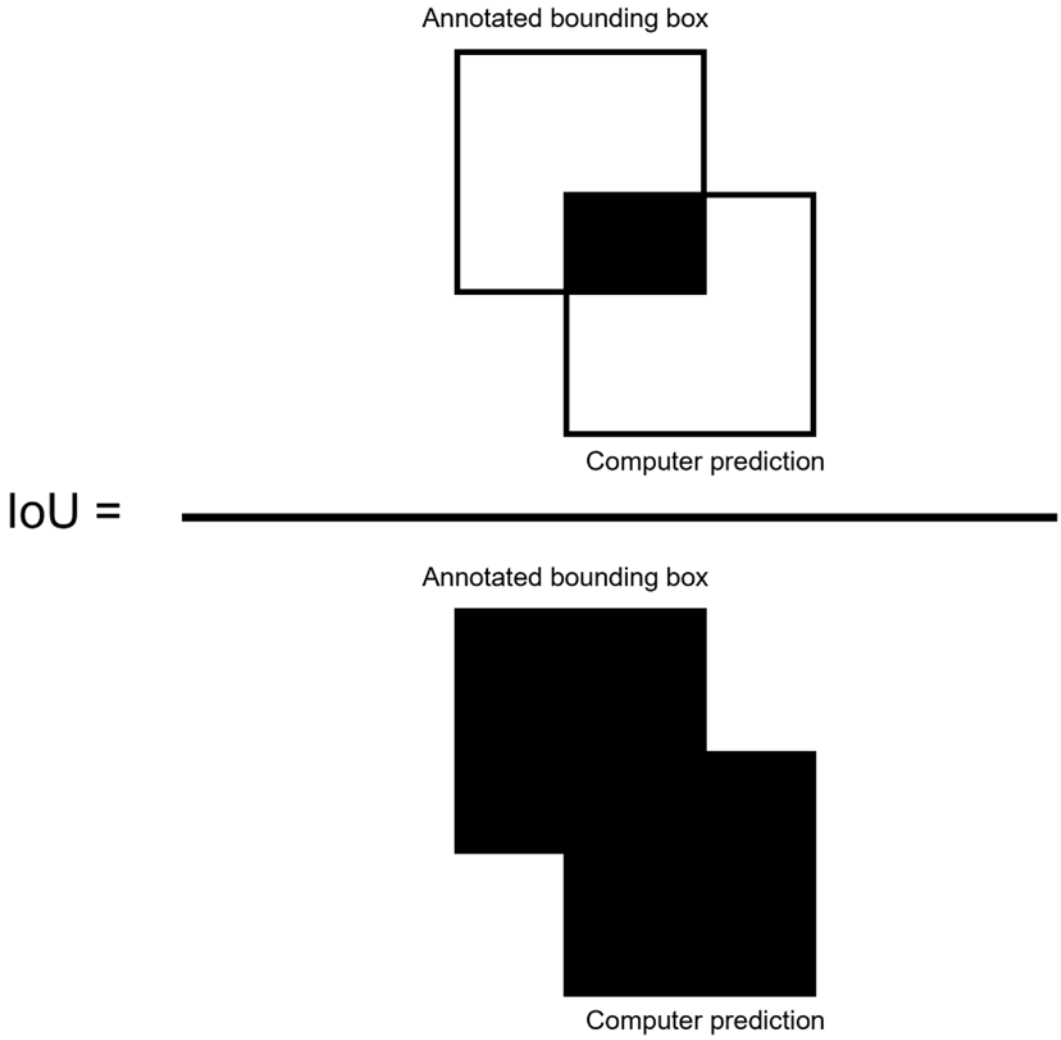

Figure 2.3 Intersection over union (IoU) equation, defined as the overlap between the ground truth annotation and the computer prediction bounding box, divided by the total area of the two bounding boxes. IoU overlaps greater than 0.5 were considered true-positive predictions, whereas overlaps less than 0.5 were considered false-positive predictions.

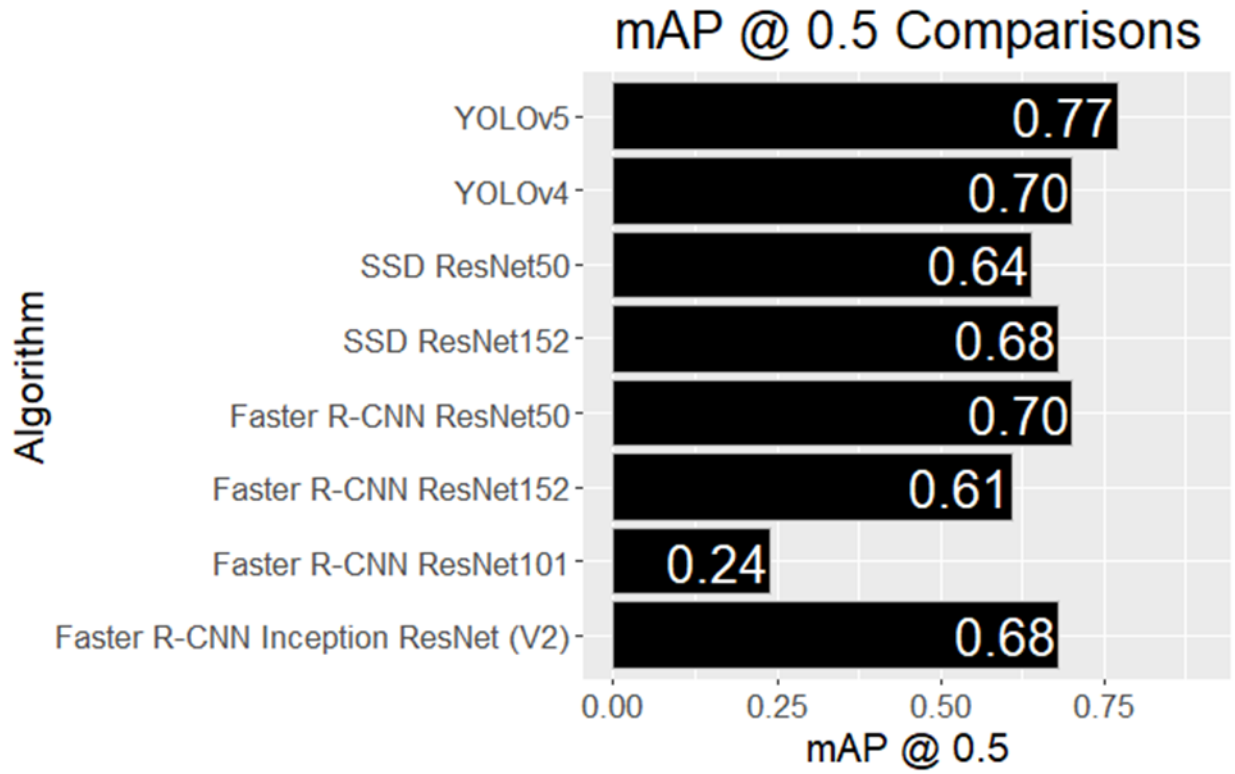

Figure 2.4 Mean average precision (mAP) results of each model after training. YOLOv5 was considered the best-performing algorithm of each tested model with a mAP of 0.77.

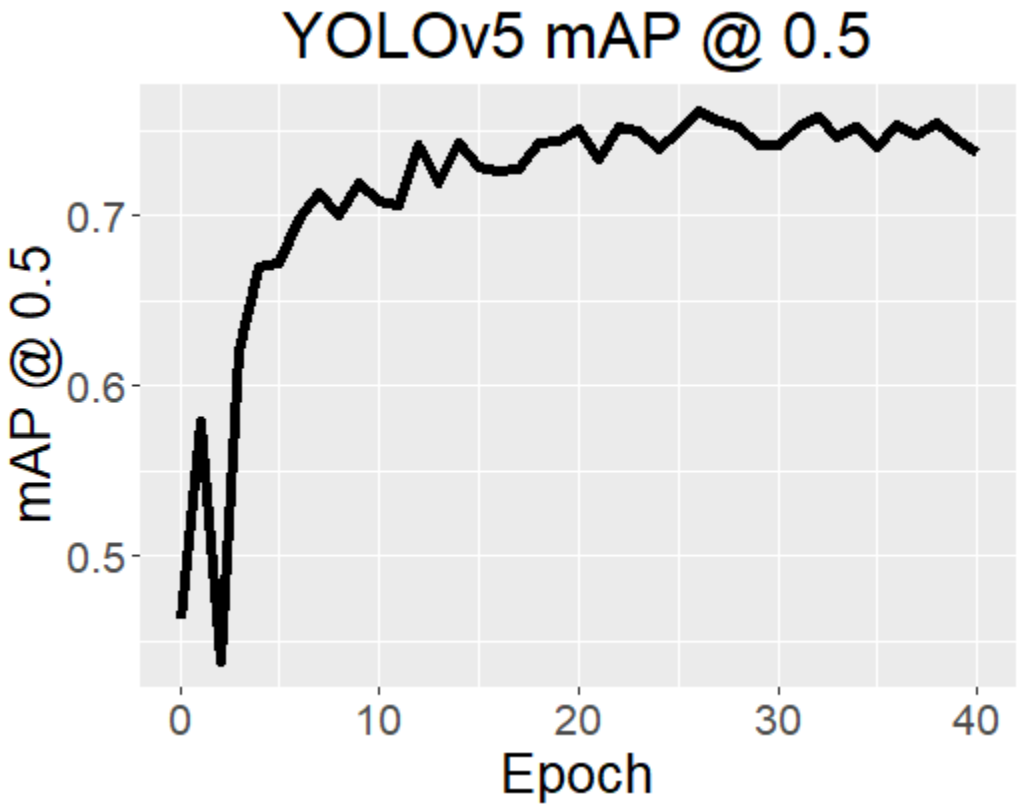

Figure 2.5 Change in mean average precision (mAP) @ 0.5 over each epoch during training. mAP was reported after the completion of each epoch. Training was terminated after visual inspection of curve and when mAP @ 0.5 curve was seen to "plateau."

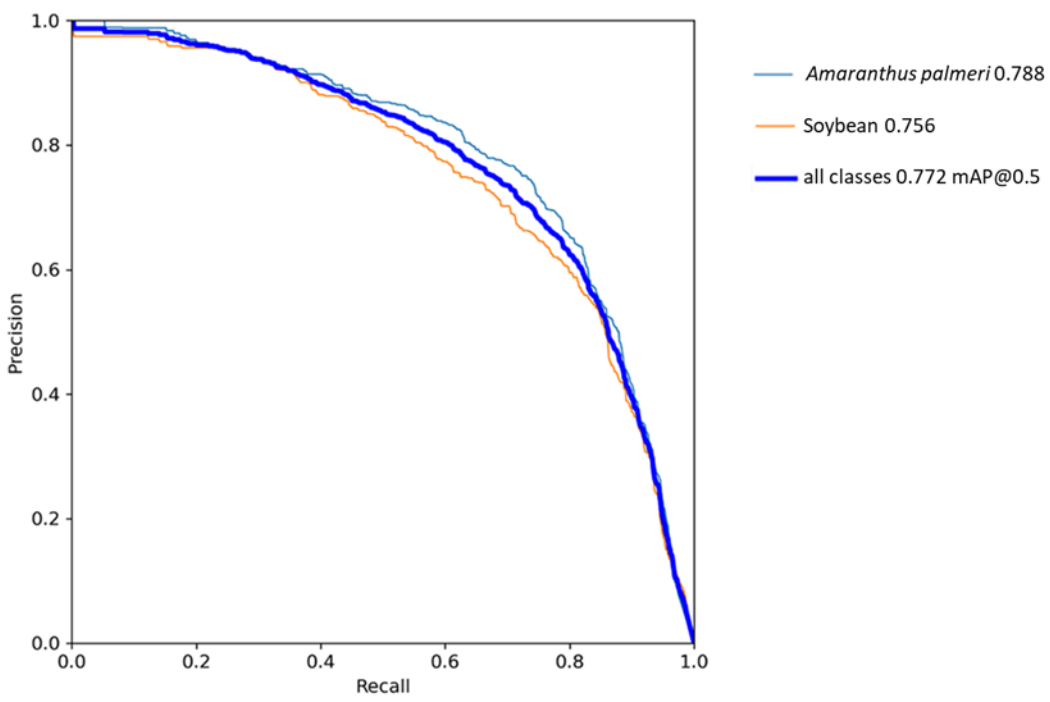

Figure 2.6 Precision–recall curve for YOLOv5. Amaranthus palmeri achieved a slightly higher average precision (AP) (0.788) than soybean. Solid blue line represents mean average precision (mAP) computed on the test data set. The AP for each class and the mAP for the overall algorithm were representative of the area of the graph under each respective curve.

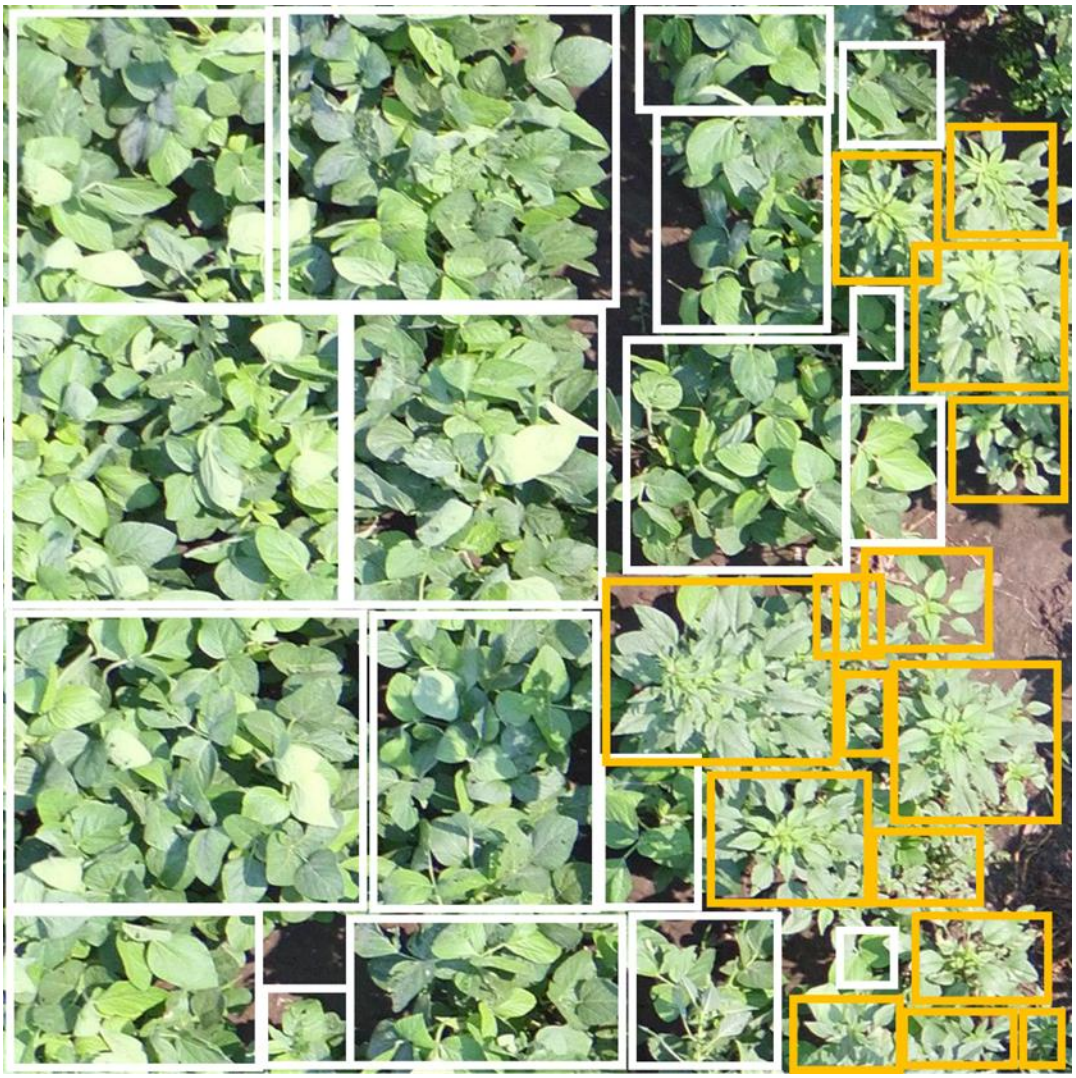

Figure 2.7 Image annotation of soybean at the R2 growth stage. As soybean populations were much higher than *Amaranthus palmeri* populations, there was a high level of soybean overlap. Therefore, it was necessary to include multiple soybean plants in each image. However, *A. palmeri* plants typically did not have as much overlap, and in most cases, it was much easier to identify and label individual plants.

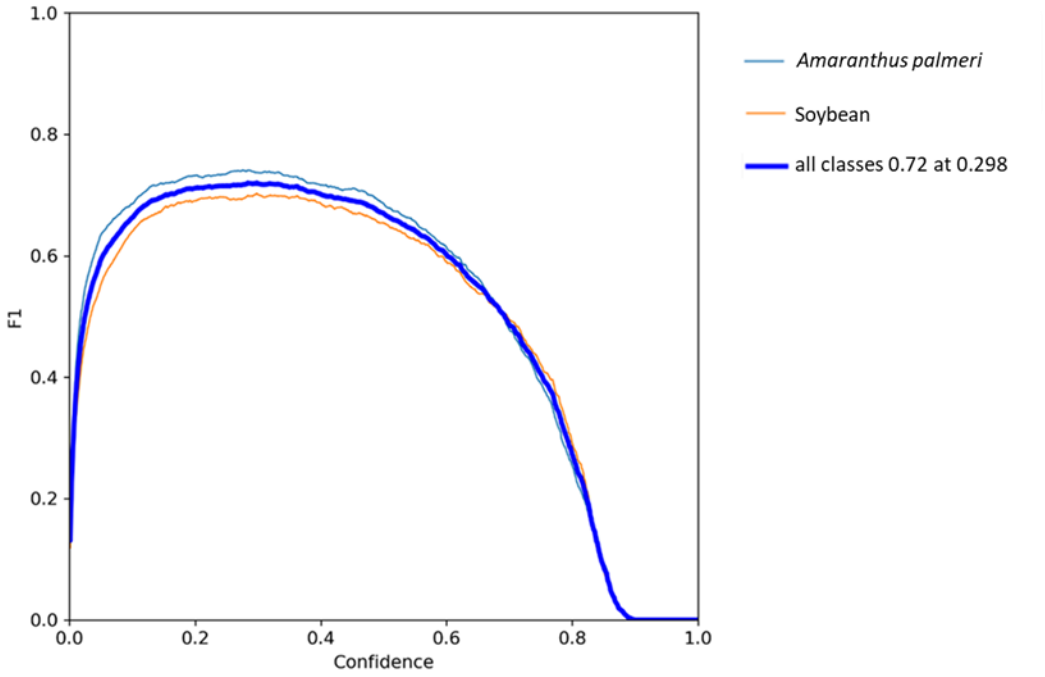

Figure 2.8 F1 scores for YOLOv5 indicating the harmonic mean between precision and recall scores. Data indicated that detection results for both species would be best at a confidence threshold of 0.298.

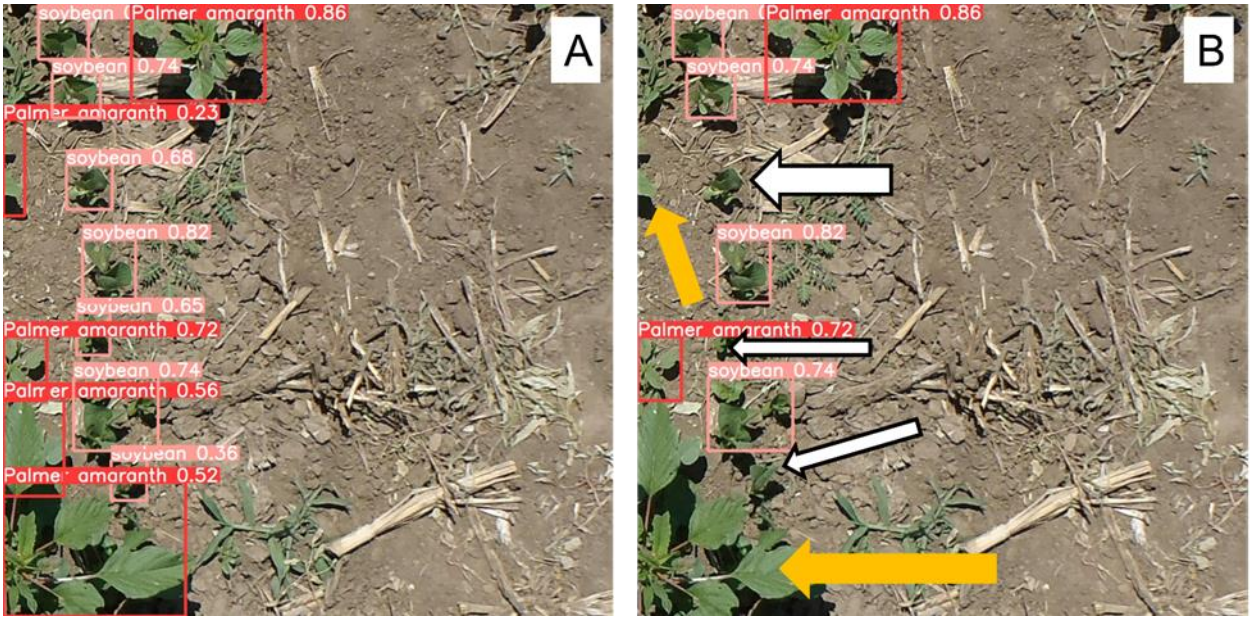

Figure 2.9 YOLOv5 detection results for *Amaranthus palmeri* and soybean using confidence thresholds of 0.15 (A) and 0.70 (B). The likelihood of false-negative (FN) detections increases as confidence thresholds increase, as can be seen in B. Objects assigned a confidence interval of less than 0.70 are not detected in B. FN *A. palmeri* and soybean detections in B are indicated by the orange and white arrows, respectively.

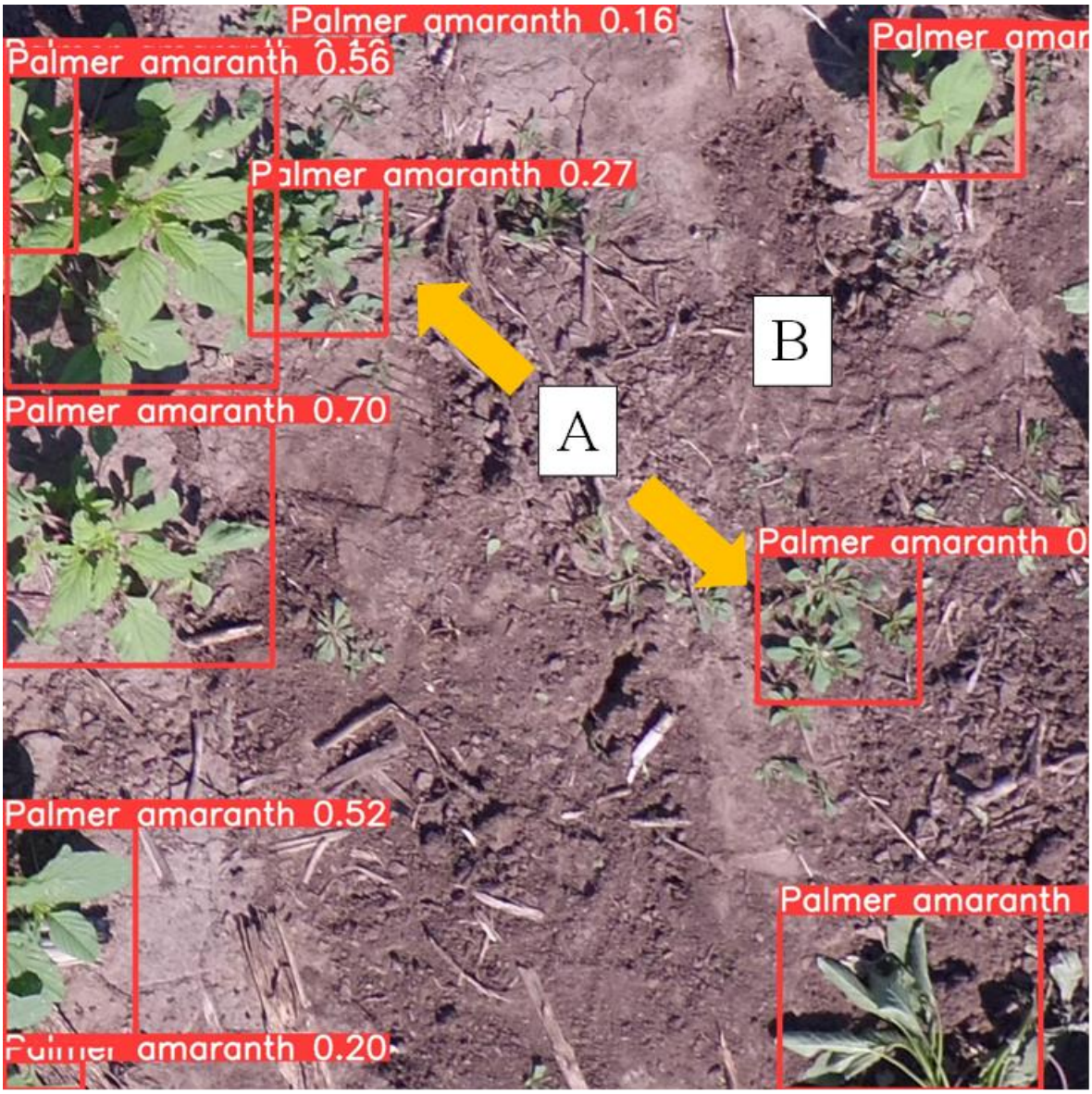

Figure 2.10 Detection results for YOLOv5 with a confidence interval of 0.15. False-positive detections of *Mollugo verticillata* and *Abutilon theophrasti* as *Amaranthus palmeri* are denoted by arrows pointing from "A" and "B," respectively.

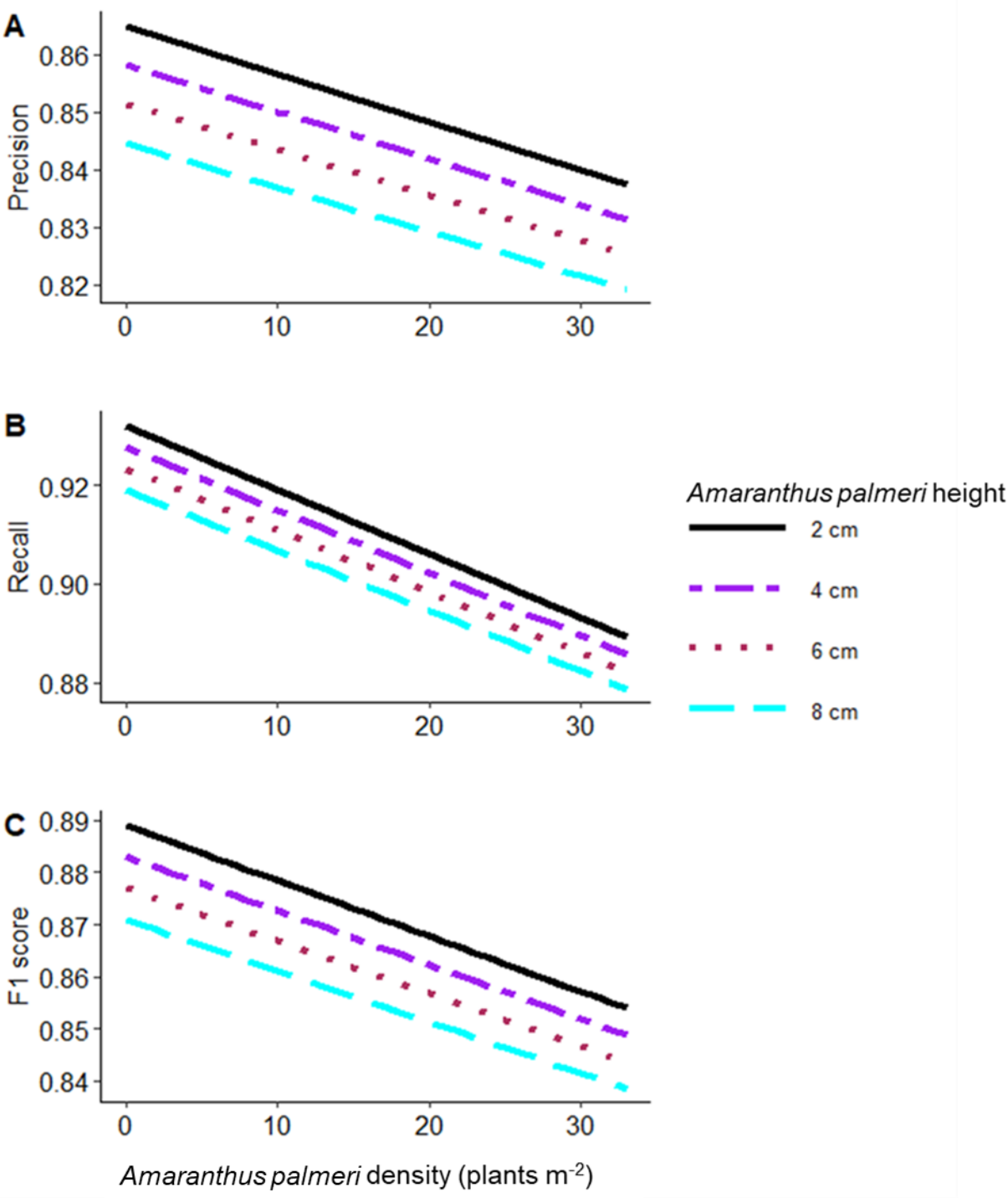

Figure 2.11 YOLOv5 precision (A), recall (B), and F1 score (C) changes as a function of *Amaranthus palmeri* density (plants m^{-2}).

2.7 Tables

Table 2.1 Dates, number of images, platform used, and height above ground for image collection at Manhattan and Gypsum, KS, field locations in 2021.

Manhattan				
Date	Images	Platform[a]	Height above ground	Image dimensions[b]
	(no.)		(m)	
May 27, 2021	35	UAV	1.5	A
June 1, 2021	90	UAV	0.5–1.5	A
June 9, 2021	17	UAV	2.8	A
June 14, 2021	44	UAV	2.0–3.0	A
June 15, 2021	14	HH	2	B
June 17, 2021	72	HH	1.2–1.5	B
June 22, 2021	150	HH	1.2–1.5	B
July 1, 2021	125	HH	1.2–1.8	B
July 8, 2021	80	HH	1.2–2.3	B
July 9, 2021	33	UAV	3.0–8.0	A
July 19, 2021	80	HH	2.3	B
July 19, 2021	61	UAV	7.0–8.0	A
July 26, 2021	40	HH	2.3	B
Gypsum				
June 21, 2021	80	HH	1.2–1.5	B
June 29, 2021	135	HH	1.2–1.5	B

July 5, 2021	80	HH	1.2–1.8	B
July 12, 2021	90	HH	1.2–1.5	B
July 12, 2021	68	UAV	6.0–7.0	A
July 20, 2021	80	HH	1.8	B
July 27, 2021	82	HH	2.3	B
July 27, 2021	44	UAV	7.0–8.0	A

[a] HH, handheld Olympus TG-510 digital camera; UAV, unmanned aerial vehicle with Zenmuse camera.
[b] Total pixel dimensions per image: A = 4,608 × 3,456; B = 4,288 × 3,216.

Table 2.2 Training information and hyperparameters used in this study.

Architecture[a]	Backbone model	Batch size	Training interval	Initial learning rate	Learning rate policy
Faster R-CNN	ResNet-50	2	100,000 steps	0.01	Cosine decay
Faster R-CNN	ResNet-101	2	100,000 steps	0.0001	Cosine decay
Faster R-CNN	ResNet-152	1	100,000 steps	0.0001	Cosine decay
Faster R-CNN	Inception ResNet-V2	1	182,500 steps	0.001	Cosine decay
SSD	ResNet-50	4	100,000 steps	0.001	Cosine decay
SSD	ResNet-152	1	100,000 steps	0.0001	Cosine decay
YOLOv4	CSPDarknet53	1	6,000 iterations	0.001	Cosine decay
YOLOv5	CSPDarknet53	4	41 epochs	0.01	Cosine decay

[a] Faster R-CNN, faster regional convolutional neural network; SSD, single-shot detector; YOLO, “You Only Look Once.”

Table 2.3 Regression models used to evaluate the effect of *Amaranthus palmeri* morphological parameters on model evaluation metrics and Akaike information criterion (AIC) used for model selection to detect *A. palmeri*. Bold type indicates that model 5 best fit the data.

Model[a]		Precision			Recall			F1 score		
		AIC	AIC Wt[b]	P-value	AIC	AIC Wt[b]	P-value	AIC	AIC Wt[b]	P-value
$y_{em} = \beta_0 + \beta_1 x_1$	1	−259.20	0	<0.0001	−304.63	0	<0.0001	−288.34	0	<0.0001
$y_{em} = \beta_0 + \beta_2 x_2$	2	−302.64	0	<0.0001	−247.97	0	<0.0001	−292.20	0	<0.0001
$y_{em} = \beta_0 + \beta_3 x_3$	3	−263.21	0	<0.0001	−268.37	0	<0.0001	−278.33	0	<0.0001
$y_{em} = \beta_0 + \beta_1 x_1 + \beta_2 x_2$	4	−337	0.28	<0.0001	−331.98	0.12	<0.0001	−349.93	0.09	<0.0001
$y_{em} = \beta_0 + \beta_1 x_1 + \beta_2 x_2 + \beta_4 x_1 x_2$	**5**	**−338.9**	**0.72**	**<0.0001**	**−335.9**	**0.86**	**<0.0001**	**−354.57**	**0.91**	**<0.0001**
$y_{em} = \beta_0 + \beta_2 x_2 + \beta_3 x_3$	6	−315.60	0	<0.0001	−275.43	0	<0.0001	−311.39	0	<0.0001
$y_{em} = \beta_0 + \beta_2 x_2 + \beta_3 x_3 + \beta_5 x_2 x_3$	7	−316.5	0	<0.0001	−274.68	0	<0.0001	−312.58	0	<0.0001
$y_{em} = \beta_0 + \beta_1 x_1 + \beta_6 x_1^2$	8	−260.90	0	<0.0001	−327.38	0.01	<0.0001	−296.14	0	<0.0001
$y_{em} = \beta_0 + \beta_2 x_2 + \beta_7 x_2^2$	9	−301.82	0	<0.0001	−246.06	0	0.0001	−291.60	0	<0.0001
$y_{em} = \beta_0 + \beta_3 x_3 + \beta_8 x_3^2$	10	−286.87	0	<0.0001	−283.37	0	<0.0001	−298.05	0	<0.0001
$y_{em} = \beta_0 + \beta_9 \log(x_1)$	11	−256.02	0	<0.0001	−285.07	0	<0.0001	−278.61	0	<0.0001

$y_{em} = \beta_0 + \beta_{10}\log(x_2)$	12	−256.03	0	<0.0001	−241.07	0	0.0009	−264.51	0	<0.0001
$y_{em} = \beta_0 + \beta_{11}\log(x_3)$	13	−262.75	0	<0.0001	−269.19	0	<0.0001	−281.14	0	<0.0001

[a] y_{em} = evaluation metric (precision, recall, F1 score), x_1 denotes density (plants m^{-2}), x_2 denotes height (cm), and x_3 denotes coverage (m^2). β_0, intercept; β_1, coefficient for *A. palmeri* density (plants m^{-2}); β_2, coefficient for height (cm); β_3, coefficient for coverage (m^2); β_4, interaction coefficient for density and height; β_5, interaction coefficient for height and coverage; β_6, coefficient for the square of density; β_7, coefficient for the square of height; β_8, coefficient for the square of coverage; β_9, coefficient for the log of density; β_{10}, coefficient for the log of height; β_{11}, coefficient for the log of coverage.

[b] AIC weight, indicating the total predictive power among all tested models.

Table 2.4 Linear regression results (model 5) for *Amaranthus palmeri* density (plants m−2) and height (cm) regressed against model evaluation metrics.

Evaluation metric	Parameter estimates[a]			R^2	RMSE[b]	P-value
	Density	Height	Density × height			
Precision	-8.6×10^{-4}***	-3.4×10^{-3}***	1.1×10^{-5}*	0.42	0.10	<0.0001
Recall	-1.3×10^{-3}***	-2.2×10^{-3}***	1.4×10^{-5}*	0.43	0.10	<0.0001
F1 score	-1.1×10^{-3}***	-3.0×10^{-3}***	1.4×10^{-5}*	0.44	0.10	<0.0001

[a] Significant at: *P < 0.05, *** P < 0.001
[b] RMSE, root mean square error

Chapter 3 - Evaluating ONE SMART SPRAY for weed control in Midwestern United States corn and soybean crops

Note: This manuscript is currently being edited and formatted for submission to Weed Science journal.

3.1 Abstract

Precision sprayers use artificial intelligence to enable on-the-go weed detection and application, thereby reducing the need to spray entire fields. A precision sprayer was evaluated for treating weeds in corn (*Zea mays* L.) and soybean (*Glycine max* [L.] Merr.) cropping systems in the Midwestern United States. Using a ONE SMART SPRAY sprayer, our objectives were to (1) evaluate the efficacy of different herbicide application programs, including one-pass versus two-pass programs, spot-spray (SS) only, and simultaneous broadcast (BCST) residual and SS foliar herbicides; (2) determine if sensor weed detection thresholds influenced weed control; and (3) determine the seasonal cost for each herbicide program compared to a traditional broadcast application. Field experiments were conducted in 2022 and 2023 near Manhattan, KS and in 2023 at Seymour, IL. Both green-on-brown (GOB; burndown applications) and green-on-green (GOG; in-crop applications) were evaluated. Main plot treatments consisted of five herbicide programs and the split-plot consisted of four weed detection thresholds: herbicide efficacy, balanced, savings, and a broadcast application. The percentage of weed-free area within each plot was estimated visually on a scale of 0 to 100, with 0 indicating complete weed infestation and 100 indicating zero weed pressure. As-applied maps were constructed using raw sprayer data collected during applications and used to compare the percentage of each plot sprayed to determine program costs. Results indicated that herbicide programs with simultaneous BCST and SS components, in many cases, resulted in weed-free area equal to or not different than broadcast

applications with the same herbicides. SS herbicide applications were less expensive than broadcast applications. Precision sprayers such as ONE SMART SPRAY demonstrated great potential to reduce herbicide input costs without compromising weed control.

Key words:

Artificial Intelligence, precision spraying, site-specific weed management, ONE SMART SPRAY

3.2 Introduction

Weeds often grow in distinct patches rather than uniformly across an entire agricultural field (Maxwell and Luschei 2005). Despite this reality, herbicides are traditionally broadcast-applied instead of only where the weeds occur (Huang et al. 2018). To address this, site-specific weed management (SSWM) has been proposed, defined as the process of adapting weed management strategies within a field to match the location of the weed infestations (Fernández-Quintanilla et al. 2018; Wiles 2009). SSWM provides opportunities for farmers to reduce total herbicide applied, reduce input costs, and minimize environmental contamination while maintaining weed control (Barroso et al. 2004; Bongiovanni and Lowenberg-DeBoer 2004; Ferreira et al. 2019). In terms of chemical weed control, this would result in herbicides being sprayed only where they are needed (Rozenberg et al. 2021). However, a major challenge to SSWM is developing a reliable and accurate method of weed detection that is robust to a multitude of field conditions (Gao et al. 2020).

In the last decade, artificial intelligence (AI) has become a major part of modern-day life and is defined as the science behind producing and creating intelligent machines (McCarthy 2007). First described by Alan Turing in a 1950 paper entitled "Computing Machinery and Intelligence" (Turing 1950), AI has evolved from a simple series of "if-then" statements to complicated algorithms that make decisions like how the human brain does (Kaul et al. 2020). A subset of AI known as deep learning is most often used for SSWM; more specifically, convolutional neural networks (CNNs) are used because they can analyze and extract features within imagery that cannot be seen with the human eye (Albawi et al. 2017; Sapkota et al. 2020). With advances in graphics processing units and computer processors, weed detection using CNNs has become more feasible. Artificial intelligence algorithms have been used to detect

weeds in many different crops including corn (*Zea mays* L.), soybean (*Glycine max* [L.] Merr.) (Ahmad et al. 2021), rice (*Oryza sativa* L.) (Yang et al. 2021), bermudagrass (*Cynodon dactylon* [L.] Pers.) turf (Xie et al. 2021), sugar beet (*Beta vulgaris* L.) (Gao et al. 2020), lettuce (*Lactuca sativa* L.) (Osorio et al. 2020), and wheat (*Triticum aestivum* L.) (Jabir and Falih 2022).

Even though AI can be used to detect weeds, the challenge is accomplishing this in real time and simultaneously delivering effective weed control. Two common types of real-time weed detection platforms are self-propelled weeding robots and field sprayers (Gerhards et al. 2022). Machines such as the Tertill® weeding robot (Tertill® Corporation, North Billerica, Massachusetts, USA) can locate weeds and use either herbicides or a mechanical string trimmer to control them. Research has shown that the Tertill® led to an 18 to 41% improvement in weed control when compared to standard cultivation (Sanchez and Gallandt 2020). Additionally, Ruigrok et al. (2020) trained the AI object detection algorithm You Only Look Once (YOLOv3) (Redmon and Farhadi 2018) to detect volunteer potatoes (*Solanum tuberosum* L.) in sugar beet crops and uploaded the trained model to an autonomous spraying robot. The authors reported that 96% of the volunteer potatoes were effectively controlled, while only 3% of the sugar beets were incorrectly sprayed.

A major drawback of current robotic weed control technology is that several robots working together are required to cover large acreage fields in a reasonable time frame (Gerhards et al. 2022); for this reason, many have turned to AI-powered field sprayers to increase efficiency and speed of weed control applications. Hussain et al. (2020) designed a sprayer to detect common lambsquarters (*Chenopodium album* L.) for herbicide applications and diseased potato plants for fungicide applications, respectively. The authors reported that chemical savings were between 42 and 43% for herbicide and fungicide applications, respectively. Jin et al. (2023)

constructed an intelligent sprayer to control weeds in bermudagrass turf and reported no differences in control of broadleaf weed species between plots receiving conventional broadcast and precision spot-spray applications. In addition to these prototype sprayers developed by research groups, commercial intelligent sprayers are becoming available on the market. Examples of such sprayer systems, both available and soon to be available in the United States, include the John Deere® See & Spray™ Ultimate (John Deere, One John Deere Place, Moline, IL, USA), Greeneye Technology™ (Greeneye Technology, Shocken Street 13, Tel Aviv-Yafo, Israel), and ONE SMART SPRAY (Bosch BASF Smart Farming, Cologne, Germany).

Because these sprayers are equipped with AI weed detection algorithms, different approaches to herbicide applications can be taken. Artificial intelligence AI algorithms usually allow for different settings known as confidence intervals, or thresholds, when detecting objects within imagery (Barnhart et al. 2022). When objects are correctly detected, they are known as true positives, whereas incorrectly detected objects or a misplaced detection are known as false positives (Ralašić 2021). Thresholds regulate the number of false positives in the final detection pass (Wenkel et al. 2021) and are often expressed as confidence intervals between 0 and 1. Based on how the algorithm was trained, object detection algorithms assign a series of confidences to objects within each image/video frame when deployed for detections. When a detection threshold is specified by users, algorithms will detect all objects with confidences equal to and greater than the specified threshold. Lower thresholds result in more false positives and thus, would maximize the chances of more weeds being detected. Conversely, higher thresholds would result in more confident detections, but would likely result in missed weed detections because some objects would have confidence values less than the specified threshold (Barnhart et al. 2022 In terms of precision spraying, these confidence intervals can translate to an efficacy

(lower) threshold with more herbicide applied or a savings (higher) threshold approach resulting in less herbicide being applied.

In addition to SS, many of these AI-enabled commercial sprayers are equipped to simultaneously broadcast soil residual herbicides and SS foliar herbicides whenever weeds are detected (Greeneye Technology 2023; John Deere 2023). Such sprayer technology becoming available in the market opens new opportunities to understand how they can be best utilized to control weeds in agronomic cropping systems. Therefore, the objectives of this study were to (1) evaluate the weed control efficacy of different commercial AI sprayer herbicide treatment programs, including One-pass versus two-pass programs, spot-sprayed treatments only, and simultaneous broadcasted residual and spot-sprayed foliar herbicides compared to traditional broadcast applications; (2) determine if sensor weed detection threshold settings influence weed control; and (3) determine the seasonal cost for each herbicide program, comparing each with a traditional broadcast treatment.

3.3 Materials and Methods

3.3.1 Description of field sites

Field experiments were established both in 2022 and 2023 in Kansas and in 2023 in Illinois. The Kansas experiments were established in rainfed corn/soybean no-till crop rotation production fields at the Kansas State University, Department of Agronomy Research Farm near Manhattan, KS. In 2022, two locations were initiated and will be referred to as MAN 1 (39.125°N, 96.648°W) and MAN 2 (39.130°N, 96.644°W). MAN 1 and MAN 2 were planted with corn and soybean in 2022, respectively, and were rotated to the subsequent crop in 2023. In 2023, additional corn and soybean field experiments were established south of the BASF

Midwest Research Farm near Seymour, IL (40.039°N, 88.403°W) (SEY Corn and SEY Soy for corn and soybean trials, respectively). Locations in IL were conventionally tilled and rainfed. For all locations, crops were planted in rows spaced 76 cm apart (Table 3.1).

Both MAN 1 and MAN 2 were located on a Smolan silty clay loam with 3 to 7% slope (Web Soil Survey 2023). MAN 1 had natural infestations of Palmer amaranth (*Amaranthus palmeri* S. Watson), shattercane (*Sorghum bicolor* [L.] Moench), common waterhemp (*Amaranthus tuberculatus* [Moq.] Sauer), smooth groundcherry (*Physalis longifolia* Nutt. Var. *subglabrata* [Mack. & Bush] Cronquist), honeyvine milkweed (*Cynanchum laeve* [Michx.] Pers.), and yellow foxtail (*Setaria pumila* [Poir.] Roem. & Schult.). In both years, MAN 1 had relatively low overall weed infestations; MAN 2, however, had greater infestations of yellow foxtail, Palmer amaranth, common waterhemp, common cocklebur (*Xanthium strumarium* L.), fall panicum (*Panicum dichotomiflorum* Michx.), and common pokeweed (*Phytolacca americana* L.). The SEY Corn and SEY Soy experiments were established in a field with Drummer silty clay loam with 0 to 2% slope (Web Soil Survey 2023). Due to drought early in the season, weed infestations in Illinois were much less than the Kansas fields, and consisted primarily of common purslane (*Portulaca oleracea* L.), velvetleaf (*Abutilon theophrasti* Medik.), common waterhemp, and morningglory (*Ipomoea*) species.

3.3.2 Field sprayer

A ONE SMART SPRAY research sprayer was used for this study. The sprayer had the same external hardware as a commercial ONE SMART SPRAY sprayer but was custom-built for small plot research. The spray apparatus consisted of an aluminum frame mounted to the front of a John Deere® 6125R™ tractor (Figure 3.1a). The sprayer was equipped with two booms (Figure

3.1b) with the front boom reserved for SS, while the rear boom was used for broadcast applications. Within each meter of boom, a camera was mounted between two red and infrared (IR) Light Emitting Diode (LED) lights to provide consistent lighting across diverse field conditions (Spaeth et al. 2024). Red-Green-Blue cameras were equipped with R/NIR filters, allowing the sprayer to distinguish between plants and other objects (Spaeth et al. 2024). Both the cameras and LED lights were mounted at a 25° angle relative to the ground. The system can detect weeds as small as 5 mm.

The front and rear boom nozzle bodies were spaced at 25.4 cm and 50.8 cm intervals, respectively, and spray swaths were 3.05 m wide for both booms. Spray pressure was provided with CO_2 pressurized tanks mounted at the rear of the spray apparatus, and pressure was manually adjusted prior to spraying. The ONE SMART SPRAY system is capable of two types of applications: green-on-brown (GOB) and green-on-green (GOG) (Quigley 2023). Green-on-brown applications refer to burndown/pre-emergence applications where no crops are present; the system does not use AI for these applications because green vegetation can be easily detected with IR and NIR light (Nguyen et al. 2012). On the other hand, GOG applications are made in-crop and therefore use AI to distinguish weeds from crops. The GOG applications with ONE SMART SPRAY currently use AI to recognize crop rows and spray green vegetation detected outside of the rows (Spaeth et al. 2024).

3.3.3 Field experiments

At each location, experiments were set up in a split-plot arrangement of treatments in a randomized complete block design with five replications. The main plot factor was herbicide application program, and the split-plot factor was sprayer threshold. For the MAN 1, SEY Corn,

and SEY Soy locations, plot dimensions were 3 m (4 crop rows) wide by 30.5 m long, whereas plot dimensions for the MAN 2 location were 3 m wide by 35.1 m long.

The five herbicide application programs were designated as 1 to 5 for explanatory purposes (Table 3.2). Program 1 consisted of a GOB application including simultaneous broadcast (BCST) residual and spot-spray (SS) foliar herbicides followed by a GOG application with only SS foliar herbicides (approximately 21 to 28 days after the GOB treatment, or DAGBT), identified as Residual Program. Program 2 consisted of a SS GOB and SS GOG, with no residual herbicides applied. Program 3 was a One-pass approach with a single GOB BCST + SS application. Program 4 was a two-pass approach and introduced a novel concept known as a "Spike" treatment, in that a minimal recommended rate of foliar herbicide was BCST at both GOB and GOG superimposed by a SS application to increase the rate of herbicide applied when weeds were detected. The minimal rate was included for general control and was increased when weeds were detected to increase likelihood of control. Finally, Program 5 was a two-pass approach with a split and overlapping application of residual herbicides for both GOB and GOG. For interpretability, programs 1 to 5 will henceforth be referred to as the 'Residual at-plant', 'SS only', 'One-pass', 'Spike', and 'Overlapping residual' programs, respectively.

The split-plot factor included four SS application detection thresholds randomized within each main treatment: Herbicide *Efficacy*, herbicide *Savings*, a *Balanced* setting, and a traditional *Broadcast* application. Although exact settings are proprietary in nature, an herbicide efficacy approach corresponds to AI algorithm thresholds that include the potential for more false positive detections; that is, in theory ensuring that all detected weeds are sprayed but may result in some crop plants being sprayed when classified as weeds. We refer to this threshold as an *"Efficacy"* threshold in that the intent was to ensure that all weeds were sprayed, not to be

confused with when “efficacy” is used to describe the effectiveness of a given herbicide. Conversely, an herbicide *Savings* approach would have the potential for more false negative detections; that is, correctly detecting most weeds but missing some. To investigate a threshold level between these two, the selected setting was chosen as a *Balanced* approach. Finally, a no-threshold (traditional *Broadcast*) treatment was included to compare to SS thresholds. In 2022, ONE SMART SPRAY thresholds were not available for GOB applications; as a result, the One-pass program had no threshold treatments applied and in 2023, the same treatment was applied .

Herbicides, adjuvants, and application rates were specific for corn (Table 3.3) and soybean programs (Table 3.4). For all corn and soybean locations, BCST applications were sprayed at a carrier rate of 93.5 l ha^{-1} and SS applications were sprayed at 140.3 l ha^{-1}. Sprayer application speed was 8 km hr^{-1} in 2022 and, due to software upgrades, application speed was increased to 9.7 km hr^{-1} in 2023. In 2022, BCST applications were made with TTI11002 flat-fan nozzles and SS applications with TP6502 even fan nozzles (TeeJet Spraying Systems Co., Wheaton, IL), pressurized at 195 and 117 kPa, respectively. With the software upgrades and speed changes made for the 2023 season, the same nozzles were used but BCST and SS boom pressures were increased to 276 and 159 kPa, respectively. All application dates and crop stages for GOG applications are in Table 3.5.

3.3.4 Data collection

Visual estimation of the percentage of weed-free area in each plot was determined from the middle two crop rows of each plot using a scale of 0 to 100%, with 0% indicating a plot completely infested with weeds and 100% indicating no weeds. For each plot, data were not taken in the first or last 1.5 m of each plot length. These assessments were taken 21 days after the

GOB treatment (DAGBT) in 2022 and 14 DAGBT in 2023, and 42 days after the GOG treatment (DAGT) at all locations and years. Weed density was determined from two randomly placed 1-m^2 quadrats within each plot at the same DAGBT, and at 14 DAGT. Total weed density across all species was collected rather than by individual weed species because ONE SMART SPRAY does not identify by weed species.

End-of-season weed biomass and final grain yield were determined at harvest at the MAN 1 and MAN 2 locations in both 2022 and 2023. Drought and lack of field space delayed planting of crops at SEY Corn and SEY Soy, and therefore did not mature for harvest. End-of-season weed biomass combined across species was sampled just prior to crop harvest from two randomly placed 0.5 m-by-1 m quadrats within each plot. Samples were oven-dried at 58 C until constant biomass was achieved. Grain was harvested from the middle two rows of each plot with a small-plot combine at physiological maturity and grain yield determined at 15.5% moisture for corn and 13% for soybean. The MAN 1 location was not harvested in 2023 due to combine mechanical issues.

3.3.5 As-applied map generation

As-applied maps were generated to determine the percentage of each plot that was sprayed. The ONE SMART SPRAY system collected geospatial data points for each nozzle on the SS boom and automatically labeled each point as “TRUE” when a nozzle was spraying or “FALSE” when not spraying. These data points were collected at a density of approximately 10 points m^{-2} (Figure 3.2). Data points were geotagged with GPS coordinates and stored as a CSV file within the machine. After each application, raw data files were imported into Jupyter Lab (Kluvyer et al. 2016) and as-applied spray maps were generated using the Python 3.9 (Python

2023) packages Geopandas (Jordahl et al. 2020), Shapely (Gillies et al. 2023), and SciPy (Virtanen et al. 2020). A grid of 0.2 m-by-0.2 m cells was overlaid across each experimental location to ensure high resolution within the resulting map. A nearest neighbor interpolation (SciPy docs 2023) was used to generate the as-applied map. A nearest neighbor interpolation assigns the value nearest to a corresponding grid cell to be the estimated value (Varella et al. 2015), with the goal of producing a binary map of 0 and 1 indicating when each nozzle was not spraying or spraying, respectively. With the high density of data points collected by the machine, a nearest neighbor interpolation method requires considerably less computational power than alternative methods such as kriging (van Stein et al. 2019). Maps were exported to QGIS 3.22.7 (QGIS 2023) where the percentage of sprayed area within each sub-plot was computed. The percentage of area sprayed within each sub-plot was multiplied by the cost ($US) ha^{-1} of a broadcast application for each herbicide tank mixture, obtaining a cost ha^{-1} for each treatment. The amounts of herbicides and adjuvants applied were computed based on the percentage of the plot where the sprayer nozzles were turned on; different herbicides and rates were accounted for in these calculations depending on the program. Herbicide costs were taken from the 2023 Kansas State University Chemical Weed Control Guide (Lancaster et al. 2023).

3.3.6 Statistical analysis

All statistical analyses were done using R 4.3.1 (R Core Team 2023). For this study, corn and soybean experiments were analyzed separately. Linear mixed effects models were used to analyze all data. Because of the absence of thresholds for GOB applications, the experiments were therefore analyzed two ways: First as a randomized complete block design to analyze overall herbicide program performance (objective 1), and secondly as a split-plot design, after

removing the One-pass program, to analyze the effect of thresholds (objective 2). To meet assumptions of the analysis, data were analyzed using a beta distribution with the glmmTMB (Brooks et al. 2017) package in R. Data were logit transformed and automatically back transformed by the package after building the model. Model residuals were checked for normality and homogeneity of variance using the DHARMa (Hartig 2022) package. ANOVA models were conducted with Type III Wald chi-square tests (as described in Miranda et al. 2022), which was the test used by the glmmTMB package. For significant models, Tukey's Honest Significant Difference post-hoc test was used to determine differences among main effect means and a confidence level of $p < 0.05$ was used. Post hoc tests were conducted with the emmeans (Lenth 2023) package.

For overall program evaluation, the response variables were percent weed-free area, weed density counts, end-of-season weed biomass measurements, and grain yield, the fixed effects were location and herbicide program, and the random effect was replication for overall program evaluation. To analyze thresholds, the fixed effects were the interaction of herbicide program and threshold, with the random effects were replication and replication by herbicide program. When conducting an additional analysis, locations often interacted with herbicide program (data not shown), because of differences in overall weed infestation levels, locations were analyzed separately. Whole-season herbicide costs (based on the percentage of each sub-plot sprayed) were limited to 2023 data because the 2022 GOB application data were lost due to a machine data decoder error. Fixed and random effects for the herbicide cost data were the same as previously described for overall program and threshold analyses. In this analysis, we did not consider the operating costs of the sprayer, but only input costs for herbicides and adjuvants.

3.4 Results and Discussion

3.4.1 Herbicide program evaluation

3.4.1.1 Green-on-brown weed-free area

Herbicide programs resulted in different amounts of weed-free area observed after the GOB application in both soybean and corn experiments. In soybean at 21 DAGBT in 2022 or 14 DAGBT in 2023, herbicide program resulted in different weed-free area observed for each location ($p < 0.0001$ for both Manhattan 2022 and Manhattan 2023, and $p = 0.01$ for Seymour 2023) (Table 3.6). Within each location, the weed-free area of all programs with residual herbicides (Residual at-plant, One-pass, and Overlapping residual) and the Spike program were not different from one another. The SS only program had no residual herbicides applied by this observation time in soybean and had less weed-free area than the One-pass program in Manhattan 2022, all other programs in Manhattan 2023, and the Residual at-plant and One-pass programs in Seymour 2023. Overall, Manhattan 2023 and Seymour 2023 had more weed-free area compared with the Manhattan 2022 location. This was likely because the MAN 2 field (Manhattan 2022 study) contained a greater weed infestation compared to the other fields.

In corn at 21 DAGBT in 2022 and at 14 DAGBT in 2023, herbicide program was significant ($p < 0.0001$) for all locations (Table 3.7). Similar to the soybean results, the SS only program resulted in the least weed-free area in Manhattan 2022 and Manhattan 2023 and was not different from only one program (“Spike”) in Seymour 2023. The Residual at-plant program contained either the most weed-free area or was not different than the highest weed-free area within each location. Both Manhattan fields had less weed-free area than the Seymour location, which experienced drought and had lower weed pressure compared to the Manhattan KS fields in 2023 (data not shown).

At this point in the season, the SS only program (the only program with no broadcasted residual or foliar herbicide) always contained less weed-free area than at least one program with a uniform broadcast application at each experiment. These results are consistent with Genna et al. (2021), as the authors found that herbicide efficacy (reduction in weed density) was often greater with broadcast applications compared to GOB SS applications. Thus far, these results suggest that including a broadcast component to ONE SMART SPRAY GOB applications could increase weed-free area compared to SS only approaches.

3.4.1.2 Green-on-green weed-free area

Like the GOB application, herbicide programs resulted in different weed-free areas observed by 42 DAGT in both soybean and corn experiments. In the soybean studies, herbicide program significantly affected weed-free area ($p < 0.0001$) at each location (Table 3.8). At Manhattan 2023 in the MAN 1 field, all programs performed well with 89 to 98% weed-free area by 42 DAGT. In general, this field (MAN 1) had less weed occurrence. The One-pass program had the least weed-free area at 42 DAGT at each location. The One-pass program at both Manhattan 2022 and at Seymour 2023 became very weedy by 42 DAGT, because no in-crop herbicide was applied. Differences between the 2023 Manhattan and Seymour locations were likely due to rainfall patterns: the Manhattan fields received rainfall early on (89 mm between planting and GOG application; Kansas Mesonet 2024), while the SEY Soy field was very dry at time of planting (35 mm between June 1 and planting; CoCoRaHS 2024) but did receive rain later in the season (111 mm between GOG application and August 31, 2023; CoCoRaHS 2024) allowing for more weeds to emerge and grow after the herbicide programs were applied.

In the corn studies, herbicide program was not significant in both the Manhattan 2022 and Seymour 2023 studies ($p = 0.08$ and $p = 0.97$, respectively), but was significant for the Manhattan 2023 study ($p < 0.0001$) (Figure 3.3). Each of the weed-free areas for the overlapping residual, Residual at-plant, and Spike programs were not different from one another. However, the One-pass herbicide program had the least weed-free area.

Multiple application passes that include residual herbicides are still recommended when using intelligent sprayer technology such as ONE SMART SPRAY. The One-pass program, which included residual herbicides applied at crop planting, resulted in the smallest percent of weed-free area in soybean at 42 DAGT across locations: 48% at Manhattan 2022, 86% at Manhattan 2023, and 33% Seymour 2023. These results are supported by other studies, in that One-pass herbicide programs led to increased weed infestations or allowed more weed escapes compared to two-pass programs (Craigmyle et al. 2013; Johnson et al. 2007; Mobli et al. 2023; Soltani et al. 2009). Interestingly, this wasn't always the case in the corn studies. Among all herbicide programs, there were no differences by 42 DAGT in percent weed-free area in both the Manhattan 2022 and Seymour 2023 studies. These results were not surprising, because corn has been shown to be more competitive against weeds compared to soybeans (Moolani et al. 1964). It is worth mentioning, however, that when differences were detected in the Manhattan 2023 study, the One-pass program had the smallest weed-free area compared with the two-pass programs. For the Manhattan fields, MAN 1 had less overall weed pressure compared to MAN 2, and corn and soybean experiments planted on MAN 2 and sprayed with the One-pass program had less weed-free area (were weedier) than the other programs. The amount of herbicide needed for precision applications is governed by overall weed pressure in each field (Melland et al. 2015), in that more weed pressure will require more herbicide for effective control than less

weedy fields. Based on our results, we suggest that in fields with lighter weed infestations, a One-pass GOB treatment could result in 89% or better weed-free area, but more weed-free area could be achieved by including both a GOB and GOG application. Two-pass applications with multiple herbicide sites of action (SOA) are generally regarded as an important part of an integrated weed management (IWM) strategy (Norsworthy et al. 2012; Smith et al. 2019).

If a farmer were interested in a complete SS only program, with both GOB and GOG applications, the weed-free area results in our study indicate that this two-pass SS only program would not provide acceptable weed control compared to programs with residual herbicide applications. This suggests that BCST residual applications are still advantageous to GOG SS technology, and that the technology does not eliminate the importance and benefit of residual herbicides. Because soil residual herbicides continue to be an important part of IWM (Owen et al. 2015), we recommend that residual applications be included in herbicide programs for intelligent sprayers.

The Spike program was used to test the effectiveness of broadcasting a base foliar herbicide rate and increasing the rate applied when weeds were detected using the SS boom. For soybean, this approach resulted in the greatest percent weed-free area at all locations and in corn this approach resulted in no differences from the treatment with the greatest percent weed-free area. Furthermore, it is likely that some weeds were not detected and thus were sprayed with the broadcast-applied minimum labeled rate of herbicides. Consistently exposing weeds to less herbicide has been shown to facilitate herbicide resistance (Manalil et al. 2011); thus, extreme caution must be exercised if Spike-spray application programs are used in the future. In this study, simultaneous BCST applications of residual herbicides and SS applications of foliar

herbicides, in most cases, provided better weed control (measured as weed-free area) compared to programs using no residual herbicides or SS only components.

3.4.1.3 Weed density

Overall weed densities measured after the GOB application were relatively low. For the corn studies, there was no effect of herbicide program on weed density in Manhattan 2022 (p = 0.84), but herbicide programs affected weed density in both Manhattan 2023 and Seymour 2023 (Table 3.9). Overall weed density at the Manhattan 2023 field (MAN 2) was more than at the Seymour IL field, which matches previously described weed infestations. The SS only program had the highest weed densities at 21 DAGBT in 2022 and 14 DAGBT in 2023 in both the Manhattan 2023 and Seymour 2023 locations. At the Manhattan 2023 location, weed densities in the Residual at-plant and One-pass programs were not different from each other (these treatments were the exact same at this point in the season), and at Seymour 2023, weed densities in the Residual at-plant, One-pass, overlapping residual, and Spike treatments were not different.

The effect of soybean herbicide programs on weed densities after the GOB application was not significant at the Manhattan 2022 field site (p = 0.61), was significant for Manhattan 2023 (p = 0.003) and not significant for the Seymour 2023 location (p = 0.16). Post hoc tests revealed that for the Manhattan 2023 location, mean (± SE) weed densities in the residual at-plant (1.7 ± 0.28), SS only (2.6 ± 0.35), one-pass (1.8 ± 0.29), and Overlapping residual (2.0 ± 0.31 weeds m^{-2}) programs were not different from one another. The only differences were weed densities in the SS only and Spike (1.3 ± 0.23) programs.

Herbicide programs resulted in different and very low weed densities after the GOG application in both soybean and corn experiments. Herbicide program in soybean at 14 DAGT

had a significant effect on weed density ($p < 0.0001$) at all locations (Table 3.10). The One-pass program had the highest weed densities at all locations. However, weed density for the SS only program was not different than the One-pass program in Manhattan 2023 and in Seymour 2023. In Seymour 2023, the Spike program was not different than both the One-pass and SS only programs. On the other hand, the Residual at-plant program was either not different from or had the lowest weed density at every location. Herbicide program had a significant effect on weed densities in corn by 14 DAGT ($p < 0.0001$) at each location (Table 3.11). Similar to soybean, weed densities were greatest in the One-pass program in Manhattan 2022 and Manhattan 2023. At Seymour, the SS only and Spike programs were not different from one another. For the corn, the overlapping residual program was either not different or had the lowest weed density in each study location. Overall greater densities were observed at Manhattan 2023 as the field had a naturally occurring higher weed population. Seymour 2023 had the lowest weed densities, likely due to late crop seeding and dry conditions.

The One-pass program had the greatest weed densities followed by the SS only program at 14 DAGT across all locations. The only exception was for the Seymour 2023 corn study, where the One-pass program was not statistically different than the programs with the lowest weed density at 14 DAGT. For both crops, programs with residual herbicides had the lowest weed densities at each location or were not different from the lowest. More information on weed density analysis will be presented in the “threshold weed density analyses” section below.

3.4.1.4 End-of-season weed dry biomass and grain yield

Herbicide program impacted end-of-season weed biomass in soybean at Manhattan 2022 ($p < 0.0001$), and in corn in Manhattan 2022 ($p = 0.04$) and Manhattan 2023 ($p < 0.0001$). The

One-pass program had the greatest weed biomass in the Manhattan 2022 soybean (Figure 3.4) and in the Manhattan 2023 corn (Figure 3.5). These were both in the MAN 2 field that had greater weed pressure overall. For the Manhattan 2022 corn, only the SS only and Spike programs were different from one another. No end-of-season data were obtained from Seymour soybean or corn studies. The least end-of-season biomass observed in soybean was in the Spike program in Manhattan 2022 and in corn, it was in the S Spike program in Manhattan 2023.

Soybean yields were only obtained from Manhattan 2022 and herbicide program impacted soybean yield (Figure 6). The spike program had the greatest soybean yield (3100 ± 70 kg ha^{-1}) but was not different from residual at plant, SS only, and overlapping residual programs. Soybean yield from the spike program was different from the one-pass program (2820 ± 70 kg ha^{-1}). All soybean plots yielded more than the 2022 average soybean yield for Riley County, KS (2370 kg ha^{-1}; USDA 2023a). Corn grain for yield was harvested from both Manhattan locations, but there were no differences among herbicide programs. Overall, Manhattan 2023 had more corn yield (7020 ± 300 kg ha^{-1}) than Manhattan 2022 (6370 ± 300 kg ha^{-1}), but yields in both years were below the 2022 average corn yield for Riley County KS (9360 kg ha^{-1}; USDA 2023b). The field conditions of the two locations differed in that MAN 1 was on a hilltop and rainfall would easily runoff, while MAN 2 was situated at the bottom of a slope and would retain rainfall more easily. Overall, 2022 was a wetter year with a total rainfall of 829 mm, compared to 2023 which only received a total rainfall of 624 mm (Kansas Mesonet 2024). Both years' rainfall amounts were below the 30-year average of 848 mm (Kansas State University 2024).

3.4.2 Weed detection threshold evaluation

3.4.2.1 Weed-free area

Green-on-green SS application thresholds were *Broadcast* (no threshold), *Efficacy* (detect all weeds and maybe some crops too), *Savings* (ensure only weeds are detected), and the *Balanced* threshold between the two, as set up in the sprayer. The thresholds were applied only in the GOG application and tested in four of the five herbicide programs, excluding the One-pass program because no GOG applications were made. Differences in weed-free area due to thresholds were observed in both Manhattan 2022 and Manhattan 2023. In Manhattan 2022, the interaction between herbicide program and threshold was significant ($p = 0.02$); post hoc test results can be seen in Table 3.12. In Manhattan 2023, the interaction between herbicide program and threshold was not significant ($p = 0.99$), but main effects were ($p < 0.0001$ and $p = 0.002$ for herbicide program and threshold, respectively). In Manhattan 2022, the greatest weed-free area was observed with the Spike program for *Efficacy* and *Savings* thresholds, but not different from any of the herbicide programs applied with the traditional *Broadcast* application (Table 3.12). The smallest weed-free area was observed with the Residual at-plant program and the *Savings* threshold and were not different from SS only or Overlapping residual programs applied with the *Savings* threshold. Overall, the *Broadcast* comparison within each program consistently had more than 86 to 97% weed-free area across the four herbicide programs, *Efficacy* ranged from 77 to 98% and *Balanced* from 77 to 92%. In Manhattan 2023, no differences in weed-free area were observed between the *Broadcast* (98% ± 0.5) and *Efficacy* (97% ± 0.9) thresholds but both had greater weed-free area than the balanced (95% ± 1.1) and savings (96% ± 0.9) thresholds.

For the corn, there was no interaction between herbicide program and threshold in Manhattan 2022, but the main effects were significant ($p = 0.007$ and 0.03 for herbicide program and threshold, respectively). At Manhattan 2023 there was a significant main effect for herbicide program, but not for threshold, and at Seymour 2023, no effect of herbicide program or threshold

was observed (data not shown). At Manhattan in 2022 (Figure 3.7), the *Balanced* and *Efficacy* thresholds did not differ from *Broadcast* comparison, but the *Savings* threshold was significantly weedier. The Residual at-pant, Spike, and Overlapping residual programs did not have different weed-free areas, but the SS only program was different than the Residual at-plant and Spike program. In Manhattan 2023, there were no differences within thresholds; the Overlapping residual (95% (±1.1) and Spike (93% ±1.3) programs did not have different weed-free areas although both had more weed-free area than the SS only (85% ±1.9) program. The Residual at-plant program weed-free area was 89% (±1.6) and was not different than the SS only or Spike programs.

Overall, traditional *Broadcast* applications resulted in the greatest weed-free area. However, for the locations discussed above, the herbicide *Efficacy* threshold was never different than the broadcast applications in terms of weed-free area. Fewer differences observed in 2023 may be because of proprietary software updates installed before the 2023 growing season. In general, when using intelligent sprayers such as the ONE SMART SPRAY, we would recommend that an herbicide *Efficacy* threshold be used, because this would decrease the likelihood that weeds are missed. Such an approach increases the likelihood of false positive detections (i.e. detecting crop plants as weeds), but in herbicide-tolerant cropping systems, this would not affect crop safety provided all product labels are followed correctly (Barnhart et al. 2022).

3.4.2.2 Weed density

Observed weed densities at 14 DAGT were influenced by main effects of weed detection thresholds and herbicide program in soybean at each location (Table 3.13). For Manhattan 2022,

there were no differences detected among any thresholds, but there were differences between thresholds detected at Manhattan 2023 and Seymour 2023. Overall, the weed densities observed in the *broadcast* and *Efficacy* thresholds were least and not different from each other in soybean. Observed weed densities at 14 DAGT were influenced by main effects of weed detection thresholds and herbicide program in corn at each location (Table 3.14). The *Broadcast* comparison consistently had the fewest weeds at each location; however, the *Efficacy* threshold was not different from broadcast at Manhattan 2022 and Manhattan 2023 weeds m^{-2}. At Seymour 2023, all SS thresholds resulted in higher weed densities when compared to *Broadcast* applications across herbicide programs. In Tables 3.13 and 3.14, only the threshold results are displayed, as herbicide program results have been previously discussed.

The threshold analyses revealed that in all locations except the Seymour 2023 corn, although the *Broadcast* applications always contained the lowest weed densities, the *Efficacy* threshold was not different. Although some thresholds contained lower weed densities than the *Efficacy* threshold at some locations (i.e. 'Savings' at Manhattan 2022 corn and 'Balanced' at Manhattan 2023 corn), it was the most consistent throughout all study locations. These results further support our recommendation that *Efficacy* weed detection thresholds should be used with SS applications. In addition, residual herbicides should be included in SS application programs, as they have been shown to significantly reduce weed densities (Bell et al. 2015; Nurse et al. 2006; Nunes et al. 2018).

3.4.3 Cost of herbicide programs and thresholds

This section focuses on the amount of herbicide applied in the different herbicide programs with each weed detection threshold. We are only able to report 2023 results because

the 2022 data were lost to the ONE SMART SPRAY raw data decoder. Furthermore, these costs were calculated based solely on geospatial data collected by the sprayer and were not validated by ground-truth measurements. This is a topic that could be expounded upon in future research.

Differences in total herbicide cost were affected by the interaction of weed detection thresholds and herbicide program for soybean at Manhattan 2023 and Seymour 2023, and for corn at Manhattan 2023 (Table 3.15). At Manhattan 2023 for both soybean and corn, all SS thresholds cost less than the equivalent *Broadcast* application across all herbicide programs, with thresholds in the SS only program costing less than in the Residual at-plant, Spike, and Overlapping residual programs. Seymour 2023 soybean costs were similar to the Manhattan results, with all thresholds costing less than their respective *Broadcast* applications. Regarding the Spike program in the Manhattan and Seymour soybean experiments, the *Efficacy*, *Balanced*, and *Savings* thresholds were more expensive than the other herbicide programs using the same thresholds. The calculated savings averaged across SS thresholds (i.e., cost difference between average SS threshold cost and broadcast threshold cost) was \$123 ha^{-1} for soybean and only \$43 ha^{-1} for corn. There are several reasons for this difference in savings between soybean and corn experiments: The MAN 2 field (corn in 2023) had greater weed pressure than MAN 1 field (soybean in 2023); timing of GOG application in corn was on taller plants at the V5 growth stage than the timing of the GOG application in soybean at the V2 to V4 growth stage. As a result, the taller corn plants had established more of a canopy making less of the row space visible, and the sprayer defaulted to a broadcast application (vs. SS threshold) when interrow space could not be seen.

At Seymour 2023, total corn herbicide cost differed by main effects of weed detection thresholds and herbicide program. Herbicide cost for the *Efficacy* (\$129 ha^{-1}), *Balanced* (\$158

ha^{-1}), and *Savings* ($128 ha^{-1}) weed detection thresholds were less than the *Broadcast* application ($188 ha^{-1}). Cost of the overlapping residual ($181 ha^{-1}), Residual at-plant ($172 ha^{-1}), and Spike ($161 ha^{-1}) herbicide programs were not different from one another, while the SS only program cost less ($90 ha^{-1}) than any of the other programs. Overall costs for corn at Seymour 2023 were greater, likely due to a late GOG application corn was late V5, making it difficult for the sprayer to see interrow space and thus, defaulting to a broadcast application more frequently compared to soybean.

Herbicide cost reductions are possible using ONE SMART SPRAY compared to traditional broadcast applications. In both soybean and corn, each SS weed detection threshold cost less than corresponding broadcast application for each herbicide program. The *Efficacy* weed detection threshold (could spray more due to false positive detections) was never different from the balanced or savings thresholds (Table 3.15). Total herbicide cost reductions are attainable even when simultaneously broadcasting residual herbicides and spot-spraying foliar herbicides, with the two-boom two-tank system. These results further support our recommendations of using herbicide efficacy thresholds for SS applications and continued use of residual herbicides in intelligent sprayer applications.

This research demonstrates that with intelligent sprayers, significant herbicide reductions are possible compared to broadcast applications without sacrificing weed-free area. Residual herbicides and multiple passes are still important when using this technology. In both corn and soybean trials, significant herbicide cost reductions were observed when simultaneously broadcasting residual and spot-spraying foliar herbicides. Growers would benefit greatly from the use of two-tank and two-boom intelligent sprayers for these simultaneous applications, as they become available on the market. Furthermore, the One-pass programs were consistently the

weediest in almost every trial, signifying that multiple passes are still necessary for weed control. It is still important to incorporate IWM principles when using this technology, which includes the use of residual herbicides, multiple herbicide SOA, and multiple sprayer passes.

In addition to these findings, there are some future research needs for intelligent sprayer applications. Currently, most intelligent sprayers are focused on weed control in crops planted in rows spaced 50 and 76 cm apart. All crops were planted in rows 76-cm apart for this research. Many crops are planted in narrower rows and are known to establish their crop canopy more rapidly than those planted in wider rows, making them more competitive against weeds (Bradley 2006), it remains to be seen how intelligent sprayer programs would best fit into these situations. In this study, weed infestations were relatively light and did not infest the entire field. We hypothesize that there will be less benefit of intelligent sprayers in fields with more weed pressure, but the "optimum" density above which the benefit of herbicide reduction ceases is unknown. Finally, especially for corn applications, earlier timing of GOG applications would likely allow the sensors to detect more weeds and would prevent the intelligent system from defaulting to broadcast applications caused by larger corn plants. Optimum POST application timing should be determined for future uses.

3.5 References

Ahmad A, Saraswat D, Aggarwal V, Etienne A, Hancock B (2021) Performance of deep learning models for classifying and detecting common weeds in corn and soybean production systems. Comput Electron Agr 184:106081

Albawi S, Mohammed TA, Al-Zawi S (2017) Understanding of a convolutional neural network. Pages 1–6 *in* Proceedings of the 2017 International Conference on Engineering & Technology. Antalya, Turkey: Institute of Electrical and Electronics Engineers

Anaele AO, Bishnoi UR (1992) Effects of tillage, weed control method and row spacing on soybean yield and certain soil properties. Soil Till Res 23:333-340

Barnhart IH, Lancaster S, Goodin D, Spotanski J, Dille JA (2022) Use of open-source object detection algorithms to detect Palmer amaranth (*Amaranthus palmeri*) in soybean. Weed Sci 70:648-662

Barroso J, Fernandez-Quintanilla C, Maxwell BD, Rew LJ (2004) Simulating the effects of weed spatial pattern and resolution of mapping and spraying on economics of site-specific management. Weed Res 44:460-468

Bell HD, Norsworthy JK, Scott RC (2015) Effect of drill-seeded soybean density and residual herbicide on Palmer amaranth (*Amaranthus palmeri*) emergence. Weed Technol 29:697-706

Bongiovanni R, Lowenberg-DeBoer J (2004) Precision agriculture and sustainability. Precis Agric 5:359–387

Bradley KW (2006), A review of the effects of row spacing on weed management in corn and soybean. Crop Manag 5:1-10

Brooks ME, Kristensen K, van Benthem KJ, Magnusson A, Berg CW, Nielsen A, Skaug HJ, Maechler M, Bolker BM (2017) glmmTMB balances speed and flexibility among packages for zero-inflated generalized linear mixed modeling. R J 9:378-400

CoCoRaHS (2024) CoCoRaHS Historical Data for Station IL-CP-62: Champaign 2.5 S. Available online: https://dex.cocorahs.org/stations/IL-CP-62/precip-summary?from=2023-07-27&to=2023-08-31. Accessed: January 14, 2024.

Craigmyle BD, Ellis JM, Bradley KW (2013) Influence of herbicide programs on weed management in soybean with resistance to glufosinate and 2,4-D. Weed Technol 27:78-84

Fernández-Quintanilla C, Peña JM, Andújar D, Dorado J, Ribeiro A, López-Granados F (2018) Is the current state of the art of weed monitoring suitable for site-specific weed management in arable crops? Weed Res 58:259–272

Gao J, French AP, Pound MP, He Y, Pridmore TP, Pieters JG (2020) Deep convolutional neural networks for image-based *Convolvulus sepium* detection in sugar beet fields. Plant Methods 16:29

Genna NG, Gourlie JA, Barroso J (2021) Herbicide efficacy of spot spraying systems in fallow and postharvest in the pacific northwest dryland wheat production region. Plants 10:2725

Gerhards R, Oebel H (2006) Practical experiences with a system for site-specific weed control in arable crops using real-time image analysis and GPS-controlled patch spraying. Weed Res 46:185-193

Gerhards R, Sanchez DA, Hamouz P, Peteinatos GG, Christensen S, Fernandez-Quintanilla C (2022) Advances in site-specific weed management in agriculture – a review. Weed Res 62:123-133

Gillies S, van der Wel C, Van den Bossche J, Taves MW, Arnott J, Ward BC, et al. (2023) Shapely. Available online: https://doi.org/10.5281/zenodo.7583915. Accessed: October 2, 2023

Greeneye Technology (2023) Our technology. Available online: https://greeneye.ag/technology/. Accessed: September 25, 2023

Grundy AC, Mead A, Burston S, Overs T (2004) Seed production of *Chenopodium album* in competition with field vegetables. Weed Res 44:271-281

Hartig F (2022) DHARMa: Residual diagnostics for hierarchical (multi-level / mixed) regression models. R package version 0.4.6. Available online: https://CRAN.R-project.org/package=DHARMa. Accessed: October 2, 2023

Huang H, Deng J, Lan Y, Yang A, Deng X, Zhang L (2018) A fully convolutional network for weed mapping of unmanned aerial vehicle (UAV) imagery. PLoS ONE 13:e0196302

Hussain N, Farooque AA, Schumann AW, McKenzie-Gopsill A, Esau T, Abbas F, Acharya B, Zaman Q (2020) Design and development of a smart variable rate sprayer using deep learning. Remote Sens 12:4091

Jabir B, Falih N (2022) Deep learning-based decision support system for weeds detection in wheat fields. Int J Elec Comput Eng 12:816-825

Jin X, McCullough PE, Liu T, Yang D, Zhu W, Chen Y, Yu J (2023) A smart sprayer for weed control in bermudagrass turf based on the herbicide weed control spectrum. Crop Protec 170:106270

John Deere (2023) See & Spray Ultimate: Targeted, in-crop spraying. Available online: https://www.deere.com/en/sprayers/see-spray-ultimate/. Accessed: September 25, 2023

Johnson WG, Gibson KD, Conley SP (2007) Does weed size matter? An Indiana grower perspective about weed control timing. Weed Technol 24:542-546

Jordahl K, van den Bossche J, Fleischmann M, Wasserman J, McBride J, Gerard J, et al. (2020) Geopandas/geopandas: v0.8.1. Available online: https://doi.org/10.5281/zenodo.3946761. Accessed: October 2, 2023

Kansas Mesonet (2024) Kansas Mesonet Historical Data. Available online: https://mesonet.k-state.edu/weather/historical/#!. (Accessed: January 14, 2024)

Kansas State University (2024) Monthly Precipitation Maps. Available online: https://climate.k-state.edu/precip/county/. Accessed: March 3, 2024

Kaul V, Enslin S, Gross SA (2020) History of artificial intelligence in medicine. Gastrointest Endosc 92:807-812

Kegode GO, Forcella F, Clay S (1999) Influence of crop rotation, tillage, and management inputs on weed seed production. Weed Sci 47:175-183

Kluvyer T, Ragan-Kelley B, Pèrez F, Granger B, Bussonnier M, Fredrick J, et al. (2016) Jupyter Notebooks – a publishing format for reproducible computational workflows. Pages 87-90 *in* Proceedings of the 20th International Conference on Electronic Publishing. Göttingen, Germany: Electronic Publishing

Lamichhane JR, Devos Y, Beckie HJ, Owen MD, Tillie P, Messéan A, Kudsk P (2017) Integrated weed management systems with herbicide-tolerant crops in the European Union: lessons learnt from home and abroad. Crit Rev Biotechnol 37:459-475

Lancaster SR, Fick WH, Currie RS, Kumar V (2023) 2023 Chemical weed control for field crops, pastures, rangeland, and noncropland. Available online: https://bookstore.ksre.ksu.edu/pubs/chemweedguide.pdf. Accessed: October 2, 2023

Lenth R (2023) emmeans: Estimated marginal means, aka Least-Squares means. R package version 1.8.6. Available online: https://CRAN.R-project.org/package=emmeans. Accessed: October 2, 2023

Maxwell BD, Luschei EC (2005) Justification for site-specific weed management based on ecology and economics. Weed Sci 53:221–227

McCarthy J (2007) What is artificial intelligence? Stanford, CA: Computer Science Department, Stanford University. 2 p

Miranda JWA, Jhala AJ, Bradshaw J, Lawrence NC (2022) Control of acetolactate synthase-inhibiting herbicide-resistant Palmer amaranth (*Amaranthus palmeri*) with sequential applications of dimethenamid-P in dry edible bean. Weed Technol 36:325-333

Mobli A, DeWerff RD, Arneson NJ, Werle R (2023) Evaluation of two-pass herbicide programs for broad-spectrum weed control in conventional tillage non-transgenic corn production in Wisconsin atrazine prohibition areas. Agrosyst Geosci Environ 6.4:e20419

Moolani MK, Knake EL, Slife FW (1964) Competition of smooth pigweed with corn and soybeans. Weeds 12:126-128

Nguyen DV, Kuhnert L, Kuhnert KD (2012) Structure overview of vegetation detection. A novel approach for efficient vegetation detection using an active lighting system. Robot Auton Syst 60:498-508

Nunes AL, Lorenset J, Gubiani JE, Santos FM (2018) A multy-year study reveals the importance of residual herbicides on weed control in glyphosate-resistant soybean. Planta Daninha 36

Nurse RE, Swanton CJ, Tardif F, Sikkema PH (2006) Weed control and yield are improved when glyphosate is preceded by a residual herbicide in glyphosate-tolerant maize (*Zea mays*). Crop Protec 25:1174-1179

Osorio K, Puerto A, Pedraza C, Jamaica D, Rodríguez L (2020) A deep learning approach for weed detection in lettuce crops using multispectral images. AgriEngineering 2:471-488

Owen MDK, Beckie HJ, Leeson JY, Norsworthy JK, Steckel LE (2015) Integrated pest management and weed management in the United States and Canada. Pest Manag Sci 71:357-376

Perkins CM, Gage KL, Norsworthy JK, Young BG, Bradley KW, Bish MD, Hager A, Steckel LE (2021) Efficacy of residual herbicides influenced by cover-crop residue for control of *Amaranthus palmeri* and *A. tuberculatus* in soybean. Weed Technol 35:77-81

Python (2023) Python 3.9.17 documentation. Available online: https://docs.python.org/3.9/index.html. Accessed: October 2, 2023

QGIS (2023) Documentation for QGIS 3.22. Available online: https://docs.qgis.org/3.22/en/docs/. Accessed: October 2, 2023

Quigley N (2023) Bosch BASF Smart Farming and AGCO announce joint development and commercialization of smart spraying capabilities. Available online: https://www.basf.com/global/en/media/news-releases/2023/04/p-23-159.html. Accessed: September 26, 2023

R Core Team (2023) R: A language and environment for statistical computing. R foundation for statistical computing. Vienna, Austria. Available online: https://www.R-project.org/. Accessed: October 2, 2023

Ralašić I (2021) A better mAP for object detection. Available online: https://towardsdatascience.com/a-better-map-for-object-detection-32662767d424. Accessed: September 27, 2023

Redmon J, Farhadi A (2018) YOLOv3: An incremental improvement. arXiv 1804.02767 [doi: 10.48550/arXiv.1804.02767]

Rehman TU, Zaman QU, Chang YK, Schumann AW, Corscadden KW (2019) Development and field evaluation of a machine vision based in-season weed detection system for wild blueberry. Comput Electron Agric 162:1-13

Rozenberg G, Kent R, Blank L (2021) Consumer-grade UAV utilized for detecting and analyzing late-season weed spatial distribution patterns in commercial onion fields. Precis Agric 22:1317-1332

Ruigrok T, van Henten E, Booij J, van Boheemen K, Kootstra G (2020) Application-specific evaluation of a weed-detection algorithm for plant-specific spraying. Sensors 20:7262

Sanchez J, Gallandt ER (2020) Functionality and efficacy of Franklin Robotics' Tertill™ robotic weeder. Weed Technol 35:166-170

Santos Ferreira AS, Freitas DM, Silva GG, Pistori H, Folhes MT (2019) Unsupervised deep learning and semi-automatic data labeling in weed discrimination. Comput Electron Agr 165:104963

Sapkota B, Singh V, Cope D, Valasek J, Bagavathiannan M (2020) Mapping and estimating weeds in cotton using unmanned aerial systems-borne imagery. AgriEngineering 2:350–366

SciPy docs (2023) scipy.interpolate.griddata. Available online: https://docs.scipy.org/doc/scipy/reference/generated/scipy.interpolate.griddata.html. Accessed: October 2, 2023

Smith A, Soltani N, Kaastra AJ, Hooker DC, Robinson DE, Sikkema PH (2019) Annual weed management in isoxaflutole-resistant soybean using a two-pass weed control strategy Weed Technol 33:411-425

Soltani N, Vyn JD, Sikkema PH (2009) Control of common waterhemp (*Amaranthus tuberculatus* var. *rudis*) in corn and soybean with sequential herbicide applications. Can J Plant Sci 89:127-132

Spaeth M, Sökefeld M, Schwaderer P, Gauer ME, Sturm DJ, Delatrée CC, Gerhards R (2024) Smart sprayer a technology for site-specific herbicide application. Crop Protec 177:106564

Tian L (2002) Development of a sensor-based precision herbicide application system. Comput Electron Agric 36:133-149

Tian L, Reid JF, Hummel JW (1999) Development of a precision sprayer for site-specific weed management. T ASAE 42:893-900

Turing A (1950) Computing Machinery and Intelligence. Mind LIX:433-460

Underwood MG, Soltani N, Robinson DE, Hooker DC, Swanton CJ, Vink JP, Sikkema PH (2017) Weed control, environmental impact, and net revenue of two-pass weed management strategies in dicamba-resistant soybean. Can J Plant Sci 98:370-379

USDA (2023a) 2023 Soybean Yield, Kansas. Available online: https://www.nass.usda.gov/Statistics_by_State/Kansas/Publications/County_Estimates/22KSsoy.pdf. Accessed: January 20, 2024

USDA (2023b) 2023 Corn Yield, Kansas. Available online: chrome-extension://efaidnbmnnnibpcajpcglclefindmkaj/https://www.nass.usda.gov/Statistics_by_State/Kansas/Publications/County_Estimates/22kscorn.pdf. Accessed: February 17, 2024

van Stein B, Wang H, Kowalczyk W, Emmerich M, Bäck T (2020) Cluster-based Kriging approximation algorithms for complexity reduction. Appl Intell 50:778-791

Varella CAA, Gleriani JM, dos Santos RM (2015) Chapter 9 – Precision agriculture and remote sensing. Pages 185-203 *in* Santos F, Borém A, Caldas C, eds. Sugarcane: Agricultural production, bioenergy, and ethanol. San Diego, CA: Elsevier, Inc.

Virtanen P, Gommers R, Oliphant TE, Haberland M, Reddy T, Cournapeau D, Burovski E, Peterson P, Weckesser W, Bright J, et al. (2020) SciPy 1.0: Fundamental algorithms for scientific computing in Python. Nat Methods 17:261-272

Ward SM, Webster TM, Steckel LE (2013) Palmar amaranth (*Amaranthus palmeri*): A review. Weed Technol 27:12-27

Web Soil Survey (2023) Web Soil Survey. Available online: https://websoilsurvey.nrcs.usda.gov/app/. Accessed: September 26, 2023

Wenkel S, Alhazmi K, Liiv T, Alrshoud S, Simon M (2021) Confidence score: the forgotten dimension of object detection performance evaluation. Sensors 21:4350

Wiles JL (2009) Beyond patch spraying: site-specific weed management with several herbicides. Precis Agric 10:277-290

Xie S, Hu C, Bagavathiannan M, Song D (2021) Toward robotic weed control: detection of nutsedge weed in bermudagrass turf using inaccurate and insufficient training data. IEEE Robot Autom Let 6:7365-7372

Yang MD, Tseng HH, Hsu YC, Yang CY, Lai MH, Wu DH (2021) A UAV open dataset of rice paddies for deep learning practice. Remote Sens 13:1358

Yang MD, Tseng HH, Hsu YC, Yang CY, Lai MH, Wu DH (2021) A UAV open dataset of rice paddies for deep learning practice. Remote Sens 13:1358

3.6 Figures

Figure 3.1 A) Front view of the ONE SMART SPRAY research sprayer used in this study. B) Dual boom system for simultaneous broadcasting and spot spraying. The left-most boom is the spot-spray boom linked to the infrared and near infrared sensors, whereas the right-most boom is the broadcast boom.

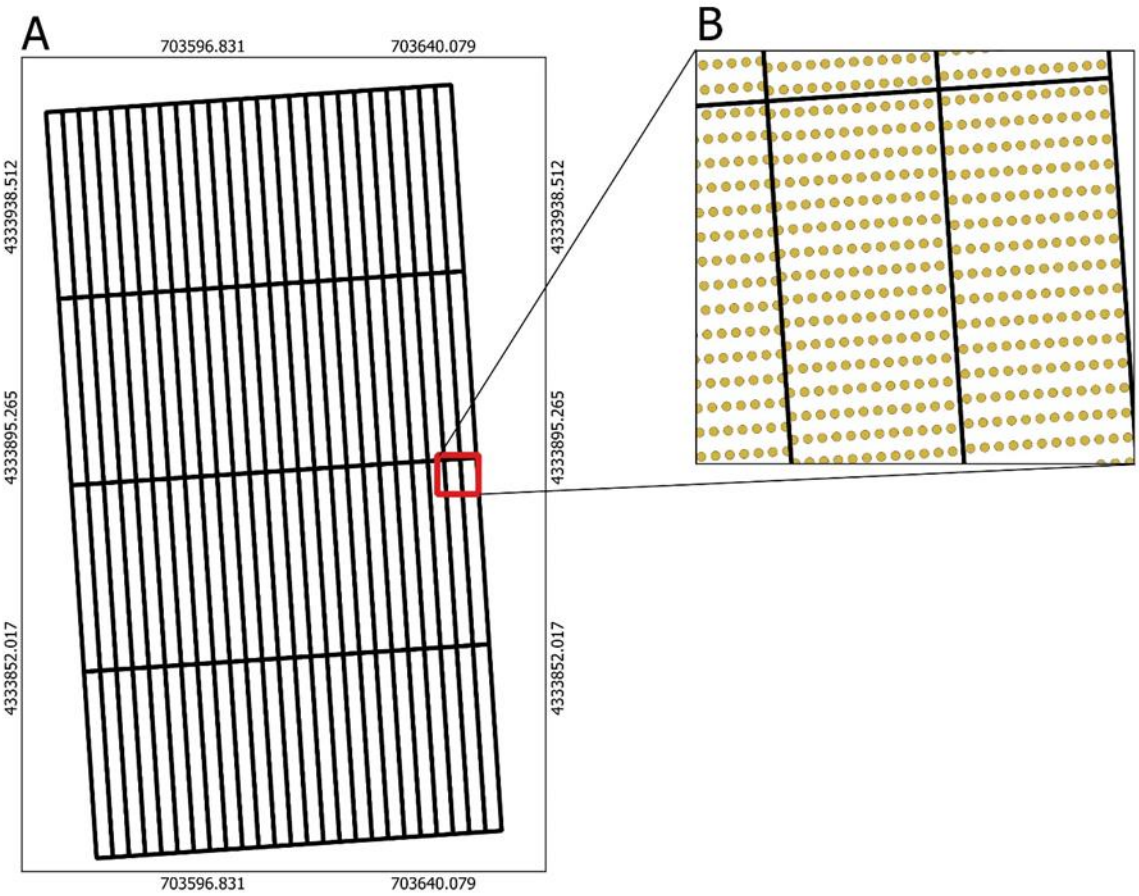

Figure 3.2 Illustration of nozzle data collected by the ONE SMART SPRAY research sprayer. (A) Whole plot view of Manhattan, KS (MAN 2) field location and (B) closeup view of the plots to illustrate number of data points recorded to create as-applied herbicide maps

.

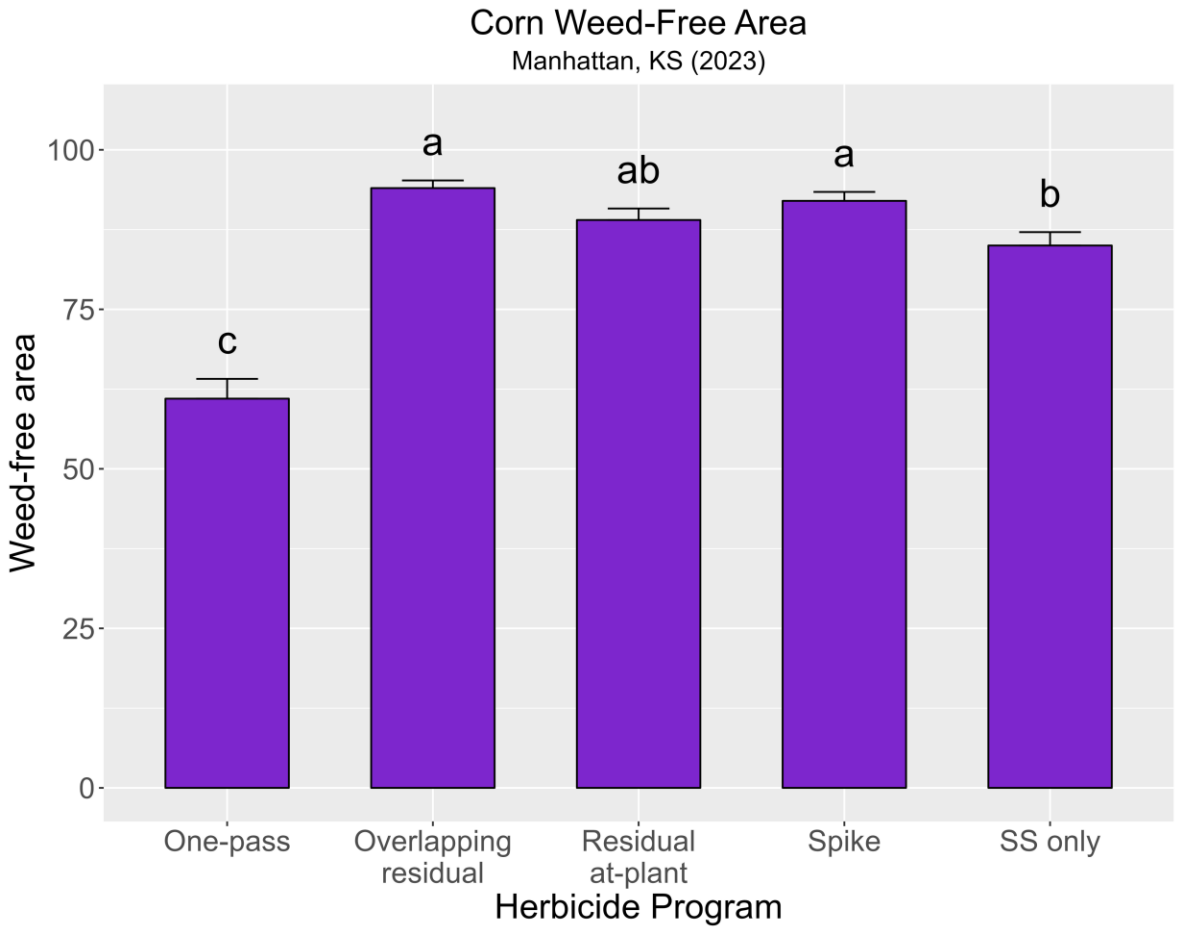

Figure 3.3 Percentage of weed-free area after the green-on-green applications for the Manhattan 2023 corn study at 42 DAGT. Corn herbicide information can be found in Table 3.3.

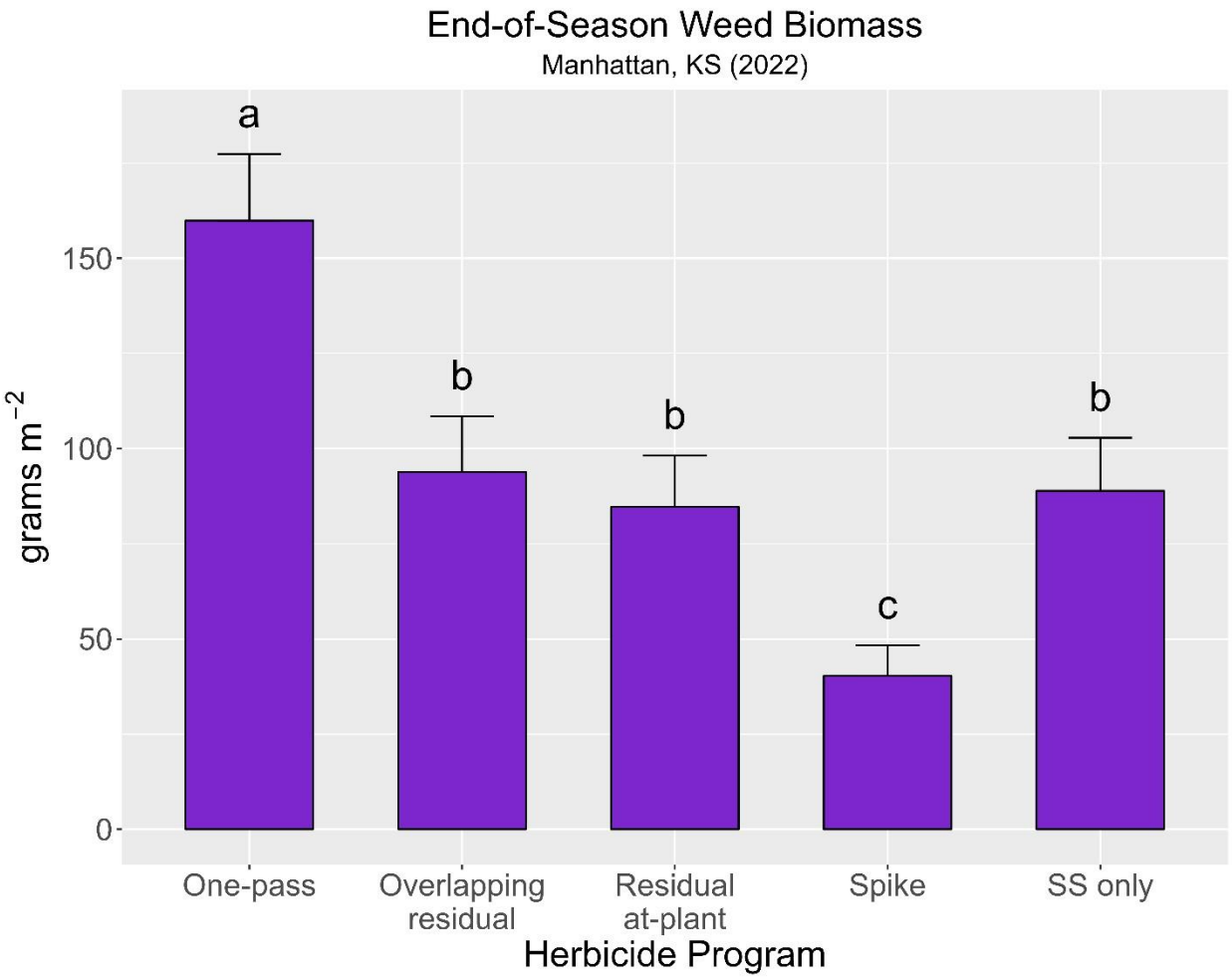

Figure 3.4 End-of-season weed biomass in soybean for the Manhattan KS 2022 field. Soybean herbicide program information can be found in Table 3.4.

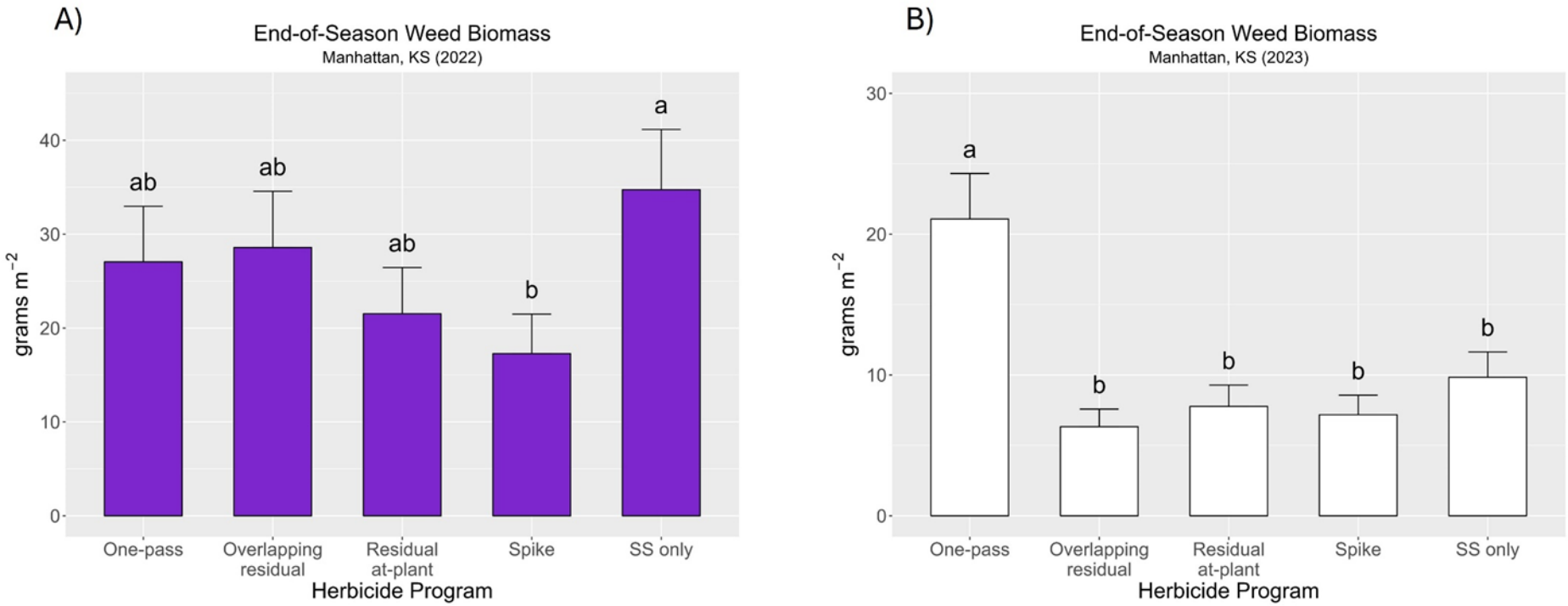

Figure 3.5 End-of-season weed biomass in corn for the A) Manhattan 2022 and B) Manhattan 2023 fields. Corn herbicide information can be found in Table 3.3.

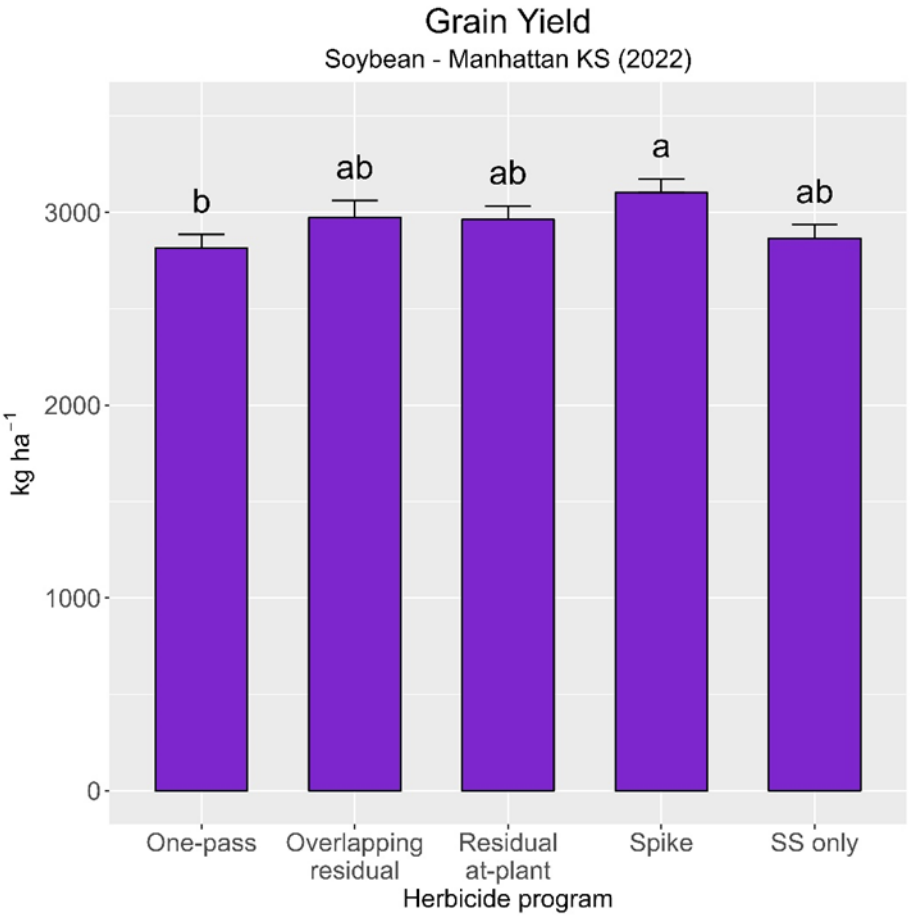

Figure 3.6 Grain yield for the soybean Manhattan KS 2022 field. Herbicide program information can be found in Table 3.4.

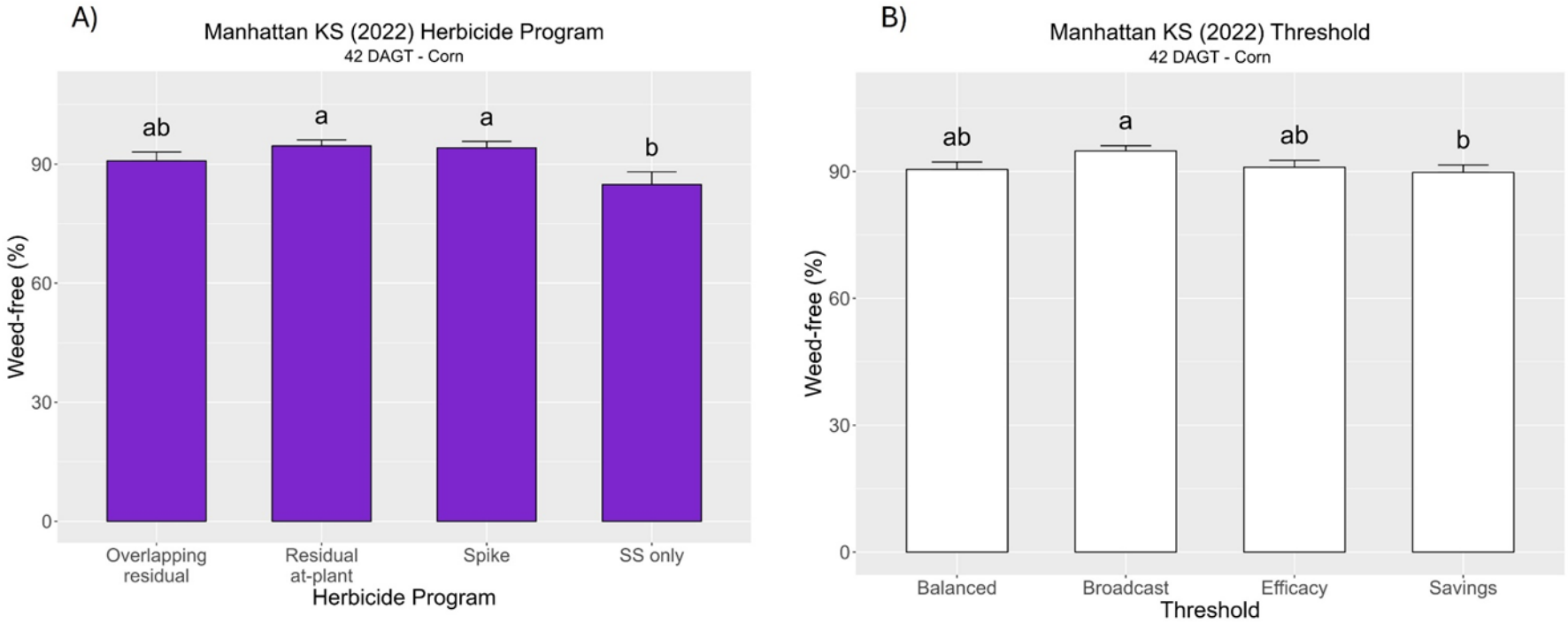

Figure 3.7 Percent weed-free area in corn at 42 DAGT for main effect of A) herbicide program and B) threshold for Manhattan, KS 2022. Herbicide programs are detailed in Table 3.3.

3.7 Tables

Table 3.1 Planting information for corn and soybean experiments evaluating ONE SMART SPRAY herbicide programs and thresholds.

	Manhattan, KS 2022		Manhattan, KS 2023		Seymour, IL 2023	
Crop	Corn	Soybean	Corn	Soybean	Corn	Soybean
Planting date	May 16	May 17	May 19	May 19	July 3[a]	July 3[a]
Planting population (seeds ha^{-1})	59,300	331,000	59,300	331,000	88,900	346,000
Seed hybrid/variety	Pioneer[b] P1089AM	Pioneer P39T61SE	Pioneer P0995AM	Pioneer P42A84E	Wyffles[c] 7878RIB	Xitavio[d] 3651E

[a] Illinois trials were planted later than usual due to drought conditions and limited space at the research farm
[b] Corteva Agriscience, 974 Center Road, Wilmington, Delaware, United States
[c] Wyffles Hybrids, 13344 US Highway 6, Geneseo, Illinois, United States
[d] Xitavio Soybean Seed, BASF Corporation, 2 TW Alexander Drive, Durham, North Carolina, United States

Table 3.2 Summary of herbicide programs used in this study. Broadcast (BCST) and spot spray (SS) applications were applied with either the broadcast boom or spot spray boom, respectively. Applications combined with a "+" sign indicate simultaneous applications. Green-on-brown (GOB) and green-on-green (GOG) applications were sprayed at-plant and 21 to 28 days after planting, respectively.

Herbicide Program	Description	GOB Application	GOG Application
1	Residual at plant	BCST + SS	SS
2	SS only	SS only	SS only
3	One-pass	BCST + SS	--------
4	Spike	Base-rate BCST + SS Spike	Base-rate BCST + SS Spike
5	Overlapping residual	BCST + SS	BCST + SS

Table 3.3 Herbicide information for corn experiments. Abbreviations: GOB, green-on-brown application; GOG, green-on-green application; BCST, broadcast; SS, spot spray.

Program	GOB BCST	GOB SS	GOG BCST	GOG SS
	---------- g ai or ae ha^{-1}----------			
Residual at-plant	dimethenamid-P[a]: 841 atrazine[b,c]: 2244	glyphosate[d,e]: 840 topramezone[f,g]: 12.3	------	glyphosate: 840 topramezone: 12.3
SS only	------	glyphosate: 840 topramezone: 12.3	------	glyphosate: 840 topramezone: 12.3
One-pass	dimethenamid-P: 841 atrazine: 2244	glyphosate: 840 topramezone: 24.6	------	------
Spike	glyphosate: 578 topramezone: 12.3	glyphosate: 578	glyphosate: 578 topramezone: 12.3	glyphosate: 578
Overlapping residual	dimethenamid-P: 841 atrazine: 1122	glyphosate: 840 topramezone: 12.3	dimethenamid-P: 420 atrazine: 1122	glyphosate: 840 topramezone: 12.3

[a] Outlook™, BASF Corporation, 26 Davis Drive, Research Triangle Park, North Carolina, United States
[b] Atrazine 4L™, Makhteshim Agan of North America (ADAMA), 3120 Highwoods Blvd., Suite 100, Raleigh, North Carolina, United States
[c] Treatments containing atrazine were applied with 10 ml crop oil concentrate L^{-1} solution
[d] Roundup PowerMax 3™, Bayer Crop Science, 800 N Lindbergh Blvd., St. Louis, Missouri, United States
[e] Treatments containing glyphosate were applied with 120 g dry ammonium sulfate L^{-1} solution
[f] Armezon™, BASF Corporation, 26 Davis Drive, Research Triangle Park, North Carolina, United States
[g] Treatments containing topramezone were applied with 2.5 ml crop oil concentrate L^{-1} solution

Table 3.4 Herbicide information for soybean experiments. Abbreviations: GOB, green-on-brown application; GOG, green-on-green application; BCST, broadcast; SS.

Program	GOB BCST	GOB SS	GOG BCST	GOG SS
	---------- g ai or ae ha^{-1} ----------			
Residual at-plant	pyroxasulfone[a]: 109	2,4-D[b]: 1067 glyphosate[c,d]: 840	------	2,4-D: 1067 glyphosate: 840
SS only	------	2,4-D: 1067 glyphosate: 840	------	2,4-D: 1067 glyphosate: 840
One-pass	pyroxasulfone: 109	2,4-D: 1067 glyphosate: 840	------	------
Spike	2,4-D: 799 glyphosate: 578	2,4-D: 266 glyphosate: 578	2,4-D: 799 glyphosate: 578	2,4-D: 266 glyphosate: 578
Overlapping residual	pyroxasulfone: 55	2,4-D: 1067 glyphosate: 840	pyroxasulfone: 55	2,4-D: 1067 glyphosate: 1346

[a] Zidua™, BASF Corporation, 26 Davis Drive, Research Triangle Park, North Carolina, United States
[b] Enlist One™, Corteva Agriscience LLC, 9330 Zionsville Road, Indianapolis, Indiana, United States
[c] Roundup PowerMax 3™, Bayer Crop Science, 800 N Lindbergh Blvd., St. Louis, Missouri, United States
[d] Treatments containing glyphosate were applied with 120 g dry ammonium sulfate L^{-1} solution

Table 3.5 Application dates for green-on-brown (GOB) and green-on-green (GOG) in both corn and soybean at all location-years. Crop stages for the GOG are provided.

Location	Year	Crop	GOB	GOG	Crop stage - GOG
Manhattan KS	2022	corn	May 19	June 17	V5
		soybean	May 20	June 17	V2
	2023	corn	May 23	June 13	V5
		soybean	May 23	June 20	V4
Seymour IL	2023	corn	July 5	July 27	V5
		soybean	July 7	July 31	V2

Table 3.6 Percent weed-free area in soybean using the program analysis for main effect of herbicide program for the green-on-brown (GOB) treatments. Ratings were taken 21 DAGBT in 2022 and 14 DAGBT 2023. Soybean herbicide programs are described in Table 3.4.

Abbreviations: DAGBT, days after GOB treatment; SS, spot-spray.

Herbicide program	Manhattan KS 2022		Manhattan KS 2023		Seymour IL 2023	
	---------- % ----------					
Residual at-plant	81 (2.7)[a]	ab[b]	97 (1.0)	a	96 (1.5)	a
SS only	73 (3.2)	b	92 (2.0)	b	90 (3.0)	b
One-pass	88 (2.1)	a	97 (0.8)	a	96 (1.6)	a
Spike	79 (2.9)	ab	98 (0.6)	a	92 (2.5)	ab
Overlapping residual	79 (2.8)	ab	96 (1.1)	a	93 (2.2)	ab

[a]Numbers in parentheses indicate standard error of the mean
[b]Letters indicate Tukey Honest Significant Difference mean separation results within a given location

Table 3.7 Percentage of weed-free area for the green-on-brown application for each herbicide program and three locations. Ratings were taken 21 DAGBT in 2022 and 14 DAGBT in 2023. Abbreviations: DAGBT, days after the green-on-brown treatment.

Herbicide program	Manhattan KS 2022		Manhattan KS 2023		Seymour IL 2023	
	---------- % ----------					
Residual at-plant	89 (1.9)[a]	a[b]	98 (0.5)	a	96 (1.2)	a
SS only	74 (3.1)	c	73 (2.4)	d	88 (2.6)	b
One-pass	89 (1.8)	a	94 (1.1)	b	96 (1.0)	a
Spike	90 (1.8)	a	85 (1.9)	c	94 (1.6)	ab
Overlapping residual	82 (2.5)	b	88 (1.70)	c	96 (1.1)	a

[a] Numbers in parentheses indicate standard error of the mean
[b] Letters indicate Tukey Honest Significant Difference mean separation results within a given location

Table 3.8 Percentage of weed-free area at 42 days after green-on-green application in soybean for each herbicide program and three locations. Herbicide programs are described in Table 3.4. Abbreviations: SS, spot spray; DAGT, days after the green-on-green treatment.

Herbicide program	Manhattan KS 2022		Manhattan KS 2023		Seymour IL 2023	
	---------- % ----------					
Residual at-plant	80 (3.1)[a]	b[b]	97 (0.8)	a	82 (4.6)	a
SS only	77 (3.4)	b	93 (1.5)	b	79 (5.2)	a
One-pass	48 (4.3)	c	89 (1.9)	c	38 (6.5)	b
Spike	95 (1.3)	a	98 (0.6)	a	82 (4.7)	a
Overlapping residual	84 (3.1)	a	93 (1.4)	b	81 (4.9)	a

[a]Numbers in parentheses indicate standard error of the mean
[b]Letters indicate Tukey Honest Significant Difference mean separation results within a given location

Table 3.9 Weed densities across herbicide programs (herbicide program analysis) for each corn location at 14 DAGBT in 2023. Herbicide programs described in Table 3.3**.** Abbreviations: SS, spot spray; DAGBT, days after the green-on-brown treatment.

Herbicide program	Weed density			
	Manhattan KS 2023		Seymour IL 2023	
	---------- number m^{-2} ----------			
Residual at-plant	6.3 (1.1)[a]	c[b]	1.1 (0.2)	b
SS only	17.4 (2.1)	a	1.8 (0.3)	a
One-pass	10.1 (1.2)	bc	0.9 (0.2)	b
Spike	11.5 (1.6)	ab	1.3 (0.2)	ab
Overlapping residual	12.0 (1.8)	ab	0.9 (0.2)	b

[a]Numbers in parentheses indicate standard error of the mean
[b]Letters indicate Tukey Honest Significant Difference mean separation results within a given location

Table 3.10 Observed weed densities in soybean at 14 DAGT for main effects of herbicide program within three locations. Herbicide programs are described in Table 3.4. Abbreviations: DAGT, days after green-on-green treatment; SS, spot spray.

Herbicide program	Weed-free area		
	Manhattan KS 2022	Manhattan KS 2023	Seymour IL 2023
	---------- weeds m^{-2} ----------		
Residual at-plant	1.5 (0.24)[a] bc[b]	0.5 (0.10) cd	0.8 (0.19) b
SS only	1.9 (0.26) b	1.1 (0.16) ab	1.3 (0.28) ab
One-pass	3.1 (0.36) a	1.4 (0.20) a	1.5 (0.32) a
Spike	0.9 (0.16) c	0.4 (0.08) d	1.3 (0.23) ab
Overlapping residual	1.4 (0.24) bc	0.8 (0.13) bc	0.8 (0.19) b

[a]Numbers in parentheses indicate standard error of the mean
[b]Letters indicate Tukey Honest Significant Difference mean separation results within a given location

Table 3.11 Weed densities in corn for each herbicide program and location (herbicide program analysis) at 14 DAGT. Herbicide programs described in Table 3.3. Abbreviations: SS, spot-spray; DAGT, days after the green-on-green treatment.

Herbicide program	Manhattan KS 2022		Manhattan KS 2023		Seymour IL 2023	
	---------- number m^{-2} ----------					
Residual at-plant	0.9 (1.6)[a]	c[b]	2.9 (3.3)	bc	0.8 (1.7)	b
SS only	1.5 (2.3)	b	3.3 (4.2)	b	2.2 (3.4)	a
One-pass	2.5 (3.5)	a	5.8 (6.7)	a	0.9 (1.8)	b
Spike	0.7 (1.4)	c	1.6 (2.6)	cd	1.4 (2.8)	ab
Overlapping residual	0.8 (1.5)	c	1.1 (1.9)	d	0.8 (1.7)	b

[a]Numbers in parentheses indicate standard error of the mean
[b]Letters indicate Tukey Honest Significant Difference mean separation results within a given location

Table 3.12 Percent weed-free area across the four threshold levels in soybean at 42 DAGT for the Manhattan, KS 2022 location. Herbicide programs described in Table 3.4. Abbreviations: SS, spot spray; DAGT, days after the green-on-green treatment.

Herbicide program	Weed-free area							
	Broadcast		Balanced		Efficacy		Savings	
	%							
Residual at-plant	92 (3.3)[a]	abc[b]	87 (4.7)	abcd	81 (6.1)	abcde	71 (7.7)	e
SS only	86 (4.8)	abcd	77 (6.7)	cde	77 (7.2)	cde	74 (7.6)	de
Spike	97 (1.6)	ab	98 (1.2)	a	92 (3.4)	abc	98 (1.0)	a
Overlapping residual	95 (2.4)	ab	83 (6.4)	abcde	84 (6.0)	abcde	79 (7.2)	abcde

[a]Numbers in parentheses indicate standard error values
[b]Letters indicate Tukey Honest Significant Difference mean separation results

Table 3.13 Threshold analysis for weed density at 14 DAGT in soybean at each location for the split plot effect of threshold. Thresholds were analyzed separately for each location.

Abbreviations: DAGT, days after the green-on-green treatment.

Threshold	Weed density					
	Manhattan KS 2022		Manhattan KS 2023		Seymour IL 2023	
	---------- number m^{-2} ----------					
Broadcast	1.54 (0.3[a])	ns[b]	0.40 (0.1)	b[c]	0.52 (0.1)	b
Efficacy	1.35 (0.2)	ns	0.68 (0.1)	ab	0.57 (0.1)	b
Balanced	1.18 (0.2)	ns	0.78 (0.1)	a	0.76 (0.2)	ab
Savings	1.40 (0.3)	ns	0.96 (0.2)	a	1.00 (0.2)	a

[a]Numbers in parentheses indicate standard error of the mean
[b] No significant difference
[c] Letters within a main effect and location indicate Tukey Honest Significant Difference mean separation results

Table 3.14 Threshold analysis for weed density at 14 DAGT in corn at each location for split plot of threshold. Thresholds were analyzed separately for each location. Abbreviations: DAGT, days after the green-on-green treatment.

Threshold	Weed Density		
	Manhattan KS 2022	Manhattan KS 2023	Seymour IL 2023
	---------- number m^{-2} ----------		
Broadcast	0.57 (0.1[a]) b[b]	1.10 (0.2) b	0.61 (0.2) b
Efficacy	0.89 (0.2) ab	1.60 (0.3) ab	1.17 (0.3) a
Balanced	1.09 (0.2) a	1.55 (0.2) ab	1.42 (0.3) a
Savings	0.87 (0.2) ab	2.23 (0.3) a	1.54 (0.3) a

[a]Numbers in parentheses indicate standard error of the mean
[b]Letters indicate Tukey Honest Significant Difference mean separation results for a given main effect within each location

Table 3.15 ONE SMART SPRAY herbicide program and threshold cost analysis for soybean (Manhattan KS 2023 and Seymour IL 2023) and corn (Manhattan KS 2023). Abbreviations: SS, spot-spray

	Herbicide Program Cost							
	Broadcast		Efficacy		Balanced		Savings	
Manhattan KS 2023 - Soybean	---------- $ ha^{-1} ----------							
Residual at-plant	217 (0)[a]	a[b]	72 (7)	d	68 (7)	d	63 (6)	d
SS only	168 (0)	b	44 (6)	de	50 (6)	de	32 (5)	e
Spike	211 (0)	a	134 (7)	bc	134 (7)	bc	127 (7)	c
Overlapping residual	217 (0)	a	74 (8)	d	76 (8)	d	73 (7)	d
Seymour IL 2023 - Soybean								
Residual at-plant	217 (0)	a	64 (7)	cde	80 (8)	c	71 (7)	c
SS only	168 (0)	b	35 (6)	de	56 (8)	cde	34 (5)	e
Spike	209 (0)	a	135 (9)	b	145 (9)	b	133 (9)	b
Overlapping residual	217 (0)	a	72 (7)	c	67 (7)	cd	75 (7)	c
Manhattan KS 2023 - Corn								
Residual at-plant	212 (0)	a	172 (3)	bc	157 (3)	cd	157 (3)	c
SS only	137 (0)	e	107 (4)	f	105 (4)	f	93 (4)	f
Spike	210 (0)	a	176 (4)	bc	181 (3)	b	178 (4)	b
Overlapping residual	214 (0)	a	170 (4)	bcd	157 (4)	c	157 (4)	c

[a]Numbers in parentheses indicate standard error of the mean
[b]Letters indicate Tukey Honest Significant Difference mean separation results for all threshold prices within a given location

Chapter 4 - On-farm evaluation of a commercial ONE SMART SPRAY in Midwestern United States corn and soybean cropping systems

Note: This manuscript is formatted to submit to Pest Management Science and is currently being edited to submit.

4.1 Abstract

Background: Herbicides are traditionally broadcast applied throughout the entire field, even where weeds are not growing. Recently, sprayers utilizing artificial intelligence have become available on the commercial market, which would allow users to simultaneously detect and spray weeds. Furthermore, some sprayers are equipped with two-tank/two-boom systems that would allow simultaneous broadcast and spot spray applications. Currently, no scientific research evaluating how these sprayers best fit within Midwestern United States corn (*Zea mays* L.) and soybean (*Glycine Max* [L.] Merr.) cropping systems has been conducted. The objectives were to investigate how spot spraying treatments compare to simulated broadcast + spot spraying approaches, and to evaluate how spot spraying applications influence herbicide costs.

Results: Simulated two-boom applications, broadcasting a base rate of foliar herbicides and spot spraying additional doses had more weed-free area than spot spray applications only. Cost of high rate broadcast + low rate spot spray applications were not different from broadcast applications, but low rate broadcast + high rate spot spray applications were always less expensive than corresponding broadcast applications.

Conclusion: Two-tank/two-boom precision sprayers show potential to provide weed control not different than broadcast applications, while costing less . Future research should also compare

simultaneous applications of broadcast soil residual herbicides and spot spraying foliar herbicides when weeds are detected.

Key words: Site specific weed control, ONE SMART SPRAY, herbicide cost, artificial intelligence, weed control

4.2 Introduction

Weed infestations are a major problem in crop production. Worldwide crop losses due to uncontrolled weeds were estimated to range between 20 and 90% when compared to weed-free crop production (Gianessi and Williams 2011; Oerke 2006; Pacanoski and Mehmeti 2021). In the United States, weed cause yield losses to average 52% in soybean (*Glycine max* [L.] Merr.) (Soltani et al. 2017), 50% in corn (*Zea mays* L.) (Soltani et al. 2016), 34% and 47% for winter and spring wheat (*Triticum aestivum* L.), respectively (Flessner et al. 2021), and 47% in grain sorghum (*Sorghum bicolor* [L.] Moench) (Dille et al. 2020). Chemical applications remain the most common method of agronomic weed control, with more than 95% of corn, soybean, cotton (*Gossypium hirsutum* L.), and sugarbeet (*Beta vulgaris* L.) fields treated with herbicides (Gianessi 2005). As input prices, including seed, pesticides, and fertilizers, have risen about 6 to 7% annually since the year 2000 (Paulson et al. 2023), the costs of herbicide applications are only expected to increase in future years. Although weeds are often distributed non-uniformly within fields (Thompson et al. 1991), herbicides are typically broadcast across entire fields, leading to increased herbicide waste, environmental contamination, and increased costs for farmers (Barroso et al. 2004; Laini et al. 2012).

Site-specific weed management (SSWM), defined as the process of adapting weed control methods to match the location of weed infestations (Fernández-Quintanilla et al. 2018), has been proposed to help reduce drawbacks associated with herbicide applications. A major challenge is creating a method reliable and accurate enough to detect and control weeds in a multitude of field conditions (Gao et al. 2020). Recently, precision sprayers using artificial intelligence (AI) for weed detection have become commercially available. These sprayers use a combination of cameras, sensors, and convolutional neural networks to locate and spray weeds

both in fallow and in-crop fields (Spaeth et al. 2024). Although these AI sprayers are relatively new, there are some reports in the literature indicating that significant amounts of herbicides can be saved compared to traditional broadcast applications. Partel et al. (2021) developed a tree fan sprayer capable of recognizing fruit trees and spraying with crop protection products as needed. The authors used a combination of LiDAR and AI algorithms to determine the need to spray based on tree leaf density and fruit count. Buzanini et al. (2023) developed a research sprayer using two sprayer nozzles to identify weeds in jalapeño pepper (*Caspicum annuum* L.) production. The sprayer was trained to identify weeds using the open source You Only Look Once v3 (Redmon and Farhadi 2018) algorithm and reported reduction in herbicide volumes by 26% and 42% for fall and spring applications, respectively. Farooque et al. (2023) developed a smart variable rate research sprayer to recognize and spray common lambsquarters (*Chenopodium album* L.) and corn spurry (*Spergula arvensis* L.) weeds with herbicides in potato (*Solanum tuberosum* L.) production, and to spray potato plants with fungicide for early blight potato diseases (caused by *Alternaria solani* Sorauer). The authors reported reduced spray volumes of 47% and 51% for herbicide and fungicide applications, respectively. This same sprayer was used by Hussain et al. (2020) and was reported to reduce spray volumes by 42% and 43% when spraying weeds and simulated diseased potato plants, respectively.

Although these studies have demonstrated real-time weed detection with precision sprayers, commercial-grade sprayers must be significantly larger and be able to spray many more acres than what can be covered by research sprayers. In the United States and Europe, examples of sprayers currently available include the John Deere® See & Spray™ Ultimate (John Deere 2024), Greeneye Technology™ (Greeneye Technology 2024), and the ONE SMART SPRAY smart sprayer (ONE SMART SPRAY 2024). More sprayers are coming equipped with features

such as two-tank/two-boom systems for simultaneous broadcast (BCST) and spot-spraying (SS) applications (i.e. the two-tank option described by John Deere (2024)). This technology allows applicators to broadcast base rates of herbicides with one boom and "spike" additional doses of same herbicide or spray other herbicides when weeds are detected. When used for targeted spraying, two-tank spray systems can increase herbicide savings over single-tank systems (Gutjahr et al. 2012). At this time, there are no other published reports evaluating commercial AI field sprayers in terms of weed control and herbicide cost savings compared to traditional broadcast applications. Therefore, the objectives are to 1) evaluate weed control of a commercial AI field sprayer using a two-tank simulated approach versus a traditional BCST approach and a SS only approach, and 2) determine herbicide cost savings with SS applications.

4.3 Materials and Methods

4.3.1 Overview of field sites

Field sites were established in 2022 at the University of Nebraska-Lincoln Research Farm southeast of Mead, NE. In 2022, NE 1 (41.170°N, 96.462°W) and NE 2 (41.170°N, 96.456°W) were planted with soybean and corn, respectively, and were rotated to the subsequent crop in 2023. Both fields were part of a no-till corn-soybean rotation and were irrigated; the exception being that NE 2 was inadvertently tilled at the beginning of the 2023 season. The NE 1 field was located on a Yutan silty clay loam (2-6% slope) and a Tomek silt loam (0-2% slope), whereas NE 2 field was located on a Yutan silty clay loam (2-6% slope) and a Filbert silt loam (0-1% slope) (Web Soil Survey 2024). Both fields contained moderate to dense infestations of waterhemp (*Amaranthus tuberculatus* [Moq.] Sauer), velvetleaf (*Abutilon theophrasti* Medik.),

and yellow foxtail (Setaria pumila [Poir.] Roem. & Schult.). All fields were planted with rows spaced 76-cm apart. Table 4.1 describes planting information.

4.3.2 Field sprayers

5 Due to equipment availability, different sprayers were used in 2022 and in 2023, although the ONE SMART SPRAY sensors and camera hardware were the same. In 2022, trials were conducted using a Fendt® RoGator™ 665 (AGCO® International GmbH, Neuhausen am Rheinfall, Switzerland) with a 36-m boom width and 2023 trials were conducted with a Hagie® STS12™ (Hagie Manufacturing, Clarion, IA, United States) with an 18.3-m boom width (Figure 4.1). Nozzles were spaced at intervals of 50 cm on both sprayers. Each sprayer was equipped with light-emitting diode (LED) lights emitting infrared (IR) and near infrared (NIR) light to provide for a consistent image across a multitude of lighting conditions (Spaeth et al. 2024). Cameras were fixed between each set of two lights and were angled approximately 25° forward from the ground so that weeds could be detected before the booms passed over them (Figure 4.2). Specific model numbers for cameras and sensors are not available because they are still considered prototypes by Bosch® (Bosch GmbH, Stuttgart, Germany).

6 The ONE SMART SPRAY system is capable of both green-on-brown (GOB) and green-on-green (GOG) applications. Green-on-brown applications are used in burndown, fallow, and/or pre-emergence situations where the sprayer detects all green vegetation and activates nozzles to spray them (Booker 2021). For GOB applications, AI is not used because vegetation can be detected effectively with IR and NIR (Knipling 1970), which

requires much less computing power. However, AI is used for GOG applications to facilitate distinguishing weeds from crop plants. This study focused on GOG applications.

4.3.3 Field studies

In 2022, treatments were established in a randomized complete block design with three replications in both NE 1 and NE 2 fields. Plot dimensions were 36 m wide by 286 m long for NE 1 (soybean) and were 36 m wide by 320 m long for NE 2 (corn), as determined by space available in each field. The main treatment factor was application program, where a SS only treatment was compared to two different "Spike" approaches where a base rate of herbicide was broadcast (BCST) and rate was "Spiked" up to the labeled herbicide rate when the ONE SMART SPRAY sensors detected weeds (Table 4.2). Treatment 1 (T1) consisted of a low BCST rate + a high SS rate, Treatment 2 (T2) consisted of a high BCST rate + a low SS rate, and Treatment 3 (T3) was a SS only treatment. In the corn experiment, only the glyphosate rates were changed for the T1 and T2 treatments, whereas an equal rate of diflufenzopyr and dicamba were applied with both BCST and SS booms. In the soybean experiment, only the glufosinate rate was changed for the T1 and T2 treatments, and an equal rate of glyphosate was applied with the BCST and SS booms. The SS only applications in T3 were the sum of the total rates applied in T1 and T2 for both corn and soybean.

In 2023, treatments were arranged in a split-plot design with four replications. The design was changed due to field space availability, a smaller boom width, and the addition of SS weed detection thresholds into the experiment (not yet available in 2022). The main treatment factor was three application programs as in 2022, and the split-plot factor was five ONE SMART SPRAY detection thresholds. Each subplot was 18.3 m wide by 31 m long. AI spraying systems

allow for different confidence intervals, or detection thresholds, to be used when making detections (Barnhart et al. 2022). Correct detections are labeled true positives, whereas incorrect (or misplaced) detections are known as false positives (Ralašić 2021). Thresholds set to smaller confidence intervals allow for more false positives, but the likelihood of correct detections is greater. On the other hand, larger thresholds result in missed detections (Barnhart et al. 2022). These thresholds represent different application philosophies; smaller thresholds would correspond to an herbicide efficacy (EFF) approach in that more herbicide would be sprayed than necessary due to false positive detections. Larger thresholds would result in an herbicide savings (SAV) approach. The ONE SMART SPRAY makes detection determinations based on weed size; although exact settings are proprietary in nature, four threshold levels were selected (presented here from smallest to largest weed detection size): Herbicide efficacy (EFF), two intermediate thresholds (INT 1, INT 2), and an herbicide savings (SAV) threshold. A broadcast (BRD) treatment was included for comparison as a traditional approach.

Applications in 2022 were made on June 21 to V5-V6 corn and on June 22 to R1 soybean. In 2023 applications were made on June 9 to V5 corn and on June 7 to V4 soybean. . Problems with the sprayer in 2022 resulted in soybean experiments being sprayed at a later growth stage. In 2022, both BCST and SS applications were made with a carrier volume of 168.4 L ha^{-1} at a pressure of 186 kPa and an application speed of 10.6 km hr^{-1}. In 2023, BCST applications were made with a carrier volume, pressure, and application speed of 140.3 L ha^{-1}, 207 kPa, and 11.1 km hr^{-1}, respectively. SS applications were made with a carrier volume, pressure, and application speed of 187 L ha^{-1}, 207 kPa, and 8.4 km hr^{-1}, respectively. For both years, T1 and T2 BCST and SS applications were sprayed separately since two-boom sprayers were unavailable. Wilger® MR110-04 flat-fan (Wilger® Inc., Lexington, TN, United States) and

a TeeJet® TP50-04 even-fan nozzles (TeeJet® Technologies, Inc., Wheaton, IL, United States) were used for 2022 and 2023, respectively. Herbicides used and application rates can be found in Tables 4.2 and 4.3 for 2022 and 2023 studies, respectively. All applications were made with dry ammonium sulfate (S-SUL™, American Plant Food Corp., Galena Park, Texas, United States) at a rate of 20.4 g L^{-1} of spray solution.

4.3.4 Field measurements

Within each plot, the percentage of weed-free area was estimated visually within an area excluding 1.5 m from the front and back of each plot. Estimations were taken 14, 28, and 42 days after treatment (DAT) using a scale of 0to 100% where a rating of 0 indicated a plot completely infested with weeds, while a rating of 100 indicated no weeds observed. In 2022 as plots spanned the entire length of the field, six random locations were selected in each plot. In 2023, as plot lengths were only 31 m, these data were collected by walking the center of each plot and estimating the weed-free area in the soybeans. For the corn, as whole-plot analysis was prohibited due to crop height, five random locations were selected throughout the crop for estimating weed-free area. Weed-free check plots were not permitted due to the farm wanting to minimize weed growth in a commercial field.

To determine herbicide application costs, as-applied maps were generated after the ONE SMART SPRAY applications (Barnhart IH, unpublished). Raw nozzle data were collected during each application documenting when each nozzle was “on” or “off.” Each point was geotagged with GPS coordinates and each point was labeled as either “TRUE” or “FALSE” to indicate whether the nozzles were spraying or not spraying, respectively. Maps were generated using a nearest neighbor interpolation, allowing for a binary map of “0” (no spraying) and “1”

(spraying) values to be produced (Fadnavis 2014). These maps were generated only for 2023 data, because the 2022 data were lost due to issues with the data decoder. Raw data files were imported into Jupyter Lab (Kluvyer et al. 2016), where the Python 3.9 (Python 3.9.17 2023) packages Geopandas (Jordahl et al. 2020), Shapely (Gillies et al. 2023), and SciPy (Scipy docs, 2023) were used to generate the maps. A 0.2m-by-0.2m grid was overlaid onto each field site, and on/off values were generated with the interpolation. After generation, maps were exported to QGIS 3.22.7 (QGIS, https://qgis.org/en/site/), where the percentage of each plot sprayed with the SS application were determined. An herbicide cost \$US ha^{-1} was determined for each application using herbicide prices found in the 2023 Kansas State University Chemical Weed Control Guide (Lancaster et al. 2023).

4.3.5 Statistical analysis

All analyses were conducted using R 4.3.1 (R Core Team 2023). Linear mixed effects models were used for all data analyses; to meet all ANOVA model assumptions, data were analyzed with the 'glmmTMB' package (Brooks et al. 2017) using a beta distribution. Data were transformed using the logit transformation and were automatically back transformed for data visualization by the package. Using the 'DHARMa' package (Hartig 2022), models were checked for normality and homogeneity of variance. The Type III Wald chi-square test was used to determine significances of models (Miranda et al. 2022), and means were separated using Tukey's Honest Significant Difference post-hoc test using the 'emmeans' package (Lenth 2023) and a confidence level of $p < 0.05$.

Due to the differences in study design, 2022 and 2023 were analyzed separately. For each year, each crop was analyzed separately. For the 2022 data, response variables of weed-free plot

area and herbicide costs were analyzed using a fixed effect of application program and a random effect of replication. In 2023, however, response variables were analyzed with fixed effects being application program and detection threshold and their interaction and random effects being replication and replication by application program.

4.4 Results

4.4.1 Weed-free area in 2022

For soybean, percent weed-free area across application programs was not different by 14 DAT ($p = 0.08$) but were different at 28 and 42 DAT ($p < 0.0001$ for both timings). The two "Spike" programs, T1 and T2, were not different from each other with both having weed-free areas of 98% and 100% by 28 and 42 DAT, respectively (Figure 4.3). The SS only treatment had 74% and 69% weed-free area by 28 and 42 DAT, respectively. Figure 4.4 illustrates the differences in weed infestation for each soybean treatment. For corn, no differences were detected in 2022 due to both sprayer malfunctions and an application of Acuron® (Syngenta Crop Protection LLC., Greensboro, North Carolina, USA) herbicide applied prior to corn emergence.

4.4.2 Weed-free area in 2023

Significant interaction between application programs and thresholds were found for each measurement date in the 2023 soybean study ($p = 0.01$, $p = 0.0006$, and $p = 0.002$ for 14, 28, and 42 DAT, respectively). Data from 42 DAT will be presented because differences were clearly observed at this time. (Figure 4.5). No differences in weed-free area were detected among all thresholds within an application program, although the greatest weed-free area was the EFF threshold in T2 (96% weed-free area). Interestingly, the EFF threshold in T1 had 91% weed-free

area and was not different than the results obtained for all thresholds with T2. In both T1 and T2, EFF outperformed the traditional BCST treatment. For T3, only INT 1 and INT 2 weed-free area were not different than the broadcast treatment.

In corn, there were no interactions between application programs and thresholds across all measurement dates ($p = 0.41$, $p = 0.07$, and $p = 0.39$ for 14, 28, and 42 DAT, respectively). Weed-free area for each application program was different at 14, 28 and 42 DAT ($p = 0.004$, $p = 0.0003$, and $p = 0.0004$, respectively). T1 and T2 were not different from each other but T3 always had less weed-free area across all measurement dates (Figure 4.6). The greatest weed-free area was observed for T2 with 96, 97 and 97% for 14, 28, and 42 DAT, respectively, though not different from T1. Conversely, the least weed-free areas were observed for the T3 treatment and were 89, 88, and 90% for 14, 28, and 42 DAT, respectively.

4.4.3 Herbicide cost

A significant interaction for total herbicide cost was observed between application programs and thresholds ($p < 0.0001$) (Figure 4.7) for soybean. Data were only collected for T2 and T3 due to an application error preventing data collection for T1. For both T2 and T3, the BRD treatment was the most expensive at \$148 ha^{-1} in both application programs. Although T2 program SS thresholds cost less than the BRD treatment, they were not different. Costs for the thresholds in the T2 program ranged from \$116 to \$127 ha^{-1} and in the T3 program ranged from \$34 to \$78 ha-1. In general for T2, EFF was the most expensive (\$126 ha^{-1}), whereas SAV was the least expensive (\$116 ha^{-1}). Conversely, all thresholds in T3 program (SS only) cost much

less than the BRD threshold, with the EFF being the most expensive ($78 ha^{-1}) and SAV being the least ($34 ha^{-1})

A significant interaction was also found between corn application programs and thresholds ($p < 0.0001$) (Figure 4.8). Like the soybean price results, the BRD treatments were the most expensive within each application program ($173, $173, and $164 ha^{-1} for T1, T2, and T3, respectively). All thresholds in T2 application program were less expensive than a BRD treatment but were not different. All thresholds cost less than the BRD treatments for T2 and T3. The EFF threshold was the most expensive threshold in T1 ($125 ha^{-1}) and T2 ($155 ha^{-1}), but each EFF threshold was not different than the INT 1 threshold for T3 ($103 and $107 for EFF and INT 1, respectively).

4.5 Discussion

A novel concept of a “Spike” approach in that a base rate of foliar herbicides can be broadcast applied when no weeds are detected and doses are increased to a predetermined rate and target applied when weeds are detected. For both years, treatments containing a broadcast base rate + a SS “Spike” application had higher weed-free area than the SS only treatments. As can be seen in the 2023 cost analyses, the T1 and T2 treatments were almost always more expensive than SS only treatments, but also resulted in better weed control. For example, 2023 soybean weed-free data, all SS thresholds provided levels of weed control similar to the broadcast applications for T2, but there were no differences in weed-free area when comparing the EFF threshold in T1 to all thresholds in T2. Utilizing an EFF threshold with a low BCST + high SS program would result in more herbicides being applied relative to other thresholds but would likely still result in significant herbicide reductions compared to broadcast applications.

Further research is needed to confirm this approach, as soybean herbicide cost data for T1 program were not available due to a data collection error.

Threshold differences were not observed in the 2023 corn likely due to absence of weed pressure and ONE SMART SPRAY application approach. Despite being irrigated, less than 76 mm of irrigation water was applied because the area was in extreme drought (data not shown), and water conservation practices were in place at that time. Therefore, weeds were not in abundance at application time. Additionally, the application was sprayed when the corn was at V5 stage (approximately 30.5 cm tall). As corn can often start to establish canopy at this stage (Curran et al. 2016), it was likely difficult for the ONE SMART SPRAY sensors to "see" between corn rows; when this occurs, the system defaults to a broadcast application to minimize chances of missing weeds (Kalvin Miller, personal communication). Although weed pressure was minimal, across all 2023 SS treatments, soybean herbicide savings compared to traditional broadcast applications were 64% but corn herbicide savings were only 43% (analysis not shown). The defaulting to broadcast applications combined with a minimal weed pressure were the likely reasons that no differences were observed among thresholds. Further research should focus on GOG applications at an earlier corn growth stage to allow ONE SMART SPRAY sensors to "see" between corn rows.

Herbicide costs for SS thresholds in T2 application program (low BCST rate + high SS rate) in both corn and soybean were not different from BRD treatment. However, herbicide costs for SS thresholds in T1 program (high BCST rate + low SS rate) in corn were cheaper than BRD treatments, but the percent weed free areas were not different. These data suggest that a low BCST + high SS rate approach using the EFF threshold may cost less (compared to the BRD applications as well as commercially acceptable weed control. Weed community was not very

dense in the corn studies, so the default broadcast application was triggered for most of the SS applications by the ONE SMART SPRAY when the cameras sensors were blocked because of tall corn. To better understand how weed densities affect ONE SMART SPRAY performance and herbicide savings, both corn and soybean studies should be established in a wide range of weed densities.

When determining base rate BCST treatments, it is worth noting that sublethal herbicide doses could increase the risk of evolution of herbicide-resistant weeds (Vila-Aiub and Ghersa 2005). The base-rate BCST treatment may have resulted in more weed-free area because undetected weeds were sprayed with the BCST application. In these experiments, the sprayer detected crop rows an eliminated them from the images, thus spraying every detectable plant not included in the crop rows, and missing weeds growing within the crop rows . Furthermore, because detecting small objects is challenging for AI systems (Li et al. 2017), it is also possible that some weeds were small enough to avoid ONE SMART SPRAY detection. Just as the repeated use of glyphosate without rotation to other herbicide modes of action helped to perpetuate the problem of glyphosate resistance (Johnson et al. 2009), it stands to reason that repeated sublethal doses of herbicides may, over time, lead to more frequent herbicide resistance cases. A proposed solution to this issue would be to rotate ONE SMART SPRAY uses, just as rotating herbicide modes of action is recommended to slow herbicide resistance in weeds (Beckie and Reboud 2009; Owen et al. 2014). For example, a proposed use of the ONE SMART SPRAY is to use two-boom/two-tank sprayers to simultaneously broadcast soil residual herbicides and SS foliar herbicides when weeds are detected. Such approaches have been shown to provide weed control not different from broadcast applications of the same herbicides but costing less (Chapter 3,). Therefore, we hypothesize that rotating between ONE SMART

SPRAY uses (i.e. rotating the "spike" treatment concept with simultaneously broadcasting residual and SS foliar herbicide treatments) may lead to significant herbicide cost savings while helping to slow the evolution of weed resistance. A dual-boom/dual-tank ONE SMART SPRAY system would allow for this versatility, but a single boom sprayer retrofitted with sensors would likely be limited to the Spike-spraying approach. We propose that the ONE SMART SPRAY be used as a tool for integrated weed management and used as diversely as possible, and not be treated as a "silver bullet" (Edwards and Hannah 2014) just to save herbicide costs. Further research is needed to understand how ONE SMART SPRAY use impacts herbicide resistance evolution. In addition, these results open opportunities to study how both weed control and weed resistance are impacted by the frequency of ONE SMART SPRAY program rotation, as well as how different herbicide combinations can influence these factors as well.

4.6 Conclusion

This study compared a novel BCST + SS "Spike" approach to both a traditional BCST and to SS only application program using a simulated two-tank/two-boom ONE SMART SPRAY. Additionally, based on 2023 data, herbicide costs were compared when using applications with SS components. Specific findings are as follows:

1. Treatments with broadcast applications (T1 and T2) often performed better than SS only (T3) applications in terms of more weed-free area. When a interaction was found between application program and thresholds in 2023, the EFF threshold with T1 program performed better than other thresholds with T1 program, and showed comparable weed-free area results to all thresholds with T2 program.

2. For both 2023 corn and soybean, cost of SS-only thresholds with T2 program were not different than BRD treatment. For corn, costs for SS components of T1 programs were less than respective BCST applications (no data available for T1 in soybean). Results suggest that using an EFF threshold with T1 program for corn will result in the greatest cost savings without sacrificing acceptable weed control. Further work should verify these findings with soybean and other crops.

4.7 Acknowledgements

Authors would like to thank the University of Nebraska-Lincoln farm staff for their assistance in establishing, planting, and harvesting trials each year.

4.8 References

Barnhart IH, Lancaster S, Goodin D, Spotanski J, Dille JA (2022) Use of open-source object detection algorithms to detect Palmer amaranth (*Amaranthus palmeri*) in soybean. Weed Sci 70:648-662

Barroso J, Fernandez-Quintanilla C, Maxwell BD, Rew LJ (2004) Simulating the effects of weed spatial pattern and resolution of mapping and spraying on economics of site-specific management. Weed Res 44:460-468

Beckie HJ, Reboud X (2009) Selecting for weed resistance: Herbicide rotation and mixture. Weed Technol 23:363-370

Brooks ME, Kristensen K, van Benthem KJ, Magnusson A, Berg CW, Nielsen A, Skaug HJ, Maechler M, Bolker BM (2017) glmmTMB balances speed and flexibility among packages for zero-inflated generalized linear mixed modeling. R J 9:378-400

Butts TR (2018) Spray Characterization and Herbicide Efficacy as Influenced by Pulse-Width Modulation Sprayers. Ph.D. Dissertation, The University of Nebraska-Lincoln

Buzanini AC, Schumann A, Boyd NS (2023) Evaluation of a smart spray technology for postemergence herbicide application in row middles of plasticulture production. Weed Technol 1-7 (2023) [doi: 10.1017/wet.2023.44]

Curran WS, Hoover RJ, Mirsky SB, Roth GW, Ryan MR, Ackroyd VJ, Wallace JM, Dempsey MA, Pelzer CJ (2018) Evaluation of cover crops drill interseeded into corn across the Mid-Atlantic region. Agron J 110:435-443

Dille JA, Stahlman PW, Thompson CR, Bean BW, Soltani N, Sikkema PH (2020) Potential yield loss in grain sorghum (*Sorghum bicolor*) with weed interference in the United States. Weed Technol 34:624-629

Edwards R, Hannah M (2014) Focus on weed control. Plant Physiol 166:1087-1089

Fadnavis S (2014) Image interpolation techniques in digital image processing: An overview. Int J Engine Res App 4:70-73

Farooque AA, Hussain N, Schumann AW, Abbas F, Afzaal H, McKenzie-Gopsill A, Esau T, Zaman Q, Wang X (2023) Field evaluation of a deep learning-based smart variable-rate sprayer for target application of agrochemicals. Smart Agric Technol 3:100073

Fernández-Quintanilla C, Peña JM, Andújar D, Dorado J, Ribeiro A, López-Granados F (2018) Is the current state of the art of weed monitoring suitable for site-specific weed management in arable crops? Weed Res 58:259–272

Flessner ML, Burke IC, Dille JA, Everman WJ, VanGessel MJ, Tidemann B, Manuchehri MR, Soltani N, Sikkema PH (2021) Potential wheat yield loss due to weeds in the United States and Canada. Weed Technol 35:916-923

Gao J, French AP, Pound MP, He Y, Pridmore TP, Pieters JG (2020) Deep convolutional neural networks for image-based *Convolvulus sepium* detection in sugar beet fields. Plant Methods 16:29

Gianessi L, Williams A (2011) Overlooking the obvious: The opportunity for herbicides in Africa. Outlook Pest Manage 22:211-215

Gianessi LP (2005), Economic and herbicide use impacts of glyphosate-resistant crops. Pest Manag Sci 61:241-245

Giles DK, Andersen PG, Nilars M (2002) Flow control and spray cloud dynamics from hydraulic atomizers. Trans ASAE 45:539-546

Giles DK, Comino JA (1989) Variable flow control for pressure atomization nozzles. J Commercial Veh SAE Trans 98:237-249

Gillies S, van der Wel C, Van den Bossche J, Taves MW, Arnott J, Ward BC, et al. (2023) Shapely. Available online: https://doi.org/10.5281/zenodo.7583915. Accessed: November 6, 2023

Gutjahr C, Sökefeld M, Gerhards R (2012) Evaluation of two patch spraying systems in winter wheat and maize. Weed Res 52:510-519

Hartig F (2022) DHARMa: Residual diagnostics for hierarchical (multi-level / mixed) regression models. R package version 0.4.6. Available online: https://CRAN.R-project.org/package=DHARMa. Accessed: October 2, 2023

Hussain N, Farooque AA, Schumann AW, McKenzie-Gopsill A, Esau T, Abbas F, Acharya B, Zaman Q (2020) Design and development of a smart variable rate sprayer using deep learning. Remote Sens 12:4091

John Deere (2024) See & Spray™ Ultimate: Targeted, in-crop spraying. Available online: https://www.deere.com/en/sprayers/see-spray-ultimate/. Accessed: April 29, 2024

Johnson WG, Davis VM, Kruger GR, Weller SC (2009) Influence of glyphosate-resistant cropping systems on weed species shifts and glyphosate-resistant weed populations. Eur J Agron 31:162-172

Jordahl K, van den Bossche J, Fleischmann M, Wasserman J, McBride J, Gerard J, et al. (2020) Geopandas/geopandas: v0.8.1. Available online: https://doi.org/10.5281/zenodo.3946761. Accessed: November 6, 2023

Kluyver T, Ragan-Kelley B, Perez F, Granger B, Bussonnier M, Fredrick J, et al. (2016) Jupyter Notebooks – a publishing format for reproducible computational workflows: Proceedings of the 20th International Conference on Electronic Publishing; 2016 Jun 7-9; Göttingen, Germany.

Knipling EB (1970) Physical and physiological basis for the reflectance of visible and near-infrared radiation from vegetation. Remote Sens Environ 1:155-159

Laini A, Bartoli M, Lamastra L, Capri E, Balderacchi M, Trevisan M (2012) Herbicide contamination and dispersion pattern in lowland springs. Sci Total Environ 438:312-318

Lancaster SR, Fick WH, Currie RS, Kumar V (2023) 2023 Chemical weed control for field crops, pastures, rangeland, and noncropland. Available online: https://bookstore.ksre.ksu.edu/pubs/chemweedguide.pdf. Accessed: November 6, 2023

Lenth R (2023) emmeans: Estimated marginal means, aka Least-Squares means. R package version 1.8.6. Available online: https://CRAN.R-project.org/package=emmeans. Accessed: November 6, 2023

Li J, Liang X, Wei Y, Xu T, Feng J, Yan S (2017) Perceptual generative adversarial networks for small object detection. Proceedings of the IEEE Conference on Computer Vision and Pattern Recognition; 2017 July 21-26; Honolulu, HI, USA

Miranda J WA, Jhala AJ, Bradshaw J, Lawrence NC (2022) Control of acetolactate synthase-inhibiting herbicide-resistant Palmer amaranth (*Amaranthus palmeri*) with sequential applications of dimethenamid-P in dry edible bean. Weed Technol 36:325-333

Oerke EC (2006) Crop losses due to pests. J Agr Sci 144:31-43

Owen MDK, Beckie HJ, Leeson JY, Norsworthy JK, Steckel LE (2014) Integrated pest management and weed management in the United States and Canada. Pest Manag Sci 71:357-376

Pacanoski Z, Mehmeti A (2021) Worldwide complexity of weeds. Acta herbologica 30:79-89

Partel V, Costa L, Ampatzidis Y (2021) Smart tree crop sprayer utilizing sensor fusion and artificial intelligence. Comput Electron Agric 191:106556

Paulson N, Schnitkey G, Sellars S, Zulaf C, Baltz J (2023) Update on growth rates of fertilizer, pesticide and seed costs over time. Farmdoc daily 13:62

R Core Team (2023) R: A language and environment for statistical computing. R foundation for statistical computing. Vienna, Austria. Available online: https://www.R-project.org/. Accessed: November 6, 2023

Redmon J, Farhadi A (2018) Yolov3: An incremental improvement. https://arxiv.org/abs/1804.02767. Accessed November 29, 2023

SciPy docs (2023) scipy.interpolate.griddata. Available online: https://docs.scipy.org/doc/scipy/reference/generated/scipy.interpolate.griddata.html. Accessed: November 6, 2023

Soltani N, Dille JA, Burke IC, Everman WJ, VanGessel MJ, Davis VM, Sikkema PH (2017) Perspectives on potential soybean yield losses from weeds in North America. Weed Technol 31:148-154

Spaeth M, Sökefeld M, Schwaderer P, Gauer ME, Sturm DJ, Delatrée CC, Gerhards R (2024) Smart sprayer a technology for site-specific herbicide application. Crop Protec 177:106564

Thompson JF, Stafford JV, Miller PCH (1991) Potential for automatic weed detection and selective herbicide application. Crop Protec 10:254-259

Vila-Aiub MM, Ghersa CM (2005) Building up resistance by recurrently exposing target plants to sublethal doses of herbicide. Eur J Agron 22:195-207

4.9 Figures

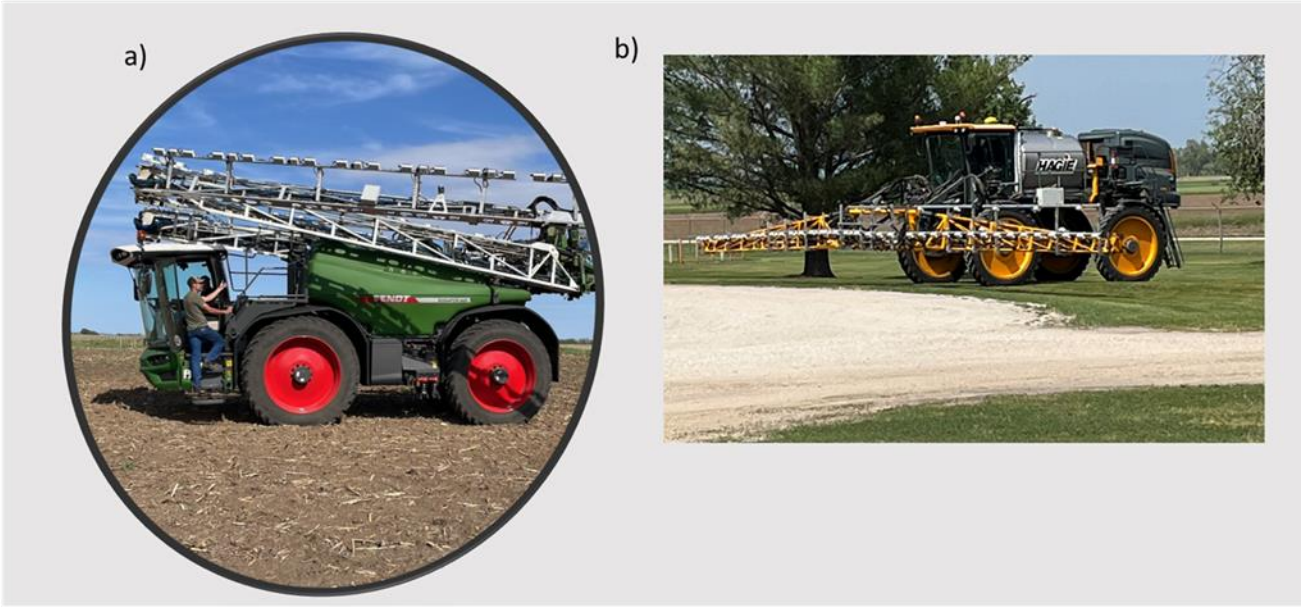

Figure 4.1 a) Fendt® RoGator™ 665 used for 2022 field study and b) Hagie® STS12™ used for the 2023 field study at Mead, NE.

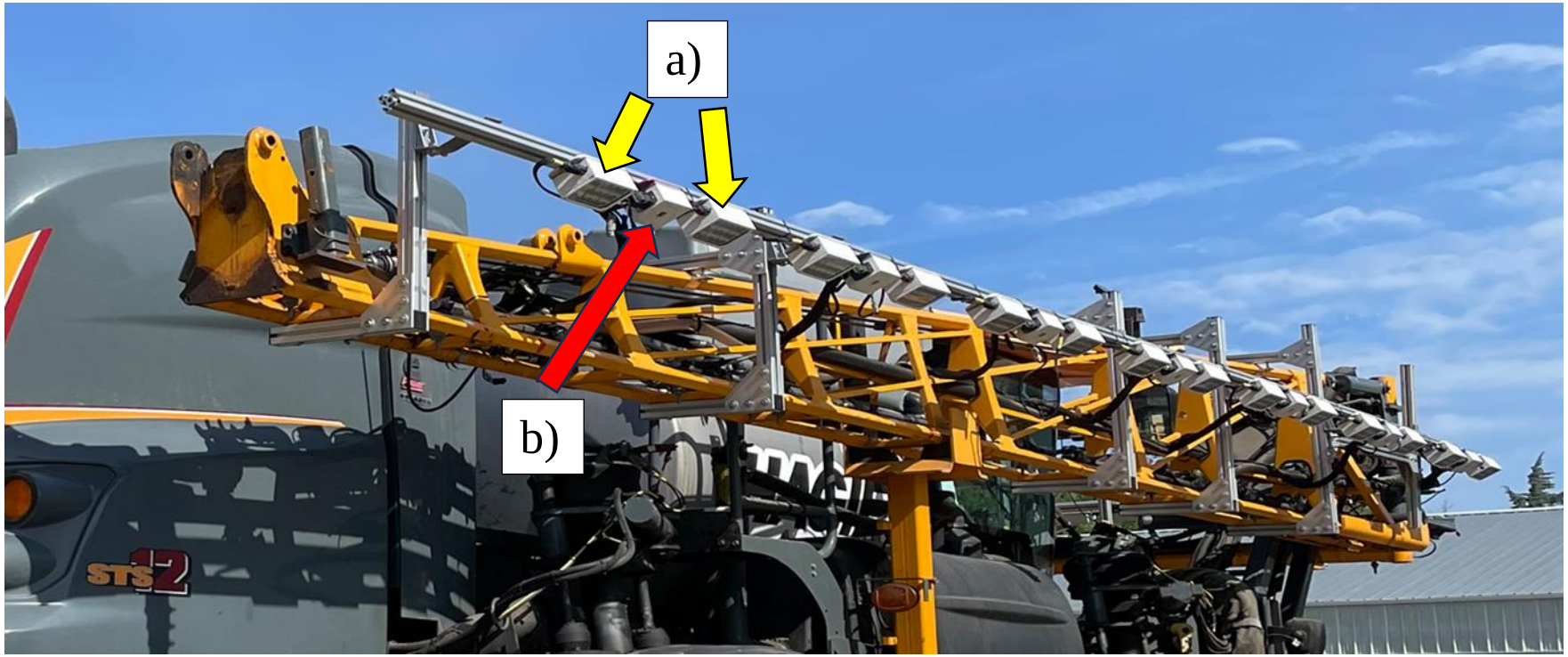

Figure 4.2 Close up view of the ONE SMART SPRAY system mounted onto the Hagie® STS12™ sprayer used in the 2023 studies. a) LED lights were attached to an aluminum rail running parallel to each boom, allowing the b) sensors to detect weeds in a variety of lighting conditions.

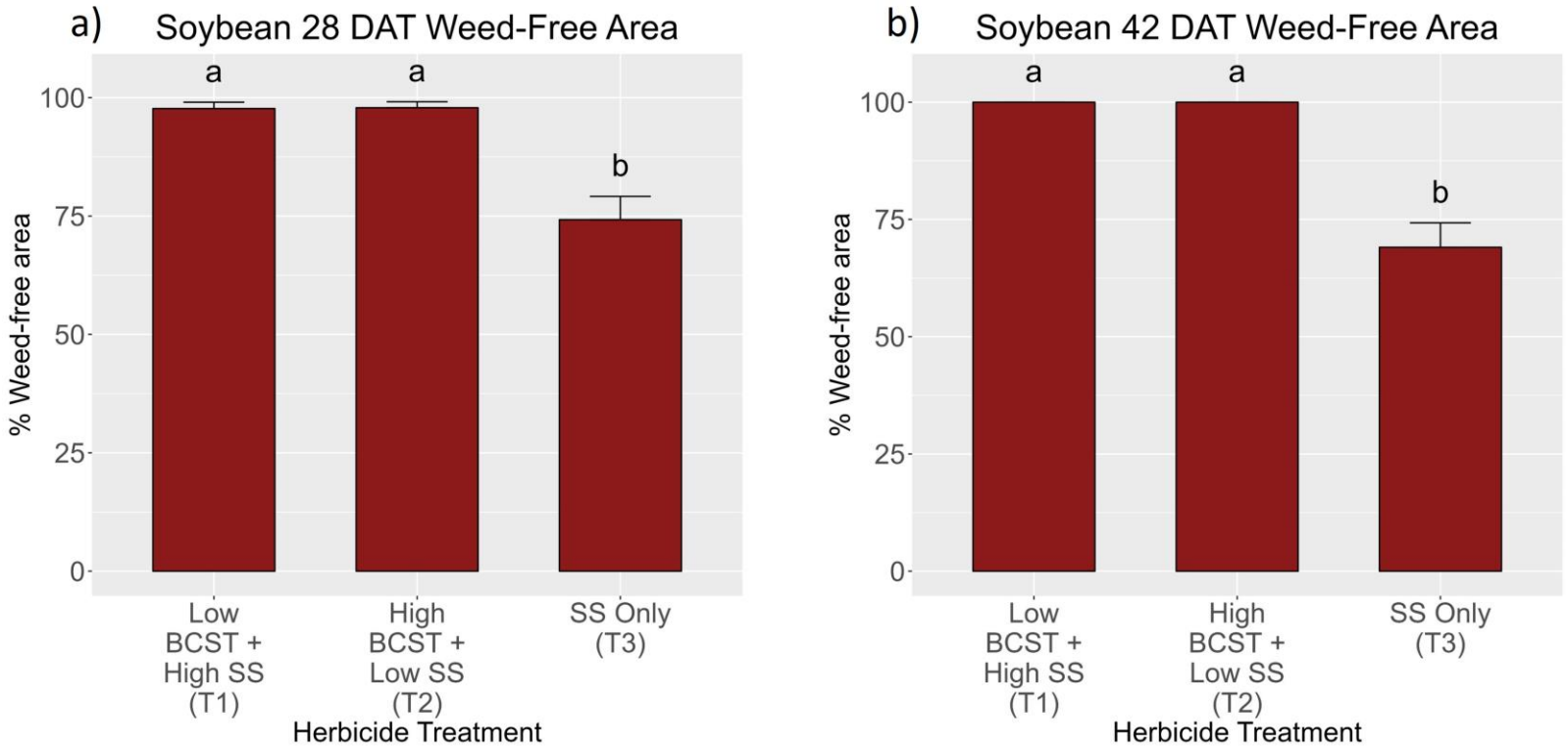

Figure 4.3 Mean percentage of weed-free area for each soybean herbicide application program at a) 28 DAT and b) 42 DAT. Weed-free areas for each plot were collected using visual estimations between 0 and 100%; ratings of 0 being completely infested with weeds, whereas ratings of 100 indicated no weed presence. A one-way ANOVA analysis was used to determine the main effect of application program on the weed-free area, and a Tukey Honest Significant Difference post hoc test ($p < 0.05$) was used for mean separation. Results indicated that T1 and T2 were not different but had more weed-free area than T3 on both measurement dates. No differences were observed between treatments with the same alphabetic letter above each bar and error bars are the standard error of

the mean for three independent replications. No error bars are above T1 and T2 for 42 DAT because the plots were completely free of observable weeds. Abbreviations: BCST, broadcast; SS, spot spray; T1, treatment 1; T2, treatment 2, T3, treatment 3, DAT, days after treatment.

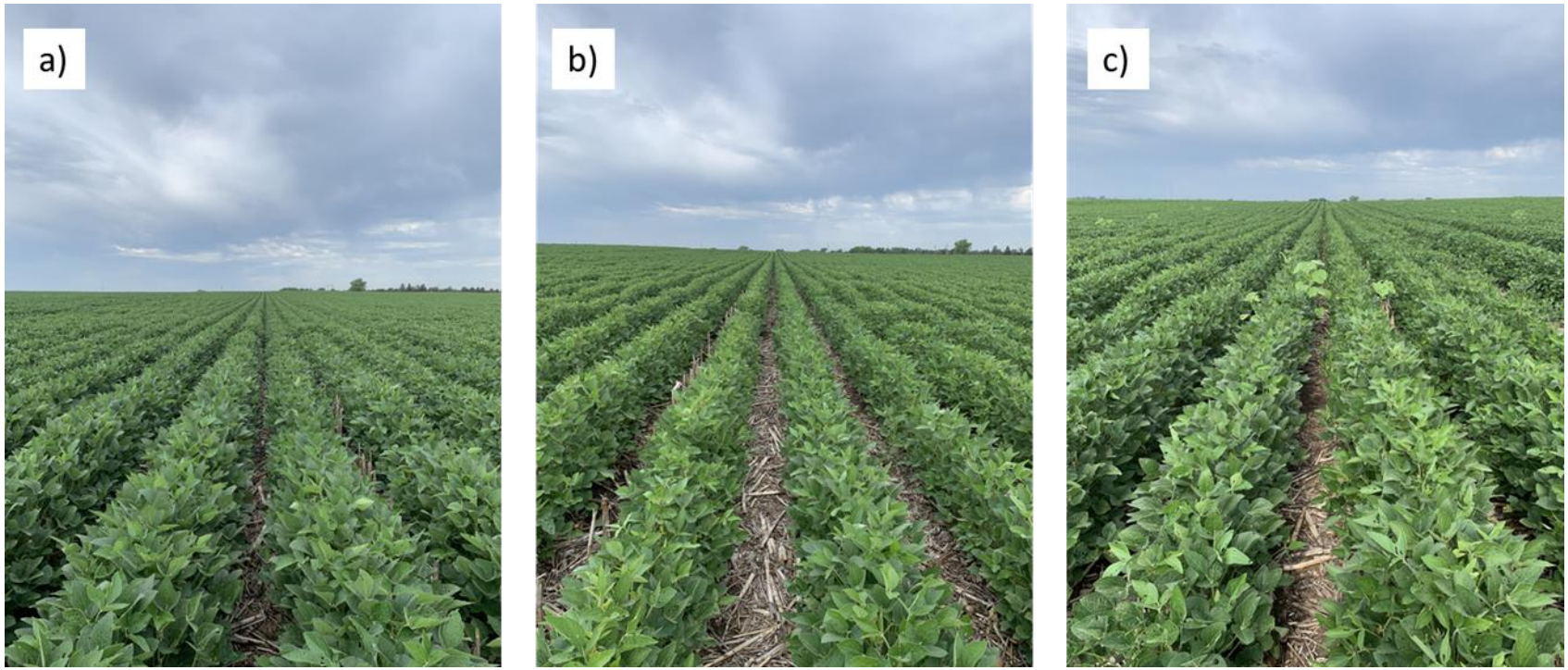

Figure 4.4 Differences in weed infestations for the 2022 soybean study by 28 DAT for a) Low BCST rate + High SS rate (T1) application program, b) High BCST rate + Low SS rate (T2) application program, and c) SS Only (T3) application program. The SS only program (T3) was characterized by denser infestations of velvetleaf (*Abutilon theophrasti* Medik.) and waterhemp (*Amaranthus tuberculatus* [Moq]. Saur) than T1 and T2 (waterhemp infestations not pictured).

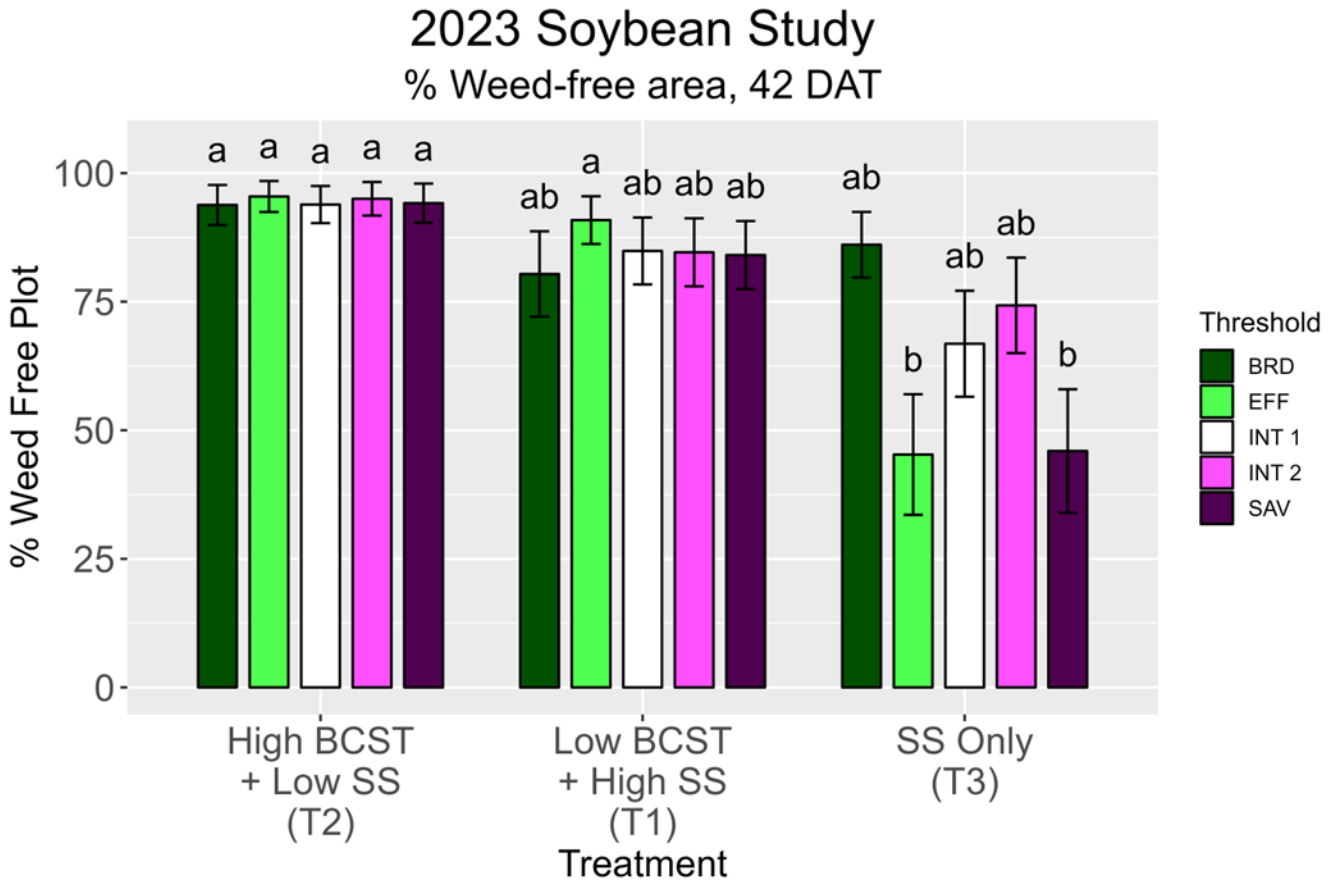

Figure 4.5 Application programs and thresholds interacted for weed-free area in 2023 soybean study by 42 DAT. Means visual weed-free area estimates of each plot, with 0 being completely infested with weeds and 100 being completely weed-free, and were analyzed with a two-way ANOVA followed by a Tukey Honest Significant Difference post-hoc test ($p < 0.05$) for mean separation. No differences were observed among n any of the thresholds in the T2 program, whereas the most weed-free area was observed for EFF threshold in T1 but was not different than the T2 results. There were no differences among observations with the same alphabetic letter above each bar. Error bars represent the standard error of the mean calculated from four independent replicates. Abbreviations: BCST, broadcast; BRD, broadcast (threshold comparison); SS, spot spray; EFF, efficacy threshold; INT 1, intermediate 1 threshold; INT 2,

intermediate 2 threshold; SAV, savings threshold; DAT, days after treatment; T1, treatment 1; T2, treatment 2; T3, treatment 3.

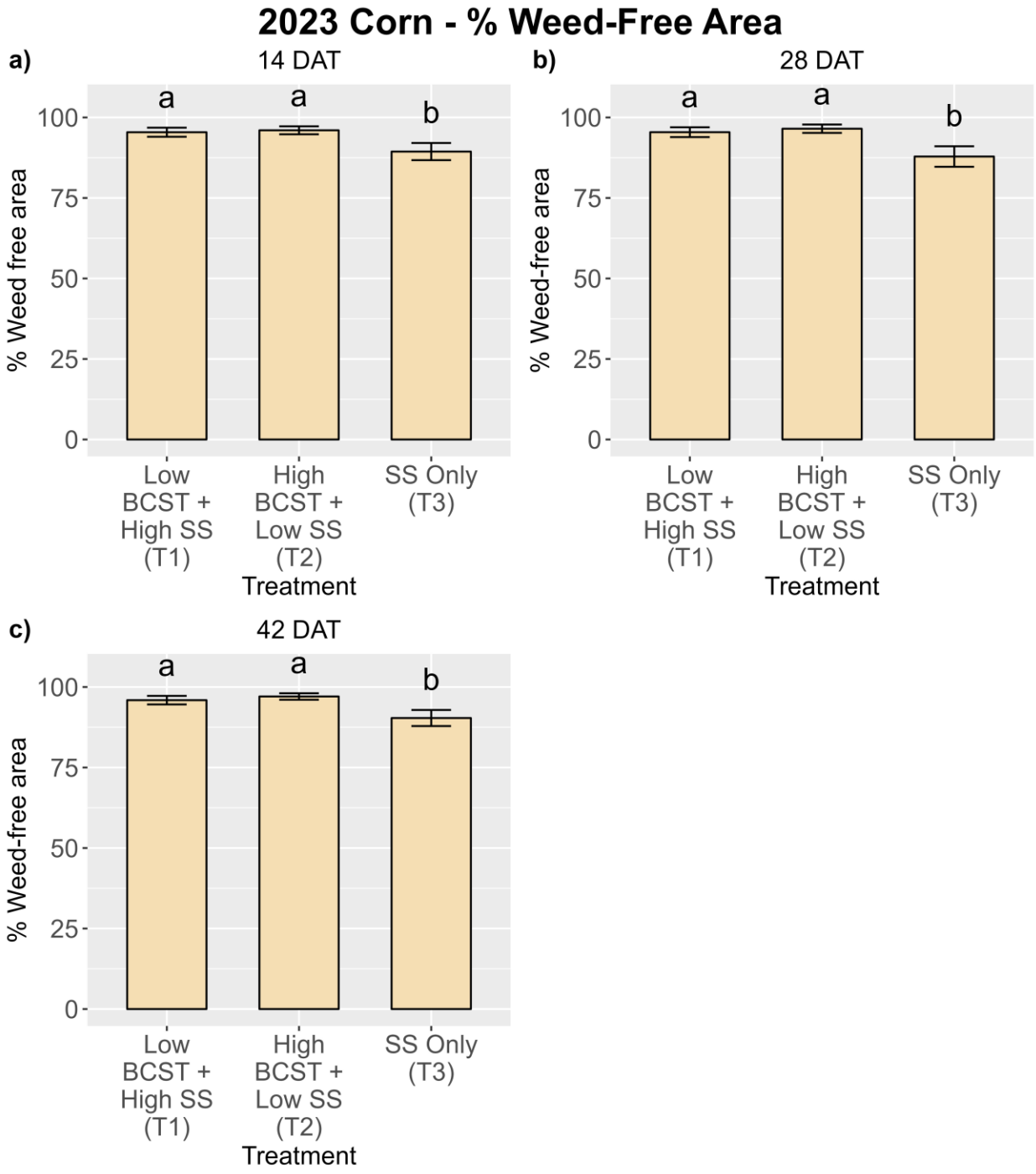

Figure 4.6 Percent weed-free area in the 2023 corn plots at a) 14, b) 28, and c) 42 DAT. Results are the average visual weed-free area estimates of each plot, with measurements of 0 indicating complete weed infestation and 100 indicating no weeds . These data were analyzed with a two-way ANOVA (main herbicide treatment and thresholds), where no significant interactions were

detected and only herbicide treatments were significant. A Tukey Honest Significant Difference post-hoc test ($p < 0.05$) was used to determine differences among means. Treatment T2 always contained the highest weed-free ratings, but T1 was never statistically different from T2. However, T1 and T2 had statistically higher weed-free area than T3 at each observation date. No statistical differences were observed between treatments with the same alphabetic letter on top of their respective bars, and error bars indicate the standard error of the mean among four independent treatment replicates. Abbreviations: BCST, broadcast; SS, spot spray, DAT, days after treatment.

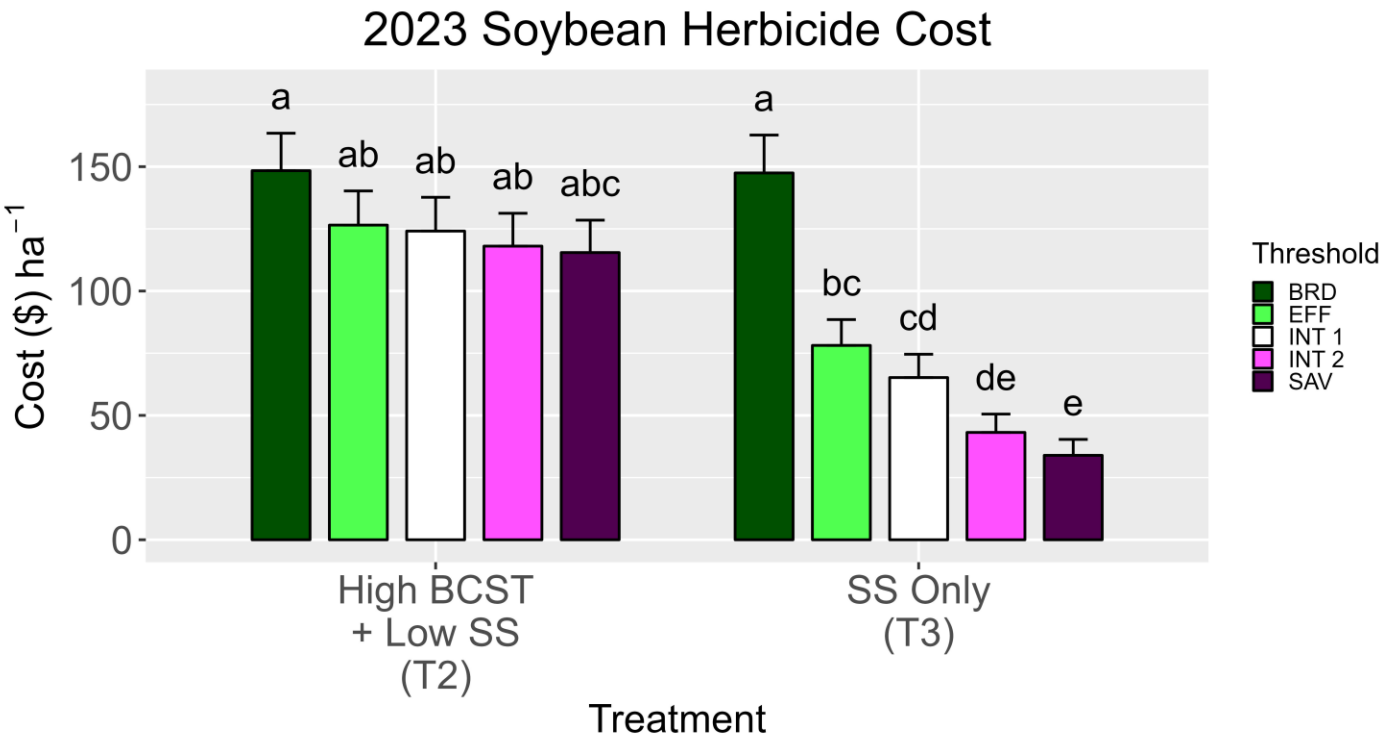

Figure 4.7 Results of the cost analysis of the 2023 soybean application programs and thresholds. Data were obtained by computing the percentage of each plot that was sprayed using the as-applied map, and includes all broadcast component costs. Data from the Low BCST rate + High SS rate (T1) were not available due to a sprayer error. A two-way ANOVA was used to determine the effect of all treatments on the cost in US$ ha^{-1}, and means were separated with a Tukey Honest Significant Difference post-hoc test ($p < 0.05$). Results indicated that, although always lower, the T2 thresholds were same cost as the BCST applications. However, T3 treatments were always cheaper than the BCST applications. No differences were observed with treatments with the same alphabetic letter over

each bar , and error bars indicate the standard error of the mean for four independent replications. Abbreviations: BCST, broadcast; BRD, broadcast (threshold comparison); SS, spot spray; EFF, efficacy threshold; INT 1, intermediate 1 threshold; INT 2, intermediate 2 threshold; SAV, savings threshold; DAT, days after treatment; T2, treatment 2; T3, treatment 3.

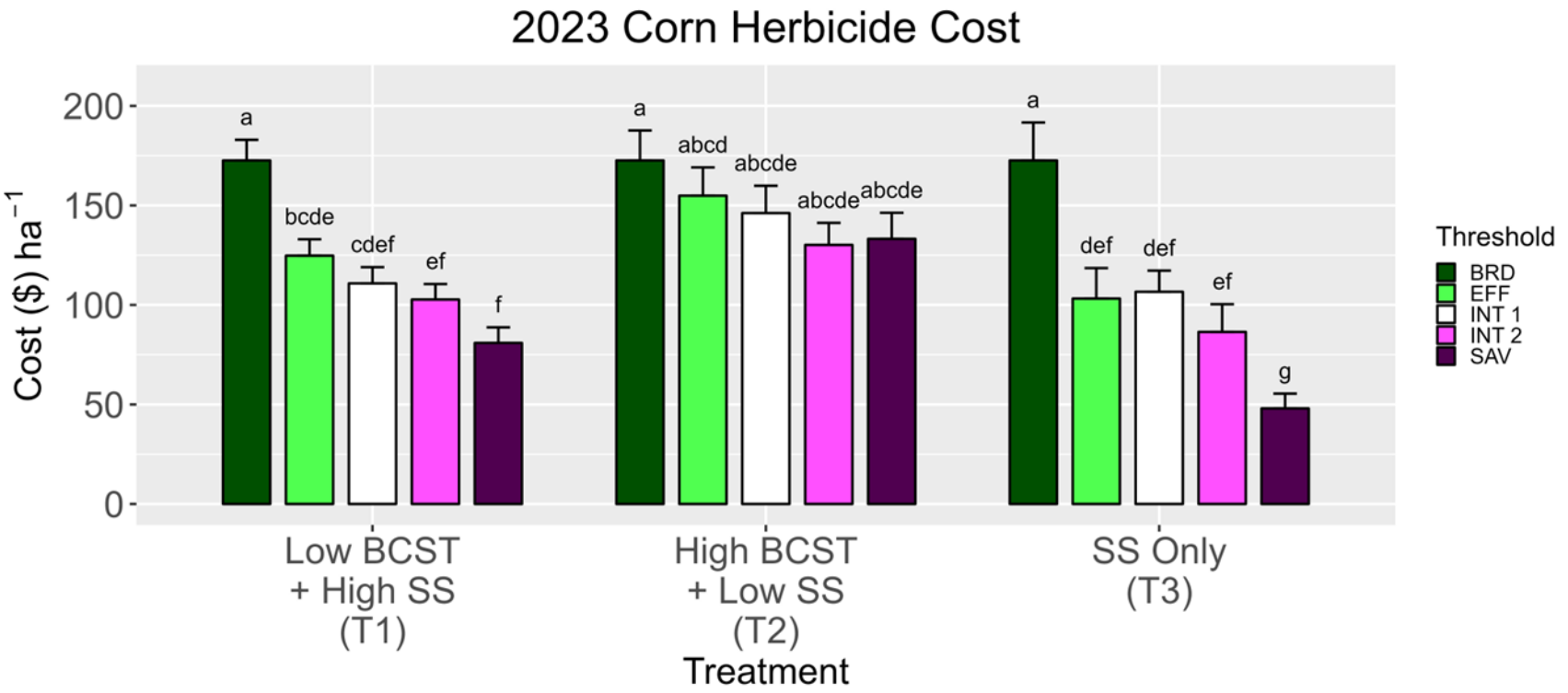

Figure 4.8 Results of the cost analysis of the 2023 corn treatments and thresholds. The percentage of each plot sprayed was computed using the as-applied maps generated using the raw sprayer data, and all broadcast treatments were included. A two-way ANOVA was used to determine the effect of corn herbicide treatment and sprayer threshold on the cost ha^{-1}, and the means were separated with a Tukey Honest Significant Difference post hoc test ($p < 0.05$). Results indicated that T2 thresholds, although lower than the BCST treatment, were not significantly lower than the BCST treatment cost, but all thresholds were significantly cheaper than the respective

BCST treatment for T1. No differences were detected among treatments with the same alphabetic letter over each respective graph, and error bars indicate the standard error of the mean for four independent replications. Abbreviations: BCST, broadcast; BRD, broadcast (threshold comparison); SS, spot spray; EFF, efficacy threshold; INT 1, intermediate 1 threshold; INT 2, intermediate 2 threshold; SAV, savings threshold; DAT, days after treatment; ha, hectare; T1; treatment 1; T2, treatment 2; T3, treatment 3.

4.10 Tables

Table 4.1 Planting information for corn and soybean trials for both 2022 and 2023 experiments.

Planting Information	2022		2023	
	Corn	Soybean	Corn	Soybean
Planting Date	April 19	May 16	May 3	May 2
Seeding population (seeds ha^{-1})	78,300	331,000	78,300	331,000
Hybrid/Variety	210-79DGVT2[†]	2622RXF[†]	59-81 RIB[‡]	2830-E3[§]

[†] Channel® Seed, Bayer Crop Science, 800 N. Lindbergh Blvd., St. Louis, MO, 63167, USA
[‡] DEKALB® Seed, Bayer Crop Science, 800 N. Lindbergh Blvd., St. Louis, MO, 63167, USA
[§] Beck's Hybrids, 6767 E. 276th Street, Atlanta, IN, 46031, USA. "E3" is a trademark of Enlist™ soybeans, Corteva Agriscience LLC, 9330 Zionsville Road, Indianapolis, IN, 46268, USA

Table 4.2 Herbicide and rate information for all 2022 treatments. Abbreviations: BCST, broadcast; SS, spot spray; ai, active ingredient; ae, acid equivalent.

Corn - 2022				Soybean 2022	
Herbicide Program	Application Method	Herbicide	Rate (g ai or ae ha^{-1})	Herbicide	Rate (g ai or ae ha^{-1})
Low BCST + High SS (T1)	BCST	glyphosate[†] + diflufenzopyr[‡] + dicamba[‡]	505 + 31 + 76	glufosinate[§] + glyphosate	246 + 631
	SS	glyphosate + diflufenzopyr + dicamba	1346 + 31 + 76	glufosinate + glyphosate	636 + 631
High BCST + Low SS (T2)	BCST	glyphosate + diflufenzopyr + dicamba	1346 + 31 + 76	glufosinate + glyphosate	636 + 631
	SS	glyphosate + diflufenzopyr + dicamba	505 + 31 + 76	glufosinate + glyphosate	246 + 631
SS Only (T3)	SS	glyphosate + diflufenzopyr + dicamba	1851 + 62 + 152	glufosinate + glyphosate	882 + 1262

[†] Roundup PowerMax 3™, Bayer Crop Science, 800 N Lindbergh Blvd., St. Louis, Missouri, United States
[‡] Status™, BASF Corporation, 26 Davis Drive, Research Triangle Park, North Carolina, United States
[§] Liberty 280 SL™, BASF Corporation, 26 Davis Drive, Research Triangle Park, North Carolina, United States

Table 4.3 Herbicide and rate information for 2023 trials. Abbreviations: BCST, broadcast; SS, spot spray; ai, active ingredient; ae, acid equivalent**.**

Corn - 2023			
Herbicide Program	Application Method	Herbicide	Rate (g ai or ae ha^{-1})
Low BCST + High SS (T1)	BCST	glufosinate[†] + diflufenzopyr[‡] + dicamba[‡] + glyphosate[§]	226 + 17 + 42 + 337
	SS	glufosinate + diflufenzopyr + dicamba + glyphosate	656 + 51 + 126 + 673
High BCST + Low SS (T2)	BCST	glufosinate + diflufenzopyr + dicamba + glyphosate	656 + 51 + 126 + 673
	SS	glufosinate + diflufenzopyr + dicamba + glyphosate	226 + 17 + 42 + 337
SS Only (T3)	SS	glufosinate + diflufenzopyr + dicamba + glyphosate	882 + 67 + 168 + 1010

Soybean 2023			
Low BCST + High SS (T1)	BCST	glufosinate + glyphosate + 2,4-D[¶]	226 + 337 + 266
	SS	glufosinate + glyphosate + 2,4-D	656 + 673 + 799
High BCST + Low SS (T2)	BCST	glufosinate + glyphosate + 2,4-D	656 + 673 + 799
	SS	glufosinate + glyphosate + 2,4-D	226 + 337 + 266
SS Only (T3)	SS	glufosinate + glyphosate + 2,4-D	882 + 1010 + 1065

[†] Liberty 280 SL™, BASF Corporation, 26 Davis Drive, Research Triangle Park, North Carolina, United States
[‡] Status™, BASF Corporation, 26 Davis Drive, Research Triangle Park, North Carolina, United States
[§] Roundup PowerMax 3™, Bayer Crop Science, 800 N Lindbergh Blvd., St. Louis, Missouri, United States
[¶] Enlist One™, Corteva Agriscience LLC, 9330 Zionsville Road, Indianapolis, Indiana, United States

Chapter 5 - Final Thoughts, Conclusions, and Further Direction

5.1 Introduction

Site specific weed management (SSWM) is a topic of interest due to an ability to reduce herbicide costs, environmental contamination, and reduce input costs for farmers. With the recent commercialization of artificial intelligence (AI) field sprayers, it is becoming increasingly feasible for farmers to use these sprayers to simultaneously detect weeds and spray them where they are growing and avoid spraying where they are not. These sprayers are a major step towards sustainability and SSWM, because AI has been shown to outperform traditional machine learning methods (i.e. support vector machines and k-means clustering algorithms) in terms of weed detection accuracy (Saini 2022). Overall, these studies demonstrate that weed detection and herbicide savings are possible and practical using AI.

5.2 Chapter 2

We determined that free and open-sourced algorithms can be trained to identify weeds without making large changes to algorithms' original code. It was found that the You Only Look Once version 5 (YOLOv5; Ultralytics 2023a) performed better than other algorithms that were tested in terms of mean average precision (mAP) (0.77), so it was chosen for further evaluation. These results revealed that the overall precision, recall, and F1 scores for 450 test images were 0.71, 0.70, and 0.71, respectively. Although these results were lower than other reported YOLO weed detectors (Jin et al. 2022; Zhuang et al. 2022), this was most likely because we had imagery from heights ranging from 1.5 m to 8 m above the ground. Studies such as Jin et al. (2022) and Zhuang et al. (2022) usually contain imagery taken at consistent heights. However,

our goal in this research was to include images that either a field sprayer or UAV would observe; we hypothesized that training algorithms for more specific detection purposes (i.e. deployments on either UAV or "smart" sprayers and not both) would lead to higher mAP, precision, recall, and F1 scores. For example, when training an object detection algorithm for an intelligent sprayer, training images should be collected from the same camera height, resolution, angle, and cameras that would be mounted on the sprayers themselves. We suggest that taking this approach would maximize the likelihood of correct weed detections.

To improve upon this study, we suggest not only tailoring algorithm training to specific objects, but collecting more imagery and increasing the number of weed species able to be detected would be beneficial. Species identification is challenging and would require a lot of data, but precise weed species identification is important because they vary in competitive ability, physical characteristics, growth habits, and even susceptibility to evolving herbicide resistance (Vasileiou et al. 2024). When collecting species data, it is important that the number of training samples for each species be balanced, as an imbalance in the number of object detection training samples often limits algorithm detection performance (Pang et al. 2019). It may also be beneficial to train newer algorithms as they are released. For example, at the time of this research, YOLOv5 was the most advanced YOLO-series model that had been released, but at the present time algorithms such as YOLO-WORLD (Ultralytics 2023b) is now available in the YOLO family (anonymous 2023). We hypothesize that object detection models will continue to improve in speed and detection accuracy as time progresses.

Additionally, we found that when deploying object detection algorithms, users can select detection confidence intervals. In our study, we found that a lower confidence interval resulted in more detections but increased the likelihood of false positives (i.e. soybean plants identified as

Palmer amaranth plants. Conversely, higher confidence intervals would result in more accurate detections, but would increase the likelihood of false negative detections (i.e. failing to detect a Palmer amaranth plant when it is, in fact, present within an image). Our recommendation is that, when deploying these weed detection algorithms, lower confidence intervals are used. In this research, the confidence interval that maximized true positive and minimized false positive detections was 0.298; this was determined automatically during model training. If deployed in an intelligent sprayer, it is currently unknown as to whether this algorithm would make detections that would provide the greatest identification and treatment of weeds. As models are trained for specific deployments, are trained on more images, and more weed species are added to the model, this optimum confidence interval may change. Further research should be conducted to understand the optimum confidence interval(s) for weed control after model deployment.

5.3 Chapter 3

We investigated different application approaches for the ONE SMART SPRAY research sprayer in corn (*Zea mays* L.) and soybean crops. The research sprayer used for this chapter was a two-tank/two-boom sprayer that was used to test spot-spray (SS) only treatments, simultaneous broadcasting (BCST) residual herbicides and SS foliar herbicides, and Spike applications in that a base rate of foliar herbicides were broadcast and "Spiked" up to a predetermined rate when weeds were detected. As discussed in chapter 2, multiple confidence intervals (referred to as thresholds from this point forward) were tested for the SS applications, and all treatments were compared with traditional broadcast applications. For this study, response variables included visual weed-free plot area estimations, weed density, end-of-season weed biomass, and grain yield.

Overall, our results indicated that two-pass approaches utilizing a broadcast application (either simultaneous broadcasting residual herbicides and spot-spraying foliar herbicides or using the Spike program) provided the most consistent weed-free area and lowest weed density. Also, the herbicide *Efficacy* threshold frequently provided weed control that was not statistically different than the broadcast treatments. The Spike programs were cheaper than broadcast treatments, but simultaneous BCST + SS treatments were, on average, cheaper than these programs. The SS only treatment was consistently the cheapest treatment across all thresholds but was almost always weedier than treatments with BCST components. Based on these data, we concluded that simultaneous BCST residual and SS foliar herbicides using the EFF threshold was the approach that provided weed control comparable to traditional BCST applications but cost significantly less.

For future research, efforts should continue to look at the BCST + SS treatments in different crops and should especially focus on narrow-row crops as the machine upgrades allow. At the present time, the ONE SMART SPRAY system is only able to spray crops planted in 76 cm apart. When machine upgrades are made so that narrower rows can be sprayed, this opens additional research questions as to how the machine can be best used. For example, soybeans can be planted in row widths including 19, 38, and 50 cm. We hypothesize that, because narrow rows establish canopy faster and are more competitive against weeds (Puricelli et al. 2003), there may be more benefits to SS only herbicide treatments compared to in 76 cm rows.

In this experiment, the Spike program included glyphosate base-rate BCST and SS rates were both 578 g ae ha^{-1}. This totals up to 1156 g ae ha^{-1} applied when weeds were detected, which is not currently labeled for glyphosate applications. The idea here was that, because these higher applications were not broadcast throughout the entire field, but only where weeds are

present, this may be a way to responsibly spray weeds with higher doses and ensure that the weeds are killed. Spot-spraying higher herbicide rates to improve SS efficacy has been suggested previously (Genna et al. 2021), although it may reduce cost savings. Herbicide labels are currently written for broadcast applications because SS technology is not as widely adopted as broadcast sprayers. However, we hypothesize that as ONE SMART SPRAY technology is increasingly adopted, there may be label changes to accommodate these new systems. Furthermore, it would be advantageous to test glyphosate application rates up to the 840 g ae ha^{-1} rate instead of the 1156 g ae ha^{-1} to understand how that would affect herbicide costs, because some of the cost savings were negated in this study due to the higher application rates.

5.4 Chapter 4

The last chapter built upon the "Spike" spray protocol but used a commercial ONE SMART SPRAY instead of a research sprayer. Due to machine availability, two different sprayers were used in 2022 and 2023, but the ONE SMART SPRAY cameras and sensors were the same for both years. For both years, Low BCST base rate + High SS (T1), High BCST base rate + Low SS (T2), and SS only (T3) applications. In 2022, we found that results were inconsistent in the corn trials (due to a strong PRE herbicide program and machine errors), but in the soybeans, both BCST + SS plots contained significantly more weed-free area than SS only plots. In 2023, these same results were observed for the corn trials, but only soybean trials saw a significant interaction between thresholds and herbicide treatments. All the thresholds used in the 2023 soybean trials were not statistically different than the broadcast application 6 weeks after application for the T2 treatments. This same weed control was not observed in the T1 treatments; however, the EFF threshold outperformed even the BCST application threshold for the T1

treatment, and the weed-free area was not statistically different from the T2 threshold results. For both crops in 2023, the T2 thresholds were not statistically cheaper than a broadcast application, but the T1 EFF threshold was cheaper than the T1 BCST application in each crop. Given that there is one year of data, these results suggest that broadcasting a low rate of foliar herbicides (i.e. glufosniate) and followed by a high "Spike" rate may provide the best weed control while allowing for significant herbicide cost savings compared to broadcast applications. Further research is needed to confirm this, as thresholds were not available in the 2022 season; consequently, we only have one year of data on these studies. Additionally, it was a very dry year, which 1) delayed canopy closure in the soybeans and 2) resulted in low weed pressure in the corn. Additional research is needed to confirm these results when adequate precipitation is available.

Especially in the soybeans, the best weed control was observed when a T2 approach was used. However, the danger of exposing weeds to sub-lethal doses of herbicide cannot be overstated. As highlighted in the chapter 4 "Discussion" section, exposing weeds to sublethal doses of herbicides has been shown to increase the likelihood of herbicide resistance development (Vila-Aiub and Ghersa 2005). The current ONE SMART SPRAY philosophy is to detect and eliminate crop rows and spray plants not within the rows. It is possible that some weeds will either be small enough to avoid detection or will be hidden by the crop rows and not sprayed with the full labeled rate. Therefore, if this method is relied upon continuously, herbicide resistance could develop at a faster rate than previously. It is worth noting that at the time of writing this chapter, the ONE SMART SPRAY will be transitioning from a crop row removal approach to an object detection approach, which will allow weed detection and future species identification (Bruno Canella-Vieira and Kalvin Miller, personal communication).

5.5 Additional Thoughts

The topic of resistance is a good opportunity to bring up the versatility of dual-tank/dual-boom sprayers. In chapter 3, we saw that the sprayers could be used in one of three ways: As a SS only, simultaneously broadcasting residual herbicides and SS foliar herbicides, and spiking an additional rate to a base-rate of foliar herbicide(s) when weeds are detected. One of the principles of integrated weed management (IWM) involves the principle of rotation (Swanton and Weise 1991). Rotating crops and herbicide modes of action have been shown to delay weed resistance development (Boerboom 1999; Beckie and Reboud 2009). We propose that to avoid development of resistance, the ONE SMART SPRAY should be rotated in terms of these use philosophies. For example, in chapter 3, the "Spike" treatment often provided the highest percentage of weed-free area. Rotating this application approach with the other treatments, coupled with rotating herbicide modes of action and crops, would likely give growers another tool for delaying weed resistance. Further research is needed to understand how these sprayers affect IWM and herbicide resistance evolution.

One of the goals of both chapters 3 and 4 was to simulate PWM applications. Although this technology could potentially turn single-boom sprayers into intelligent sprayers, we observed in chapter 3 that this approach resulted in less herbicide savings than simultaneous BCST + SS approaches. In many cases, the BCST + SS approaches provided weed-free area equal to or not statistically different than PWM "Spike" treatments. Although sprayers retrofitted with intelligent technology and PWM nozzles would, in theory, prevent farmers from having to purchase new sprayers, we would like to point out that the dual-tank/dual-boom sprayer we used was shown to be more versatile compared to single-boom sprayers. Therefore, to reap maximum

benefits from these sprayers, we suggest dual-tank/dual-boom sprayers be used when they come to market.

Finally, a topic of further research should be discovering the weed densities in which the ONE SMART SPRAY is best suited. We suggest that, at some density threshold, weed infestations will be heavy enough that a SS application will not provide cost savings compared to a traditional BCST application. While it is true that weeds often grow in non-uniform spatial distributions (Cardina et al. 1997), some fields will likely be completely infested with weeds and would require a broadcast application. In our studies, most of our fields contained light to very light weed infestations, which provided substantial herbicide savings. In chapter 3, the Manhattan KS Field 2 site had the highest weed densities, and significant savings were still observed. More studies across a variety of weed densities should be carried out to better understand the weed density at which SS herbicide savings are no longer statistically different than traditional BCST applications.

In closing, the future is bright for AI and weed control. As computing power, graphics processing units, and object detection algorithms improve over time, we suggest that further opportunities will emerge for on-the-go precision weed management tools to be created. As long as intelligent sprayers remain on the market, software upgrades are expected to improve performance and enable further improvements in precision weed management. This research demonstrates that there is tremendous potential for AI and intelligent sprayers to continue to be adapted to Midwestern United States' cropping systems and demonstrates that it is possible to significantly reduce herbicide costs and quantity applied while achieving weed control comparable to traditional BCST applications.

5.6 References

Anonymous (2023) YOLOv8 vs. YOLOv5: Choosing the best object detection model. Available online: https://www.augmentedstartups.com/blog/yolov8-vs-yolov5-choosing-the-best-object-detection-model. Accessed: November 21, 2023

Barnhart IH, Lancaster S, Goodin D, Spotanski J, Dille JA (2022) Use of open-source object detection algorithms to detect Palmer amaranth (*Amaranthus palmeri*) in soybean. Weed Sci 70:648-662

Beckie HJ, Reboud X (2009) Selecting for weed resistance: herbicide rotation and mixture. Weed Technol 23:363-370

Boerboom CM (1999) Nonchemical options for delaying weed resistance to herbicides in Midwest cropping systems. Weed Technol 13:636-642

Cardina J, Johnson GA, Sparrow DH (1997) The nature and consequence of weed spatial distribution. Weed Sci 45:364-373

Cheng T, Song L, Ge Y, Liu W, Wang X, Shan Y (2024) YOLO-World: Real-time open-vocabulary object detection. arXiv 2401.17270

Gao J, French AP, Pound MP, He Y, Pridmore TP, Pieters JG (2022) Deep convolutional neural networks for image-based Convolvulus sepium detection in sugar beet fields. Plant Methods 16:29

Genna NG, Gourlie JA, Barroso J (2021) Herbicide efficacy of spot spraying systems in fallow and postharvest in the Pacific Northwest dryland wheat production region. Plants 10:2725

Jin Z, Sun Y, Che J, Bagavathiannan M, Yu J, Chen Y (2022) A novel deep learning-based method for detection of weeds in vegetables. Pest Manag Sci 78:1861–1869

Pang J, Chen K, Shi J, Feng H, Ouyang W, Lin D (2019) Libra r-cnn: Towards balanced learning for object detection. Pages 821-830 *in* Proceedings of the IEEE/CVF conference on computer vision and pattern recognition. Long Beach, California, United States: Institute of Electrical and Electronics Engineers

Puricelli EC, Faccini DE, Orioli GA, Sabbatini MR (2003) Spurred anoda (*Anoda cristata*) competition in narrow- and wide-row soybean (*Glycine max*). Weed Technol 17:446-451

Saini P (2022) Recent advancement of weed detection in crops using artificial intelligence and deep learning: A review. Advances in Energy Technology: Select Proceedings of EMSME 2020, 631-640

Swanton CJ, Weise SF (1991) Integrated weed management: the rationale and approach. Weed Technol 5:657-663

Ultralytics (2023a) Comprehensive Guide to Ultralytics YOLOv5. Available online: https://docs.ultralytics.com/yolov5/. Accessed: November 21, 2023

Vasileiou M, Kyrgiakos LS, Kleisiari C, Kleftodimos G, Vlontzos G, Belhouchette H, Pardalos PM (2024) Transforming weed management in sustainable agriculture with artificial intelligence: A systematic literature review towards weed identification and deep learning. Crop Protec 176:106522

Vila-Aiub MM, Ghersa CM, Building up resistance by recurrently exposing target plants to sublethal doses of herbicide. Eur J Agron 22:195-207 (2005)

Zhuang J, Li X, Bagavathiannan M, Jin X, Yang J, Meng W, Li T, Li L, Wang Y, Chen Y, Yu J (2022) Evaluation of different deep convolutional neural networks for detection of broadleaf weed seedlings in wheat. Pest Manag Sci 2022:521–529

Appendix A - List of abbreviations

A. palmeri – Palmer amaranth (*Amaranthus palmeri*)

AI – artificial intelligence

AIC – Akaike information criterion

ANN – artificial neural networks

ANOVA – analysis of variance

AP – average precision

BCST – broadcast application

BRD – broadcast threshold

CNN – convolutional neural network

COCO – Microsoft "Common Objects in Context" image set

DAGBT – days after the green-on-brown treatment

DAGT – days after the green-on-green treatment

DAT – days after treatment

DCNN – deep convolutional neural network

DL – deep learning

EFF – efficacy threshold

fb – followed by

FN – false negative

FP – false positive

GOB – green-on-brown application

GOG – green-on-green application

GPS – global positioning system

IL – Illinois

ILSVRC – ImageNet Large Scale Visual Recognition Challenge

INT 1 – intermediate threshold 1

INT 2 – intermediate threshold 2

IoU – intersection over union

IR – infrared radiation

IWM – integrated weed management

KS – Kansas

LED – light-emitting diode

LiDAR – light detection and ranging

MAN 1 – Manhattan, Kansas field 1

MAN 2 – Manhattan, Kansas field 2

mAP – mean average precision

ML – machine learning

MOA – (Herbicide) mode of action

MS – milliseconds

NE – Nebraska

NE 1 – Nebraska field 1

NE 2 – Nebraska field 2

NIR – near infrared radiation

PWM – pulse width modulation

R-CNN – regional convolutional neural network

SAV – savings threshold

SEY 1 – Seymour, Illinois field 1

SEY 2 – Seymour, Illinois field 2

SS – spot spray application

SSD – Single Shot Detection

SSWM – site-specific weed management

T1 – treatment 1; low broadcast rate + a high spot-spray rate

T2 – treatment 2; high broadcast rate + a low spot-spray rate

T3 – treatment 3; spot-spray only

TP – true positive

UAV – unmanned aerial vehicles

WAP – weeks after planting

WSSA – Weed Science Society of America

YOLO – You Only Look Once

YOLOv3 – You Only Look Once, version 3

YOLOv4 – You Only Look Once, version 4

YOLOv5 – You Only Look Once, version 5

YOLOv8 – You Only Look Once, version 8